THESIS

ANALYSIS OF SELENIUM CYCLING AND REMEDIATION IN COLORADO'S LOWER ARKANSAS RIVER VALLEY USING FIELD METHODS AND NUMERICAL MODELING

Submitted by

Erica C. Romero

Department of Civil and Environmental Engineering

In partial fulfillment of the requirements

For the Degree of Master of Science

Colorado State University

Fort Collins, Colorado

Fall 2016

Master's Committee:

Advisor: Timothy K. Gates
Co-Advisor: Ryan T. Bailey

Dana L. K. Hoag

ABSTRACT

ANALYSIS OF SELENIUM CYCLING AND REMEDIATION IN COLORADO'S LOWER ARKANSAS RIVER VALLEY USING FIELD METHODS AND NUMERICAL MODELING

Groundwater and surface water concentrations of selenium (Se) threaten aquatic life and livestock as well as exceed regulatory standards in Colorado's Lower Arkansas River Valley (LARV). Se is naturally present in surface shale, weathered shale, and bedrock shale in the region. Excess nitrate (NO_3) from irrigated agricultural practices oxidizes Se from seleno-pyrite present in shale and inhibits its chemical reduction to less toxic forms. Irrigation-induced return flows and evapotranspiration induce high concentrations of Se in the alluvial groundwater resulting in substantial nonpoint source loads to the stream system.

This research uses three main components to address the need to better describe and find solutions to the problem of Se pollution in the LARV: (1) Se data collection in streams to characterize solute and sediment concentrations, (2) development of a conceptual model of in-stream Se reactions, and (3) application of existing calibrated groundwater models to explore alternative Se remediation strategies. Data in the form of Se solute samples, Se sediment samples, and related water properties were collected during four different sampling events in 2013 and 2014 at several locations in the stream network in an effort to understand the various species of Se and how they cycle through the surface water environment. A conceptual representation of the major chemical reactions of Se in the water column and sediments of streams was described and incorporated into the OTIS (One-Dimensional Transport with Inflow and Storage) computational model of stream reactive transport for future coupling to the

MODFLOW-UZF and RT3D-UZF groundwater models. The new version of OTIS, now called OTIS-MULTI, allows for simulation of the cycling of multiple Se species in the river environment. Lastly, five best management practices (BMPs) were tested using MODFLOW-UZF and RT3D-UZF: improved irrigation efficiency (reduced irrigation), lining or sealing of canals to reduce seepage, lease fallowing of irrigated fields, improved fertilizer management (reduced fertilizer), and enhancement of riparian buffers. The impact of each of these BMPs on Se loading to the stream network was evaluated individually over three scenarios in which the adaption of each BMP is incrementally increased. In addition, various combinations of three and four BMPs were simulated and compared.

Water samples gathered from the Arkansas River had total dissolved Se concentrations ranging from 6.1 to 32 μg/L (ICP method), compared to the Colorado chronic standard of 4.6 μg/L, while concentrations in samples gathered from tributaries ranged from 6.04 to 29 μg/L (ICP method). The groundwater and drinking water standard from the National Primary Drinking Water Regulations for selenium is 50 μg/L (USEPA, 2016). Concentrations of total Se (sorbed, reduced, and organic) in river bed sediments ranged from 0.16 to 0.36 μg/g with concentrations in river bank samples ranging from 0.26 to 1.78 μg/g. About 70 to 80% of Se in bed and bank sediments was found to be in a reduced or organic form. Analysis also reveals statistically significant high correlations of 0.70-1.00 between sorbed SeO_3 (bed sediment (μg/g) and sorbed SeO_4 (bed sediment) (μg/g); sorbed SeO_3 (bed sediment (μg/g) and estimated precipitated and organic Se (bed sediment) (μg/g); sorbed SeO_4 (bed sediment) (μg/g) and estimated precipitated and organic Se (bed sediment) (μg/g); ammonium (mg/L) and nitrite-nitrogen (NO_2-N) (mg/L); NO_3-N (mg/L) and total dissolved Se (μg/L); and sorbed SeO_4 (bank sediment average (μg/g) and an estimate of precipitated and organic Se (bank sediment average)

(µg/g). The conceptualization of key Se reactions was incorporated into OTIS-MULTI and must now be tested and calibrated for future application. The groundwater model results indicate that the individual BMP scenarios that most effectively decrease Se total mass loadings to the Arkansas River and its tributaries are: lease fallowing, resulting in a 15% decrease in predicted mass loading; reduced irrigation, with an 11% decrease; canal lining or sealing, with a 10% decrease; enhanced riparian buffer, with a 7% decrease; and reduced fertilizer, with a 3% decrease. In comparison, a BMP combination of lease fallowing, canal lining or sealing, enhanced riparian buffer, and reduced fertilizer was predicted to reduce loads by 46% and a combination of reduced irrigation, canal lining or sealing, enhanced riparian buffer, and reduced fertilizer by 44%. The hope, to be proven by future investigations, is that these reduced loads will contribute to lower concentrations in the river system.

ACKNOWLEDGMENTS

I am very grateful to the Nonpoint Source Program of the Water Quality Control Division of the Colorado Department of Public Health and Environment and to the Colorado Agricultural Experiment Station for their financial support of this work. I would like to thank my advisor, Dr. Timothy K. Gates, and co-advisor, Dr. Ryan T. Bailey for the opportunity to work on this project and for all of their advice and help. I am grateful to Dr. Dana Hoag for the chance to work with him on this project and to learn more about an alternative perspective. I would like especially to thank to my fellow graduate and undergraduate students who worked and helped me on this project: Misti Sharp, Mike Weber, Corey Wallace, Cale Mages, Brent Heesemann, Alex Huizenga, Caroline Draper and Chaz Meyers. I am very grateful to Brent Heesemann for his help in performing the statistical analysis on the collected field data, for creating Figure 3 of this thesis for shared use, and for helping me with other numerous questions along the way. Special thanks are extended to Misti Sharp for keeping me as positive as possible while working on this thesis (she is the best study buddy ever). My other friends' encouragements in my times of need are much appreciated. Most of all, I would like to thank Carl, my husband, and my family for their support and words of wisdom in helping me complete my MS degree.

TABLE OF CONTENTS

LIST OF TABLES

LIST OF FIGURES

Chapter 1: Introduction

1.1 Background and Problem Statement

Selenium (Se) is a required micro-nutrient for life; however, at high levels Se is toxic to humans, livestock, and aquatic species alike. For humans, the recommended range for dietary health lies between 40-400 micrograms/day (µg/day) (Levander and Burk, 2006). Once intake exceeds 400 µg/day a person is susceptible to selenosis with symptoms of defective nails and skin, hair loss, unsteady gait, and paralysis according to the United States Agency for Toxic Substances & Disease Registry Toxicological Profile for Se (USHHS, 2003). Acute oral exposure to high Se doses leads to nausea, vomiting and diarrhea, and sometimes cardiovascular symptoms (Lenz and Lens, 2009). For aquatic life, the toxic threshold for Se varies with regards to species and with the location where Se is measured, whether in water, soil, or tissue. The bioaccumulative nature of Se in the river system, especially in stagnant water areas, contributes to why different thresholds exist in different mediums. However, Hamilton (2004) suggests a toxicity threshold for fish near 3 µg/L and for sediment 4 µg/g as a general guide. When organisms or specific fish species are in danger, the literature should be consulted to determine a more suitable toxicity threshold. Two other important factors to consider in determining an aquatic toxicity threshold is the location in a water system, whether in the lotic (streams and rivers) or lentic (backwaters, side channels, reservoirs) areas, as well as whether the fish in question are a cold water or warm water variety (Hamilton 2004). In the embryo-larval stages of life, terotogenesis will develop in wild birds and fish whose parents were exposed to high levels of Se (Lemly, 1999; Hamilton, 2004). The side effects of terotogenesis in fish include curvature of lumbar and the spine; deformity of the head, mouth, gill cover, and fin; as well as edema, and problems of the brain, heart, and eye (Hamilton, 2004).

An early documentation of Se toxicity to livestock due to high plant and soil concentrations occurred in South Dakota in the middle 19th century (USHHS, 2003). Other investigations have been made, predominantly in the western United States. Of these areas, Kesterson Reservoir, CA was fed with high Se loadings from the irrigated soils of the San Joaquin Valley. The examination of Kesterson Reservoir was documented in hundreds of reports and publications (Hamilton, 2004) potentially making it the most famous case of Se poisoning (Bailey, 2012). The wildlife most visually affected in the area were various specious of duck: embryos shown in Figure 1-1 (Ohlendorf et al., 1986; Hoffman et al., 1988).

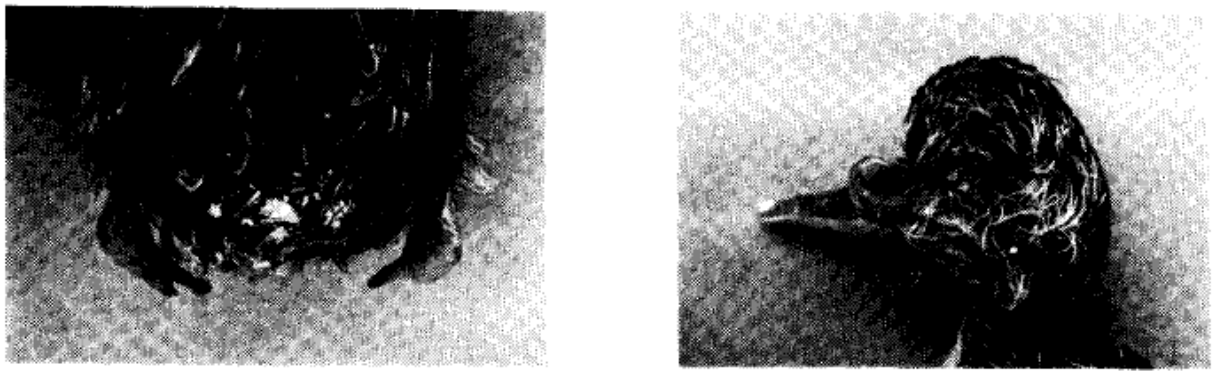

Figure 1-1. Abnormal embryos from eggs of aquatic birds at Kesterson from Ohlendorf (1986). The image on the left shows an American coot with truncated feet. The image on the right is a Black-necked stilt with abnormalities of the lower beak, poorly developed eyes, and no legs or one wing.

Following the closure and capping of Kesterson Reservoir, Se loading still continues to the Central Valley, San Joaquin River, the San Joaquin-Sacramento Delta, and San Francisco Bay (Hamilton, 2004). Further mitigation measures may be necessary to prevent continued pollution downstream.

In Colorado, the Colorado River received Se in irrigation return flows, reported as early as 1935 by Williams and Byers (1935). The extent of the study of Se on the Colorado River ranges from the headwaters in Colorado to the Colorado River Delta in Mexico where elevated concentrations prevail (Garcia-Hernandez et al., 2001). Due to the evidence of threshold-

exceeded concentrations in biota documented in Garcia-Hernandez et al. (2001), suggestions have been made that the Colorado River water should be mixed with agricultural drainage water to reduce toxic thresholds, that wetlands should have an outflow to decrease organic carbon and thereby lower Se concentrations, and that no dredging should be allowed to reduce toxicity in fish.

Of primary consideration in the Colorado River in Colorado are endangered species including the Colorado pikeminnow (*Ptychocheilus lucius*) and razorback sucker (*Xyrauchen texanus*) (Osmundson et al., 2000). Osmundson et al. (2000) discusses the difficulty in quantifying the extent of the Se problem with a method that does not cause fish sacrifice. Muscle plugs were taken from the fish and analyzed by neutron activation. The average Se concentrations found in the muscle tissue of the Colorado pikeminnow exceeded the toxic threshold of 8 μg/g dry weight from 1994-1996 (Osmundson et al., 2000). Since the 1960s, advocates have called for the protection for endangered fish along Colorado River as described in Hamilton (2004). Hamilton (2004) also discusses a controversy over the threshold toxicity concentration for fish predominantly and he disproves the hypothesis that certain fish species may have evolved to live in Se-rich environments.

Due to phosphate mining, the Blackfoot River watershed of southeastern Idaho has been impacted by Se as described by sampling of water, surficial sediment, aquatic plants, aquatic invertebrates, and fish in nine streams in 2000 (Hamilton et al., 2002). Water samples only exceeded the national water quality standard of 5 μg/L for Se at two sites. Most creek samples contained the same amount of inorganic elements; however, Dry Valley Creek had high amounts of aluminum, copper, iron, and magnesium. The most serious of results were those of concentrations in fish because at seven sites Se concentrations were > 4 μg/g in the whole body.

Se is also a serious issue in surface water and groundwater of the Lower Arkansas River Valley (LARV) in Colorado with potential toxic impacts on aquatic life and livestock since all three segments of the Lower Arkansas River were designated in 2004 as "water quality limited" with respect to Se and have been placed on the current Clean Water Act 303(d) list for total maximum daily loads (TMDL) development. Collected data indicate that Se concentrations are double the Colorado chronic standard of 4.6 µg/L for aquatic life in an Upstream Study Region (USR), which is shown in Figure 2 within Segment 1B of the river. The USR is named as such due to its location upstream of the John Martin Reservoir. More details on the data collection and analysis of Se in the region are discussed in Chapter 2. The affected segments of the river are designated by the Colorado Department of Public Health and the Environment (CDPHE) as COARLA01A (Segment 1A) COARLA01B (Segment 1B), and COARLA01C (Segment 1C) (Figure 2).

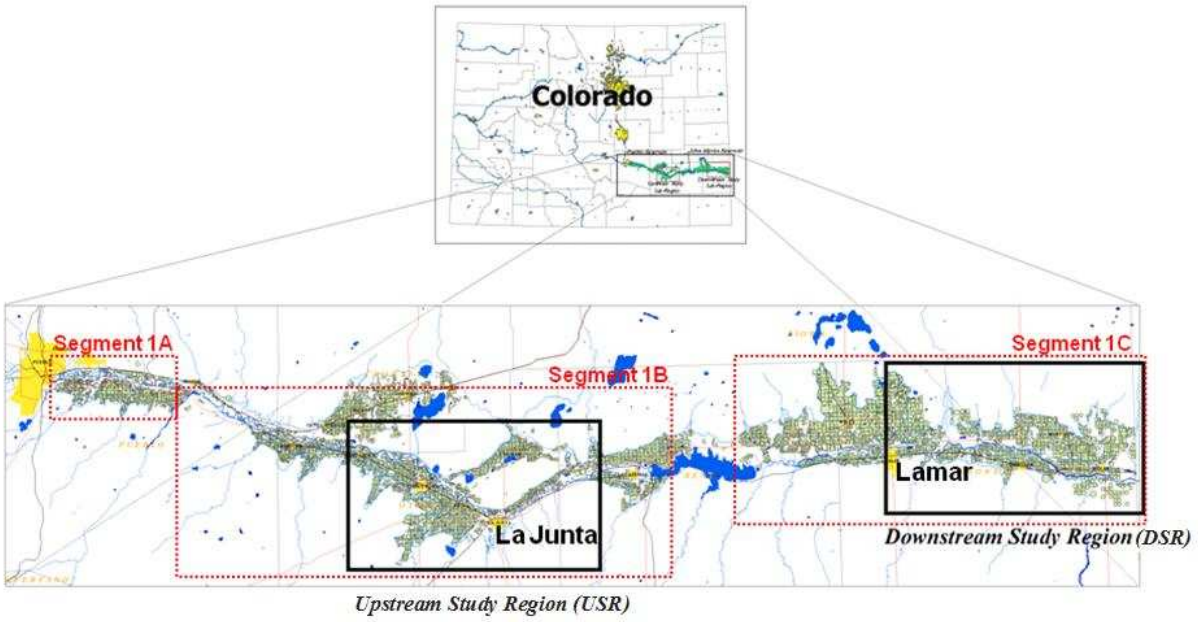

Figure 1-2. The Lower Arkansas River Valley in Colorado with two CSU study regions (black boxes) within Segments 1B and 1C of the Arkansas River

The Se problem in the LARV has developed over time since Se is naturally present in marine shale, which underlays and outcrops from the alluvial valley and is released from $FeSe_2$ through reduction of oxidative species such as dissolved oxygen and NO_3 into surface water and groundwater (Fernandez-Martinez and Charlet, 2009). For over a hundred years, irrigated farming has been prevalent in the area, growing crops such as melons, corn, alfalfa, onions, grass, sorghum and others. The irrigation water, containing high amounts of dissolved oxygen and NO_3, applied on the land has increased the dissolution of Se from weathered, bedrock, or surficial shale deposits. More recently, due to the application of fertilizers for farming productivity, the level of NO_3 has increased in the groundwater and surface water of the LARV thereby enhancing the dissolution of Se from shale via redox reactions (Bailey et al., 2012).

1.2 Objectives

To better address the problem of Se and N pollution in the LARV, the Nonpoint Source Program (NPS) of the Water Quality Control Division (WQCD) of the Colorado Department of Public Health and Environment (CDPHE) funded a project entitled "Identifying Arkansas River Selenium and Nitrogen Best Management" in 2012. A major aim was to use calibrated groundwater and stream models to estimate current Se loadings to the Arkansas River and tributaries and to examine the potential for alternative best management practices (BMPs) to reduce Se loadings and consequently lower solute concentrations toward compliance with regulatory standards. Key stakeholders and water agencies are being engaged for their input on the feasibility and desirability of considered BMPs. Economic analysis of the costs and benefits of the alternative BMPs also is being conducted. An ultimate goal is to develop a plan for implementation of a pilot program to test the effectiveness of the BMPs identified to be most promising. A companion project, supported by the Water Quality Improvement Fund (WQIF),

provided supplemental funds not only for modeling but also for field data collection and analysis to characterize how Se and N are processed in the stream system.

A major goal of the research in the LARV is to create calibrated regional-scale groundwater-surface water flow and reactive transport models that can be used to simulate the spatial and temporal distribution of Se and N concentrations in both the aquifer and the Arkansas River and its tributaries for characterization and for finding ways to lower these concentrations to meet regulatory and performance standards. The research presented in this thesis is important because it takes intermediate steps to reach this goal. The primary objectives are to:

1. Collect additional field data on Se concentrations and related water quality parameters in the Arkansas River and its tributaries to enhance the existing database and to inform both groundwater and stream models,

2. Develop a conceptual model along with mathematical expressions of the major processes involved with Se cycling in the stream system for use in a computational model of reactive fate and transport, and

3. Use existing calibrated and tested groundwater flow and transport models to explore and rank alternative BMPs for abatement of Se loading in groundwater and, consequently, for lowering Se concentrations in the Arkansas River and its tributaries.

Background, methods, and results associated with meeting these objectives are documented herein. Chapter 2 provides a literature review, discussing the background of Se chemistry, sources of Se, field sampling of Se in water and soil, Se in the environment, Se modeling research, prior CSU characterization and modeling of Se in the LARV, and remediation strategies. Chapter 3 describes the methods of field collection, description of Se surface water

cycling relationships, and groundwater modeling of BMPs for mitigating Se loading to streams of the LARV. Results are presented and discussed in Chapter 4. Chapter 5 summarizes the research, presents major conclusions, and suggests future work.

1.3 Study Region

The USR in the LARV, where the current study focuses, extends from just west of Manzanola, CO to near Las Animas, CO (Figure 1-2). Of the total 50,600 hectares (ha) (125,000 acres), 26,400 ha (65,300 acres) are irrigated lands which receive water from canals or pumping wells (Gates et al., 2009). As detailed in Gates et al., (2009), data have been collected focusing on Se and Se-related ions for both the USR and Downstream Study Region (DSR) extensively from 2003 to 2011. Monitoring of Se was implemented in the shallow unconfined alluvial aquifer and in the tributaries and drains of the Arkansas River. A total of 16 sampling events were conducted in the USR over the period June 2006 – May 2011. The routine surface water and groundwater samples were collected in 45 groundwater observation wells, four locations in tributaries and drains, and 10 locations along the river. Groundwater and surface water samples were collected for analysis of total dissolved Se concentration, dissolved uranium (U) concentration, and major salt ion concentrations including sodium, potassium, magnesium, calcium, nitrate, sulfate, chloride, bicarbonate, carbonate, and boron. Water quality properties including pH, electrical conductivity (EC), temperature, dissolved oxygen (DO), and oxidation reduction potential (ORP) also were measured in-situ.

Data collection for the present study was based on the previous methods reported in Gates et al. (2009); however, a few key differences exist. In addition to gathering and analyzing water samples from the Arkansas River and its tributaries, sediment samples also were collected from the top 0.2 – 0.3 m of the channel bed and banks for analysis of sorbed and reduced (and

organic) Se. Three complete surface water and sediment sampling events were conducted in March 2013, June 2013, and March 2014 for analysis of total and dissolved Se concentrations, dissolved U concentrations, and the same specific related ions as reported in Gates et al. (2009). In March 2013, eight locations in the Arkansas River and seven locations in five different tributaries were sampled. In June 2013, nine locations in the Arkansas River and seven tributary locations were sampled. In March of 2014, four Arkansas River and four tributary locations were sampled. One abbreviated sampling event was conducted in August 2013 but, due to insufficient flows, could not be completed. Only three river and one tributary location were sampled during this event. The locations of previous groundwater and surface water monitoring sites compared to the current project monitoring locations are shown in Figure 1-3.

Key findings of Gates et al. (2009) were that the average measured Se concentration (C_{Se}) in the Arkansas River exceeds the CDPHE chronic standard of 4.6 µg/L (85th percentile) for aquatic habitat on average by a factor of about 2.5 to 3 in the USR. The livestock water standard also was substantially elevated with the averaged measured C_{Se} in groundwater at 57.7 µg/L, compared to the standard of 30 µg/L. The spatial and temporal variability is large, indicating varying management solutions may be needed.

Correlation was found to be moderate between C_{Se} and salinity as represented by total dissolved solids (TDS) and EC in both groundwater and surface water. Values of C_{Se} in groundwater are strongly correlated with up-gradient distance to the identified near-surface shale (L_s) in the USR. High correlation exists between C_{Se} and the concentration of U (C_U) in groundwater and surface water. The ratio of C_{Se} in groundwater to that in water diverted for irrigation from the river is too large to be explained by the evaporative concentration alone, implying oxidative dissolution of Se from geologic strata. Values of C_{Se} in groundwater are

strongly correlated to the concentration of nitrate (C_{NO_3}) indicating that NO_3 enhances the dissolution of Se from soil and rock and its retention in solution. Finally, threshold concentration levels of roughly 10 mg/L for C_{NO_3} and 7 mg/L for DO appear to inhibit chemical reduction and promote oxidative dissolution from shale deposits as determined from analysis of the influence of C_{NO_3} and DO on the correlation of C_{Se} and C_U with L_s.

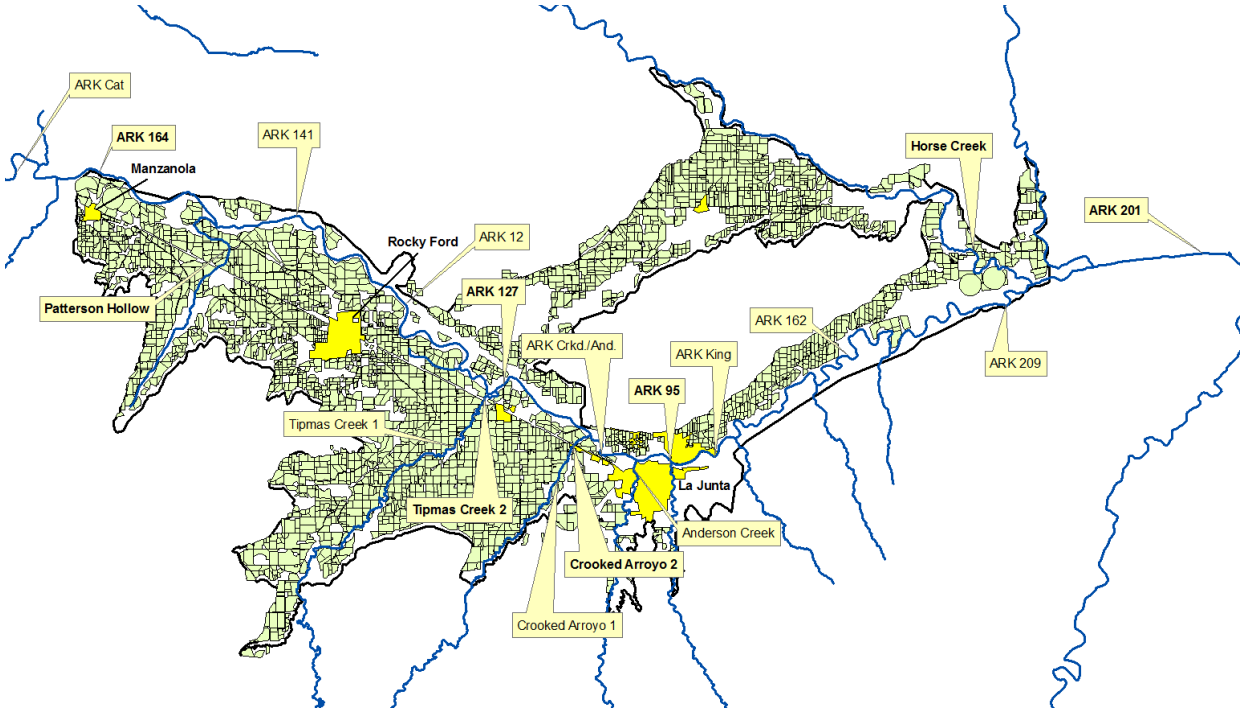

Figure 1-3. The USR showing the locations of the previous groundwater and surface water monitoring sites as well as the surface water locations sampled in this study (bold) in the Arkansas River and its tributaries.

Chapter 2: Literature Review

2.1 Selenium Chemistry

Se is a nonmetal with an atomic number of 34, relative mass of 78.971 and electron configuration [Ar] $3d^{10}$ $4s^2$ $4p^4$ as described by the Royal Society of Chemistry (Periodic Table-Selenium, 2014). The element is present in four main oxidation states (+VI), (+IV), (0), and (-II) in nature (Barceloux, 1999); in organic and inorganic forms; in solid, liquid, and gas phases; and in six stable isotopes (Lenz and Lens, 2009). The soluble oxyanions of Se are selenate (SeO_4^{-2}) and selenite (SeO_3^{-2}). The fully oxidized Se(VI) form, SeO_4^{-2}, exists in solution as biselenate ($HSeO_4^-$) or SeO_4^{-2} (Seby et al., 2001); although, SeO_4^{-2} is the dominant form at high redox potentials and has low adsorption and precipitation capacities (Alemi, 1988; Balistrieri and Chao, 1987). The two forms of Se(IV) are SeO_3^{-2} and the gas selenium dioxide, SeO_2; SeO_3^{-2} also can exist as three weak acid species including H_2SeO_3, $HSeO_3^-$, or SeO_3^{2-} depending on the pH of the solution. SeO_3^{-2} is the major species in the moderate redox potential range, and its mobility is mainly governed by sorption/desorption processes on various solid surfaces such as metal hydroxides (Balistrieri and Chao, 1987; Papelis et al., 1995), clays (BarYosef and Meek, 1987), and organic matter (Gustafasson and Johnsson, 1994).

Non-soluble elemental Se or Se(0) occurs in the form of at least 11 allotropes, seven crystalline and four non-crystalline (Minaev et al., 2005). The final two oxidation states, (-II) and (-I), occur in a variety of metallic selenides and many organic compounds and are stable under strongly reducing conditions (Fernandez-Martinez and Charlet, 2009). Other forms of Se found in surface water, groundwater, or wastewater include non-volatile organic selenides such as seleno amino-acids and volatile methylated forms of selenides such as dimethylselenide (DMSe) and dimethyldiselenide (DMDSe) (Fernandez-Martinez and Charlet, 2009).

2.2 Sources of Selenium

Earth's crust contains, in general, low concentrations of Se (Kabata-Pendias and Mukherjee, 2007; Fordyce, 2007). However, certain regions contain much more naturally-occurring Se than others. The usual Se content in soil is between 0.1 and 1 mg/kg; however, soil concentrations can be as high as 2 to 100 mg/kg (Cooper et al. 1974). Se is found in three major types of source rocks in the western United States: volcanic rocks, Cretaceous marine sedimentary rocks (mostly shales), and Permian marine sedimentary rocks (Presser, 1994). The Se substitutes for S in pyrite (FeS_2) to form seleno-pyrite ($FeSe_2$) since Se can isomorphically substitute in S-containing minerals (Kabata-Pendias and Mukherjee, 2007). Se is associated with other host minerals such as chalcopyrite and sphalerite, and about 50 Se minerals are known to exist including the following three examples: klockmanite, CuSe; berzelianite, $Cu_{2-x}Se$; and tiemannite, HgSe (Kabata-Pendias and Mukherjee, 2007). Sediments erode from Se-bearing rock on the ground surface and may deposit in streams. Se also can leach into the groundwater if stratigraphic layers intercept or bound an aquifer. Wildfires and volcanic activity also are natural sources of Se (Chapman, 2010).

Anthropogenic sources of Se contamination include power generation, oil refining, mining, irrigation drainage (Presser et al., 2004), and waste water treatment (Chapman, 2010). Since shale typically contains Se, crude oil from geologic formations, including marine shale, brings more Se to the surface. For example, mining of the Permian Phosphoria Formation, which is a marine, oil-generating shale unit, has resulted in death of livestock due to excess Se in southeast Idaho (Presser et al., 2004). Methods of power generation like combustion of fossil fuels, including coal and oil, also have introduced Se into the environment. In Belews Lake, North Carolina, fish tissues contain high Se due to inputs from the coal-fired Belews Creek Stream Station since late 1974 (Sorensen, et al., 1984). Cumbie and Van Horn (1980) found that

fish deaths were predominantly due to dietary intake of benthic insects which accumulated much higher amounts of Se than organisms living in the water (Hodson, 1988). Examples of agricultural exacerbated Se areas already have been discussed in Section 1.1 including the San Joaquin River Valley in CA, the Colorado River Valley in CO and Mexico, and the Lower Arkansas River Valley, CO. Finally, mining activities for ores such as coal, phosphates, and sulfides produce waste rock contributing to Se contamination. Waste rock piles, tailings impoundments, backfilled mining excavations, and reclaimed mined areas can leach Se when uncontrolled and end up in aquatic ecosystems (Chapman, 2010).

2.3 Selenium Cycling in Soil and Water

The cycling of Se in the environment is governed by the biological processes that affect the oxidation state of Se and subsequently its toxicity in the environment (Frankenberger Jr. and Arshad, 2001). Also the ability of Se to move through a river system is dependent on the form of Se. Dominant processes of Se conversion in soil and water include reduction of Se-oxyanions, oxidation of elemental Se, and volatilization. Toxic Se oxyanions, SeO_4 and SeO_3, can be reduced in water by a bacterium to elemental Se which is biologically unavailable because it is insoluble (Losi & Frankenberger Jr., 1997). Bacteria use SeO_4 and SeO_3 as terminal electron acceptors in energy metabolism or dissimilatory reduction; bacteria also can reduce and incorporate Se into organic compounds such as SeMet via assimilatory reduction (Fernandez-Martinez and Charlet, 2009). The oxidation of elemental Se in soil is mostly biotic in nature and occurs at relatively slow rates (Losi & Frankenberger, 1998). The methylation or volatilization of Se in soil and water differs in relation to the microorganisms that mediate the conversion. Bacteria are thought to be the active Se methylating organisms in water (Thompson-Eagle & Frankenberger Jr., 1991; Chau, et al., 1976), and DMSe gas is the main species produced

(Karlson & Frankenberger Jr., 1988). The major Se-methylating organisms in soil are fungi as well as bacteria (Janda & Fleming, 1978; Challenger et al., 1954).

This thesis focuses on the reactions of Se in deposited sediment (predominantly sediment that can reside in the bed of a stream but also can be transported) and suspended sediment (sediment carried by the flow of water in a stream) as opposed to soil (present in non-hydrologic environments or former hydraulic environments). Sediment in general and in this context is defined as a porous medium, laid down by streams, and exists in a predominantly aerobic environment. Due to the inherent differences between deposited and suspended sediment, and soil, the fractionation of Se varies in each setting. Se cycling in soil has been extensively studied compared to that of suspended and deposited sediments. However, the key differences must be examined.

Se in soil exists in several forms including elemental Se, selenide, SeO_4, SeO_3, and organic forms of Se including SeMet (Jezek et al., 2012). The speciation in soil (taken from three different areas given different amounts of agricultural drainage water) is important because it drives the availability in biota, and oxidized forms are generally more biologically available (Zalislanski & Zavarin, 1996). In their study of Kesterson Reservoir sediments (in this case the sediments the authors refer to are formerly ponded sediments but the reservoir ponds are now dry), Zalislanski and Zavarin (1996) monitored six fractions of Se: soluble Se(IV), soluble Se(VI), adsorbed Se, organic Se, carbonate Se, and refractory Se. The most significant observations occurred in surface soils within 0-0.10 m depth or Type A soils. Type B soils were collected from to 0.45 to 0.55 m below the ground surface. In Type A soils contained the largest percentage of refractory Se compared to soluble Se dominating Type B soils. Although

seemingly reversed, the history of Se deposition at Kesterson explains that surface soils (Type A) are generally more aerobic than deeper soils.

Zawislanski and Zavarin (1996) also conclude that the largest change in Se species was a 50% oxidation of refractory Se to soluble Se(VI). First order oxidation rates were between 0.058 and 0.27 yr^{-1} for organic Se and between 0.11 and 2.4 yr^{-1} for refractory Se. Methylation effects were not observed, indicating insignificance in soil. A Na_2HPO_4 solution was used to remove both the soluble and adsorbed fractions of Se from the sample rather than K_2HPO_4 as used in Fio et al., (1991) and Guo et al. (2000) due to the sodic nature of the soils tested from the Kesterson Reservoir.

A few studies have delved into the Se cycling in stream sediments, including that of Cook and Burland (1987) who proposed a diagram on biogeochemical Se cycling in water. Cook and Burland (1987) described the following processes: a) reductive assimilation of SeO_4 and SeO_3 into organic Se (bound by organisms); b) release of organically bound selenide back into solution; c) assimilation of dissolved organic selenide by organisms; d) oxidation of dissolved organic selenide to SeO_3; e) conversion of dissolved dimethylselenonium ions ($DMSe^+$-R) to DMSe; f) direct release of DMSe to solution; g) release of DMSe to the atmosphere; h) oxidation of DMSe to SeO_3 and/or SeO_4. Other authors have built off the research of Cook and Bruland (1987). For example, Fan et al. (2002) examined the speciation in food chain organisms.

Fractionation in suspended and deposited sediment differs in the various forms of Se present and the source of Se. Bowie et al. (1996) studied the Se cycling in Hyco Reservoir, North Carolina from 1985 to 1989 were the relative importance of major Se cycling processes in the water column and bed sediments were studied. The Se (IV) loading in the water column is from coal fly ash pond effluent which drives the Se biogeochemical cycle in Hyco Reservoir. In

sediments, the porewater contained five of the most important Se cycling processes. Diffusion was the second most important process for both the water column and sediments. Another key difference is that Se (IV) and Se (-II) suspended in the water column tended to follow oxidation tendencies in contrast to conditions in sediments where Se (VI) and Se (IV) follow reductive tendencies.

The presence of other chemical species has an effect on the cycling of Se in suspended sediment in the water column and in soil. Another study of the upper layer of the soil profile indicated that Se would be reduced and transformed into immobile species, from SeO_4 to organic Se for example, if enough C is present (Neal and Sposito, 1991). Although, these results are informative, they do not include the influence of other chemical species in the soil water and groundwater (Bailey, 2012a). No studies could be found on the effects of C on Se in stream sediments. Influences of O_2 and NO_3 on Se have been studied extensively in groundwater, revealing that Se is only consumed after the concentrations O_2 and NO_3 have been decreased to a certain threshold value (Weres et al., 1990; Oremland et al., 1990; Benson, 1998). Fio et al., (1991) found that O_2 and NO_3 prevent the chemical reduction of mobile Se and encourage Se leaching.

Sorption of SeO_3 and SeO_4 in soil is very different for each oxyanion (Jezek, 2012). SeO_3 is more strongly attached than SeO_4 to positively charged binding sites in soil (Eich-Greatorex, 2007) and creates stable complexes with iron hydroxides. Selenide is formed in soils in more acidic and reducing conditions, and also forms stable complexes with iron hydroxides (Kabata-Pendias, 2007).

2.4 Field Sampling of Selenium in Water and Sediments

Observations in the field characterize the nature and variability of Se in an environmental system and provide a base for theoretical analysis and numerical modeling (Ji, 2008). Once a

sample is collected in the field, it must be analyzed at a laboratory for any chemical species of interest. The method for determining the amount of Se in a sample varies based on the media and the species of Se of concern. The two media focused on here are water and sediments. Methods used for sampling fluvial sediments for Se analysis are highly dependent on the type of material present, ranging from large gravels to fine grain materials. It should be determined if only sediments are to be analyzed and/or if suspended sediment in the water column are to be studied as well. Also, depending on the goals of the project, a certain type of sampler should be selected based upon the size of the river or stream being sampled since each sampler has a maximum velocity and maximum flow depth or other limiting criteria for which it can be used. In general, the following types of samplers are available for use: depth-integrating, suspended-sediment samplers; point-integrating, suspended-sediment samplers; pumping samplers; bed-material samplers; and bedload samplers (Edwards & Glysson, 1999). An example of each type of sampler is shown in Figure 2-1. The last two samplers listed are for sediment alone. All other types are for sampling suspended sediments in water.

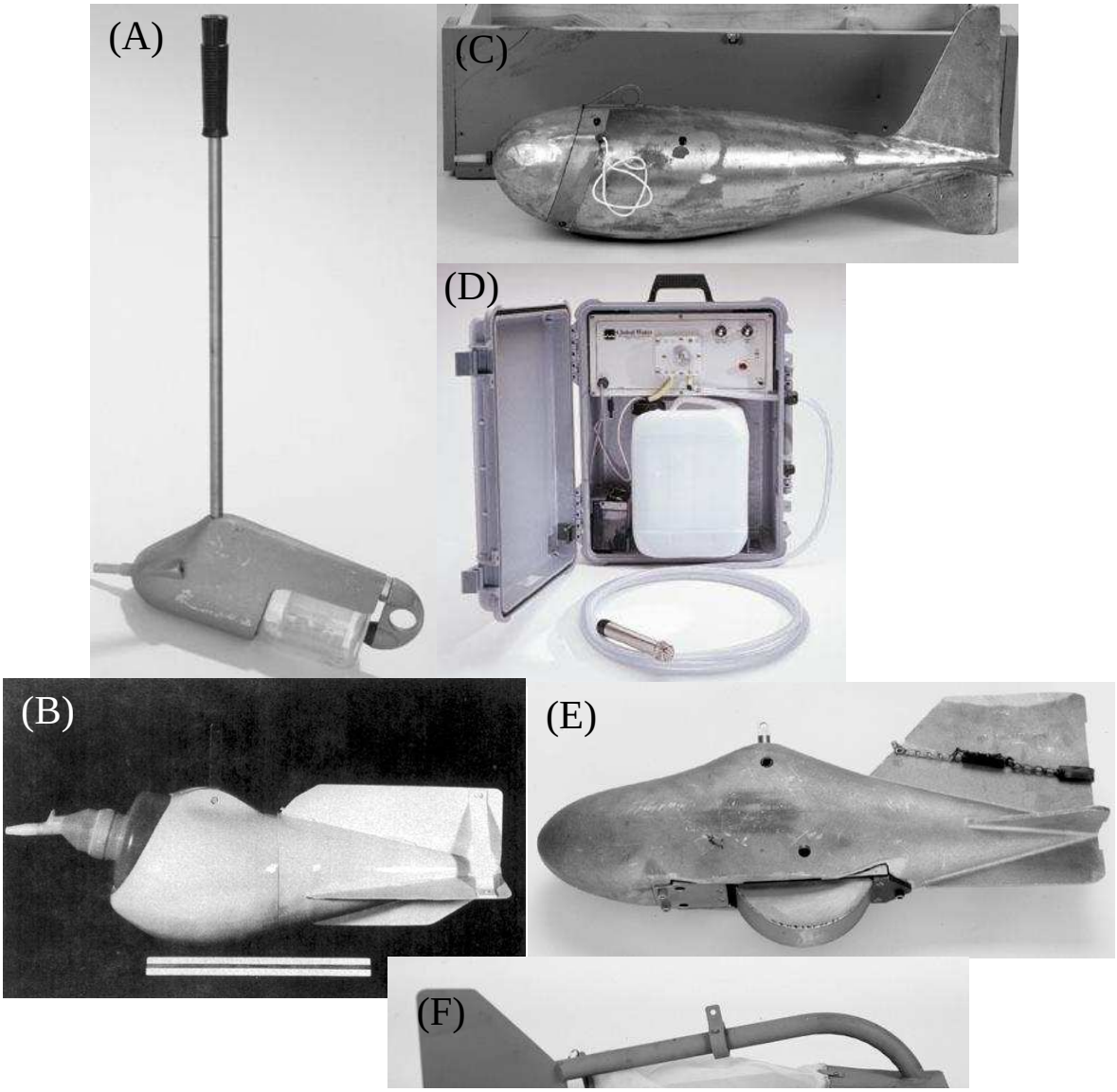

Figure 2-1. Images of the following samplers: (A) Depth-integrating wading type US DH-48; (B) depth-integrating suspended type US D-77; (C) point-integrating suspended sediment US P-72; (D) pumping sampler (www.geoscientific.com); (E) bed-material US BMH-60; and (F) bedload sampler US BL-84 (*Depth-Integrating Samplers*, 2009 for A-C and E-F)

The depth-integrating DH-48 sampler is for use in smaller rivers that can be waded into safely, which is why they are lightweight (*Depth-Integrating Samplers*, 2009). In general, DH samplers designated with a larger number are used for larger rivers and/or those below freezing temperatures. Point samplers can be used to collect a sample at any point underneath the surface of a stream or over a range of depth. Bed material samples are used to collect samples from

within the bed of a stream. Bedload samplers are made to sample the material in a stream which is in suspension above the bed and frequently maintains contact with the bed (Julien, 2010).

More than 26 different samplers are discussed in Edwards and Glysson (1999). In some cases, simple methods may be used for gathering samples in the case where the bed material is made up predominantly of coarse-grained sand to clay grain sizes. A bedload sampler would be used only to sample for material near the bed and mobilized fractions. The sediment of concern in this study is the material composing the bed must also be sampled to a depth of about 15 cm (6 in). None of the samplers discussed are suitable for extraction at this depth. Thus, plastic tubes placed vertically in the sediment of the bed or banks of the river with plastic end caps were used to collect sand and fine grained material from the surface to approximately 15 cm below the ground surface.

Numerous methods exist for collecting surface water samples for Se; however, only a few examples are discussed herein to illustrate the diversity. Zhang and Moore (1996) studied Se fractionation in Benton Lake National Wildlife Refuge, Montana and collected water samples by filtering water samples through a 0.45 μm membrane filter using a 60 mL plastic syringe that was decontaminated using an acid wash and deionized water rinse. The sample was placed into clean polyethylene bottles that had been rinsed two times by the filtered sample water (Zhang and Moore, 1996).A comprehensive study was conducted by the USGS on the collection of both surface water and sediment samples for analysis of Se. The USGS investigated four sites of the middle Green River basin that has been irrigated for over 60 years to investigate the effects of native Monaco Shale on land, water quality, and wildlife (Stephens et al., 1992). The sampling techniques used for surface water included taking grab samples of water for well-mixed low discharges and using an equal-width, depth-integrated method and a DH-48TM sampler.

Sediment samples were collected with a hand auger, composited by depth interval and placed into plastic bags or bottles. The method of analysis used for Se water samples was a hydride-generation methodology with a potassium permanganate in a hot acid solution.

The methods used for analyzing Se species in water are selective hydride generation or ion-chromatography using atomic fluorescence spectrometry or inductively coupled plasma-mass spectrometry (ICP-MS) (Maher et al., 2010). Zhang and Moore (1996) used a XAD (Alpha Products, Dankers, MA) resin separation method to determine Se species including SeO_3, SeO_4, and organic Se in water as well as soluble and adsorbed fractions in sediment according to Fio and Fujii (1990). Continuous-flow hydride-generation atomic absorption spectrometry was used to determine the Se concentrations in all samples (Zhang. and Moore 1996).

Multiple procedures have been used to analyze for Se in sediments. According to Maher et al. (2010), Se speciation in sediments primarily is measured by selective extraction procedures (SEP) and X-ray absorption. For example, studying the sediments in source shales, alluvial sediments, and evaporative pond sediments near Kesterson Reservoir, Martens and Suarez (1997) used hydride generation atomic absorption measurements to test for SeO_3, $SeO_4$and selenide that were soluble due to their extraction process. Not only were various Se species analyzed, but the analysis included organic carbon. The results of the study contend that Se concentrations and organic carbon are related in two different stages of release near Kesterson Reservoir. The first initial release of organic associated forms of Se is due to the oxidation of carbon that has accumulated because of anaerobic conditions. The second release is of refractory Se and occurs much slower due to the ecosystem change from the former Kesterson evaporation pond ecosystem (1978-1986) to a native semiarid grassland (1986-present). The results express the need to prevent refractory Se oxidation to prevent more soluble Se from entering the system.

Another study concentrating on Se speciation from source shale and testing sediments is by Kulp and Pratt (2004). Major and minor ions, total carbon, total sulfur, acid-insoluble sulfur, and total Se were tested. Kulp and Pratt (2004) also used hydride-generation atomic absorption spectrophotometry; however, they determined the concentrations of many more forms of Se including total Se, dissolved Se [SeO_3 and SeO_4], ligand exchangeable [SeO_3 and organic Se], base soluble [SeO_3 and organic Se], elemental Se, acetic acid soluble [SeO_3 and organic Se], sulfide/selenide associated Se (-II), and residual organic Se concentrations between the detection limit of 2 mg/L and 30 mg/L Se. The study determined that the mineralogy of the sediment and what type of organic matter is associated with each rock type indicates differences in the environmental chemistry and release of Se into the environment due to weathering (Kulp & Pratt, 2004).

Similar methods for water quality sampling have been conducted by the USGS in the Arkansas River in Colorado which have focused on measuring dissolved solids, Se, and uranium loads; unmeasured source and sinks for streamflow; and aggregating data on dissolved solids, Se and uranium loads. Ivahnenko et al. (2013) studied dissolved solids, Se, and uranium loads from June through December 2009 and from May through October 2010. Their dissolved constituents were filtered after collection through a 0.45 micrometer capsule filter and field preserved with acid to a pH of 2. Se concentrations in the Arkansas River from near Avondale to Las Animas were found to range from 8.4 to 12.2 μg/L, exceeding the 4.6 μg/L chronic standard. Se concentrations increased between Nepesta to La Junta and were generally higher in the tributaries. Flows from the La Junta Waste Water Treatment Plant (WWTP) had the highest median Se concentration of 18.9 μg/L. No Se concentrations at any sites exceeded the U.S.

Environmental Protection Agency primary drinking-water standards which were 50 µg/L for dissolved Se (USEPA, 2011) (Ivahnenko et al., 2013).

In the LARV, the most recent study of surface water samples collected from the Arkansas River and its tributaries for Se analysis were gathered from 2006 to 2011 using a peristaltic pump (Gates et al., 2009). Samples for total dissolved Se concentration were filtered through disposable in-line 0.003 or 0.006 m^2 0.45-µm capsule filters and placed into clean 0.12-L plastic bottles for storing dissolved metals. The location within the stream where the samples were taken was from about mid-flow depth at about the middle of the cross-section. The samples were sent to Olson Biochemistry Laboratories at South Dakota State University in Brookings, SD (USEPA certified) for analysis. The samples were analyzed via the Official Methods of Analysis of AOAC International, 17th edition, test number 996.16 Selenium in Feeds and Premixes, Fluorometric Method which can determine total dissolved Se, SeO_3, and total recoverable Se. SeO_4 is estimated by subtracting the SeO_3 from the total dissolved Se (Gates et al., 2009). Gates et al. (2009) states that dissolved Se concentrations are about double the CDPHE chronic standard of 4.6 µg/L

2.5 Se Modeling

The development of computational groundwater and surface water models of Se transport begins with conceptual models of the related processes. Significant advances have been made in recent years in groundwater modeling; however, little progress has been made in the modeling of Se in surface waters.

2.5.1 Modeling Se in Groundwater (Saturated and Unsaturated)

To better understand Se cycling in groundwater in numerical modeling studies from small to large scales, several models have been developed, as summarized in Table 2-1. These models first addressed one-dimensional (1D) soil column flow and have progressed into the

representation of two-dimensional (2D) vertical profile flow. Recently, more finite difference models are beginning to be advanced that incorporate Se cycling in 2D to three-dimensional (3D) domains. However, a significant deficiency in these models is the lack of consideration of solute interactions such as those among C, DO, NO_3 and Se.

Table 2-1. Summary of characteristics included in Se numerical modeling studies (modified from Bailey 2012)

Study	Model Dim.	Saturated Flow	Unsaturated Flow	SeO_4	SeO_3	Redox	Volatilization	Plant Uptake	Org. Matter Decay
Alemi et al. 1988	1D	X		X					
Fio et al. 1991	1D	X		X	X				
Alemi et al. 1991	1D		X	X	X				
Liu and Narasimhan 1994	1D	X				X			
Guo et al. 1999	1D	X		X	X	X	X		
Mirbagheri et al. 2008	1D		X	X	X	X	X	X	X
Tayfur et al. 2010	2D		X	X	X	X	X	X	X
Rajabli et al. 2013	2D	X	X	X	X	X	X	X	X
Myers 2013	3D	X		X					

The simplest Se models address 1D transport of Se species but do not include both sorption and redox reactions in saturated and un-saturated conditions (Bailey, 2012a). At least three studies have used 1D models to study sorption of SeO_4 and/or SeO_3 (Alemi et al., 1988; Fio et al. 1991; Alemi et al., 1991). The first study to include the redox reactions analyzed the vertical movement of Se in groundwater by using DYNAMIX, a redox-controlled, multiple species chemical transport model beneath Kesterson reservoir (Liu and Narasimhan, 1994). Guo et al. (1999) used saturated column leaching experiments and batch adsorption tests to analyze Se sorption, volatilization, and redox reactions with parameters fitted through model calibration.

Studies that have progressed in the simulation of additional Se cycling processes in the subsurface include Mirbagheri et al. (2008), Tayfur et al. (2010), and Rajabli (2013). These studies have incorporated all major Se processes including redox reactions, sorption, volatilization, mineralization and immobilization, and plant uptake of Se. Mirbagheri et al. (2008) simulated Se transport in an unsaturated soil column using a 1D dynamic mathematical model using a finite difference implicit method to converge on a solution. Tayfur et al. (2010) implemented a 2D finite element model that simulates Se transport in saturated and unsaturated soils. The reactions defined in Tayfur et al. (2010) are much simpler; for example, elemental Se and selenide are combined into one term. The model was tested using two datasets from Mendota, CA. The finite-element mesh for the model testing is 616 elements and 669 nodes. The mean absolute error for the both the 1990 and 1992 dataset is 8.9% and the mean absolute error is 48.5 μg/L (Tayfur et al., 2010). The model by Rajabli et al. (2013) extends the research by Mirbagheri et al. (2008) by adding the simulation of saturated media as well as unsaturated media in a modified 3D model. The test was applied in soil columns with various fractions of silt, clay and sand. The total depth of the soil columns were 200 cm. The model was tested using data by Nasiri, et al. (2012) from the Gonbad-e-Kavous site in the Golestan province of Iran. Simulated results are supposedly in good agreement with measured values; however, at two out of eight depths the simulated results match three or fewer of the nine measured values.

Finally, Myers (2013) implements MODFLOW-2000 to simulate groundwater flow and MT3D to simulate groundwater Se transport but does so in a non-robust manner. Myers (2013) assumes that SeO_4 is the primary species of Se in the groundwater in the geologic formation simulated and does not incorporate any of the other Se processes that are included by Rajabli (2013) or Tayfur (2010).

The Se cycling relationships presented in this thesis are slightly different than those addressed in the models developed by Rajabli (2013) and Mirbagheri (2008) since they are extended to a river system. Se cycling, in general, is very similar in a surface water system as compared to a groundwater environment. However, volatilization is enhanced in the surface water environment due to the potential availability of volatilizing plants, algae, fungi, or bacteria. Reaction rates dependent on temperature can increase during the heat of the day or decrease during the winter.

2.5.2 Modeling Se in Surface Water and Sediments

Hamer et al. (2012) discuss the LAKEVIEW model of Beaver Creek which calculates concentrations of radium-226, Se, U, and TDS in a 3D water quality transport and constituent speciation model for lakes and rivers, created by SENES Consultants Limited to simulate mine waste effects. The model includes transport between the water column and sediments with three parameters: "the mass transfer coefficient between water and sediment porewater (K_1), the adsorption coefficient in the sediment for a given constituent (K_{D_sed}), and the adsorption coefficient of the setting solids in the water column for a given constituent (K_{D_Wat})" (Hamer et al., 2012).

2.6 CSU Modeling of Salinity and Se in the Arkansas River Valley

Since 1974, several regional-scale waterlogging and salinity models of the LARV have been developed. Goff et al, (1998) created a 2D flow and solute transport model of 17.7 km of the Arkansas River. A previously calibrated solute transport model in 1973 of an 17.7 km [11-mile (mi)] reach of the Arkansas River was tested and found faulty by Konikow and Person (1985). Person and Konikow (1986) improved the previous model by incorporating salt transport throughout the unsaturated zone and refining the input data using regression relationships for estimating salinity from specific conductance data. Brendle (2002) developed a

steady-state groundwater flow model of a terrace alluvial aquifer, St. Charles Mesa, south of the Arkansas River and southeast of Pueblo, CO. The model was used to evaluate the decline of the water table using various scenarios such as lining of ditches, installing dewatering wells, as well as others. All methods would lower the water table except for reduced recharge to irrigated areas and the installation of two drains enough that some groundwater wells would no longer produce water.

In 2002, a much more expansive steady-state, three-dimensional model of groundwater flow and salt transport in the USR in the LARV was published by Gates et al (2002). Later models of transient flow and salt transport in the USR were developed and applied by Burkhalter and Gates (2005, 2006) to evaluate alternative management scenarios to remediate waterlogging, salinization, non-beneficial consumptive use, and salt loading. The more refined groundwater flow model of the USR developed by Morway et al. (2013) was used in this thesis along with the reactive transport model of Bailey et al (2014) to evaluate several alternative best management practices for Se remediation.

The CSU groundwater flow model applied to the period of 1999-2007 of the USR in the LARV is a regional-scale (~10^4-10^5 ha) model of the irrigated alluvial aquifer system (Morway et al., 2013). The objectives of model development were to adequately simulate "groundwater levels, recharge to infiltration ratios, partitioning of ET originating from the unsaturated and saturated zones, and groundwater flows, among other variables" (Morway et al., 2013) under historic baseline conditions and to simulate changes in these variables under alternate BMPs over the same time period. The model builds on earlier CSU models by using a more detailed representation of hydrologic conditions and water-budget components over a greater spatial and temporal extent as well as using larger observation data sets for calibration for the USR. To

inform the model construction and calibration, a database was built with field data collected over a period of nine years, including groundwater hydraulic head, groundwater return flow, seepage from earthen canals, actual crop evapotranspiration (ET) within the soil zone, and upflux to ET from the water table under naturally vegetated and fallow land, and estimates of ratios of water table recharge to infiltrated irrigation water. Use of the nine year data set was maximized by the following unique features implemented in the regional models:

- The time period was lengthened by six years compared to previous studies (Burkhalter and Gates, 2005; Burkhalter and Gates, 2006) so that it includes wet, dry, and near-average hydrological conditions.
- The unsaturated-zone flow (UZF1) package (Niswonger et al., 2006) developed for MODFLOW was incorporated and used to simulate unsaturated-zone flow processes over a regional scale.
- To create realistic spatiotemporal irrigation patterns and to preserve historical canal diversion records, a water allocation algorithm was developed.
- For increased numerical stability during calibration (easing cell wetting and drying problems), MODFLOW-NWT (Niswonger et al., 2011) was used.
- Spatially-varying estimates of precipitation and potential ET rates were employed in place of uniform estimates for each region.
- Estimates of actual ET were accounted for by using highly resolved land-use and crop-planting calibrated data classification.
- The rates and timing of seepage losses from earthen canals have been improved.
- Hydraulic conductivity and specific yield values were constrained by hundreds of stratigraphic logs.

The period of time simulated by the regional models is from 1999-2007 for the USR and 2002-2007 for the DSR. The grid cells have uniform areal dimensions of 250 m x 250 m in the horizontal plane which translates to a total of 15,600 active nodes in the USR. Two layers represent the alluvial aquifers of the LARV where the top layer is 5 m thick to take into account the maximum extent of deeply-rooted crops for alfalfa. The lower layer reaches from the bottom of the top layer to the impervious shale which forms the lower boundary of the modeled alluvial aquifer.

The models for each study region were calibrated using both automated and manual methods (Morway et al., 2013). The automated calibration methods used were UCODE (Poeter et al., 2005) and PEST (Doherty, 2002) which were tasked with minimizing the residual differences between simulated and observed values of target variables. Six target variables were used in calibration. Two targets, observations of hydraulic head and groundwater return flows, were used in automated calibration. The parameters undergoing automated calibration were hydraulic conductivity and river conductance values for changing seepage. These parameters were "varied to achieve an acceptable match between model-simulated values of hydraulic head (h) and groundwater return flow to the river (Q_{GW}), and values determined from field measurements" (Morway et al, 2013). The four targets used in manual calibration are canal seepage measurements (Martin, 2013; Shanafield et al., 2010; Susfalk et al., 2008), total actual ET calculated by the RESET model using satellite imagery (Elhaddad and Garcia, 2008), field estimates of groundwater ET (Niemann et al., 2011), and estimates of recharge to infiltration ratios (Gates et al., 2012). Using these observed data groups, manual adjustments were "made to values of canal conductance, potential ET, extinction depth, and a multiplier applied to the K_s" (saturated vertical hydraulic conductivity of the unsaturated zone) array (Morway et al., 2013).

Finally, engineering judgment was used to ensure that the final selected values of all calibrated parameters fell within realistic ranges (Morway et al., 2013).

The groundwater flow model for the USR was used to compute groundwater levels and flows for use in a variably-saturated reactive transport model (Bailey et al., 2014). The reactive transport model was developed by applying UZF-RT3D (Bailey et al., 2013) and accompanying Se and N reaction models (Bailey et al. 2013a) to the USR to simulate all species of dissolved Se and N in the system. Other constituents simulated are sulfur and dissolved oxygen. The Se reactions accounted for near-surface Se cycling due to agricultural processes, plant-soil interactions, sorption, and oxidation-reduction reactions. Most redox reactions include chemical reduction of dissolved oxygen and NO_3 (denitrification), nitrification and volatilization of ammonium, volatilization of SeMet, sorption of SeO_3, and oxidation-reduction of SeO_4, SeO_3, elemental Se, and selenide. The chemical reactions are modeled using first-order kinetics. The most important reaction is the "inclusion of autotrophic reduction of O_2 and NO_3 in the presence of residual Se in marine shale and the associated release of SeO_4 into the alluvial aquifer system" (Bailey et al., 2015). Johnsson et al. (1987) and Birkinshaw and Ewen (2000) presented mass-balance equations that were patterned for the LARV's N cycling module. There are seven dissolved-phase species including O_2, NH_4-N, NO_3-N, N_2, SeO_4-Se, SeO_3-Se, and SeMet. There are 16 solid-phase species. In this section, the notation for NH_4-N, NO_3-N, SeO_4-Se, SeO_3-Se will be written as NH_4, NO_3, SeO_4, SeO_3. "UZF-RT3D solves a system of advection-dispersion-reaction (ADR) equations for chemical species in both the dissolved phase and solid phase using the operator-split method (Yeh and Tripathi, 1989), with one ADR equation for each species" (Bailey et al., 2015). The ADR equation will be defined below for dissolved-phase Se species

(SeO_4, SeO_3, and SeMet) and the terms will be defined below the following equations from Bailey et al. (2015):

$$\frac{\partial(C_{SeO_4}\theta)}{\partial t}R_{SeO_4} = -\frac{\partial}{\partial x_i}(\theta v_i C_{SeO_4}) + \frac{\partial}{\partial x_i}\left(\theta D_{ij}\frac{\partial C_{SeO_4}}{\partial x_j}\right) + q_f C_{f_{SeO_4}} + F_{SeO_4} - U_{SeO_4}$$

$$+\varepsilon(\mathrm{r}_{s,Se}^{\min} - \mathrm{r}_{s,Se}^{\mathrm{imm}}) + \theta(r_{f,SeO_4}^{auto} - r_{f,SeO_4}^{het}) \quad (1a)$$

$$\frac{\partial(C_{SeO3}\theta)}{\partial t}R_{SeO_3} = -\frac{\partial}{\partial x_i}(\theta v_i C_{SeO_3}) + \frac{\partial}{\partial x_i}\left(\theta D_{ij}\frac{\partial C_{SeO_3}}{\partial x_j}\right) + q_f C_{f_{SeO3}} + F_{SeO3} - U_{SeO_3}$$

$$+\theta(r_{f,SeO_4}^{het} - r_{f,SeO_3}^{het(Se_s)} - r_{f,SeO_3}^{het(SeMet)}) \quad (1b)$$

$$\frac{\partial(C_{SeMet}\theta)}{\partial t} = -\frac{\partial}{\partial x_i}(\theta v_i C_{SeMet}) + \frac{\partial}{\partial x_i}\left(\theta D_{ij}\frac{\partial C_{SeMet}}{\partial x_j}\right) + q_f C_{f_{SeMet}} - U_{SeMet}$$

$$+\theta(\mathrm{r}_{f,SeO_3}^{het(SeMet)} - \mathrm{r}_{f,SeMet}^{het}) \quad (1c)$$

C = solute concentration ($M_fL_f^{-3}$), with the subscript f denoting fluid phase

D_{ij} = hydrodynamic dispersion coefficient (L^2T^{-1})

v = pore velocity (L_bT^{-1})

ϕ = porosity ($L_f^3L_b^{-3}$)

θ = volumetric water content ($L_f^3L_b^{-3}$)

q_f = volumetric flux of water representing sources and sinks (($L_f^3T^{-1}L_b^{-3}$), e.g. irrigation water, canal and river seepage, groundwater discharge to the river, or pumped groundwater, with b denoting the bulk phase

C_f = solute concentration of the source or sink ($M_fL_f^{-3}$)

r_f and r_s = represent the ratio of all reactions that occur in the dissolved phase ($M_fL_f^{-3}T^{-1}$) and solid phases ($M_sL_s^{-3}T^{-1}$), respectively

ε = the volumetric solid content ($L_s^3 L_b^{-3}$) with s denoting the solid phase and is equal to 1 – ϕ

R_m = the retardation factor for species m and is equal to $1+(\rho_b K_{d,j})/\theta$, where

ρ_b = the bulk density of the porous media ($M_b L_b^{-3}$) and

$K_{d,m}$ = partition coefficient ($L_f^3 M_b^{-1}$)

F = inorganic fertilizer application rate ($M_f L_b^{-3} T^{-1}$)

U = potential uptake rate ($M_f L_b^{-3} T^{-1}$)

Other superscripts to note are min and *imm* which signify mineralization and immobilization respectively; and *auto* and *het* represent autotrophic and heterotrophic chemical reduction, respectively. The complete set of equations for NH_4, NO_3, and O_2 are all included in Bailey et al. (2013) but are not included here.

Monod terms are used for rate law expressions and to quantify the r_f terms to include the dependence of reaction rate on water content, soil temperature, organic carbon being present for microbial consumption, and the concentration of the reacting solute. Also, the chemical reduction of Se species is slowed by the presence of O_2 and NO_3. Shown below are the equations for the heterotrophic denitrification and SeO_4 reduction with all equations defined in Bailey et al. (2013):

$$r_{f,NO_3}^{het} = \lambda_{NO_3}^{het} C_{NO_3} \left(\frac{C_{NO_3}}{K_{NO_3} + C_{NO_3}} \right) \left(\frac{CO_{2,prod}}{K_{CO_2} + CO_{2,prod}} \right) \left(\frac{I_{O_2}}{I_{O_2} + C_{O_2}} \right) E \qquad (2a)$$

$$r_{f,SeO_4}^{het} = \lambda_{SeO_4}^{het} C_{SeO_4} \left(\frac{CO_{2,prod}}{K_{CO_2} + CO_{2,prod}} \right) \left(\frac{I_{O_2}}{I_{O_2} + C_{O_2}} \right) \left(\frac{I_{NO_3}}{I_{NO_3} + C_{NO_3}} \right) E \qquad (2b)$$

Where λ_m = the base rate constant for species m (T^{-1})

K_m = the Monod half-saturation constant for species m ($M_f L_f^{-3}$)

I_{O_2} and I_{NO_3} = the O_2 and NO_3 inhibition constants ($M_f L_f^{-3}$)

$CO_{2,prod}$ = the total mass of CO2 produced during organic matter decomposition and signifies available organic carbon; and

E [-] =an environmental reduction factor that accounts for soil moisture and soil temperature.

Below are the solid-phase Se species for litter L_{Se} and humus H_{Se} equations with equations for related carbon and N:

$$\frac{\partial(C_{L_{Se}}\varepsilon)}{\partial t} = \alpha_{Rt,Se}P_{Rt} + \alpha_{St,Se}P_{St} + \varepsilon(\mathrm{r}^{dec}_{s,Se(L\to H)} + \mathrm{r}^{dec}_{s,Se(\mathrm{M}\to\mathrm{L})} + \mathrm{r}^{dec}_{s,Se(\mathrm{L}\to\mathrm{L})} - \mathrm{r}^{dec}_{s,Se(\mathrm{L})} + \mathrm{r}^{imm}_{s,Se(\mathrm{L})} - \mathrm{r}^{\min}_{s,Se(\mathrm{L})})) \quad (3a)$$

$$\frac{\partial(C_{H_{Se}}\varepsilon)}{\partial t} = \varepsilon\left(\mathrm{r}^{dec}_{s,Se(L\to H)} - \mathrm{r}^{dec}_{s,Se(\mathrm{H})}\right) + \varepsilon\left(\mathrm{r}^{imm}_{s,Se(\mathrm{H})} - \mathrm{r}^{\min}_{s,Se(\mathrm{H})}\right) \quad (3b)$$

Where

P_{Rt} and P_{St} = the application rates of root and after-harvest stover mass, respectively

$\alpha_{Rt,Se}$ and $\alpha_{St,Se}$ = the portions of the root and stover mass attributed to Se with dec signifies organic matter decomposition

L and H = the litter and humus pool, respectively, with the arrow representing the direction of mass flow

Expressions for each r_s term are found in Bailey et al. (2013).

As described above in equations (3a) and (3b), soil organic matter cycling from litter (fast-decomposing), humus (slow-decomposing), and manure is also simulated. The movement of solute mass from crops in the growing season to deposition of organic Se and N to the litter pool with the death of the plant is also taken into account. Finally, during plowing, the remaining root mass and above-ground crop mass not removed at the harvest (stover) is taken into the litter pool (Bailey et al., 2014).

The simulation time period employed by Bailey et al. (2015) was from January 1, 2006 through October 31, 2009 with the calibration period being January 1, 2006 through March 31, 2008 and the remaining time used as the testing period. Daily time steps were used. The finite difference surface grid and cell grid dimension in the horizontal direction were exactly the same as those used by Morway et al. (2013) in the groundwater flow model. However, the vertical discretization was modified from two layers to seven so that localized chemical reactions and physical processes like root growth, solute uptake, and dead root mass/stover mass additions could be more accurately represented. The top two layers compose the root zone and are each 0.5 m thick. The third layer is 1.0 m thick and ends the unsaturated zone. Layers 4-6 make up the saturated zone. Since layer 4 corresponds to the depth at which most groundwater samples were taken from observation wells, it was used when comparing the observed concentrations to simulated concentrations.

2.7 Best Management Practices for Se

In prior modeling work leading up to this thesis, BMPs examined for their potential impact on Se concentrations and return loads to the Arkansas River included reduced fertilizer application (loading), reduced Se concentration in canals, reduced irrigation application, enhanced riparian buffer zones, and a combination of these individual BMPs (Bailey, 2012). BMPs not considered by Bailey (2012a) include canal sealing to reduce seepage and rotational lease fallowing of irrigated land.

2.7.1 Enhanced Riparian Buffer Zones

Numerous publications detail the progress made in understanding the capability of riparian buffer zones to remediate solute concentrations in return flow to streams. However, in order to model enhanced riparian buffer zones, information is needed on uptake and volatilization rates of trees and grasses native to the LARV USR and on reaction rates of

heterotrophic chemical reduction. Two such native species in the region are salt grass (*Distichlis stricta*) and cottonwood (*Populus sargentii*) (Lindauer, 1983). Tamarix (*Tamarix chinensis*), a non-native species of tree has extensively invaded the riparian zones of the Arkansas River and its tributaries. An important factor to consider when planting more or different vegetation in the LARV is the highly saline environment. Lindauer (1983) observed that a change in more alkaline-salt tolerant species was taking place and already one-third of the floodplain contained tamarix.

Se uptake rates by plants native to the LARV were difficult to find in the literature. Se uptake by a native Colorado plant, Brassicaceae (*Stanleya pinnata*), was studied by Freeman et al. (2010) but did not result in first-order uptake rates. Volatilization rates were found for salt grass (*Distichlis spicata* L.) and aquatic plants. Wu and Huang (1991) found that 1-m^2 salt grass will volatilize 180 µg of Se per day; although salt grass accumulated less Se than any other salt-tolerant plant species in the Kesterson, CA area. The mean and standard deviation of Se volatilization rates by of salt grass grown in sand culture irrigated with a 2 mg/L Se treatment was 65 ± 14 µg g^{-1} day^{-1}.

Most plant species are termed nonaccumulators in that they can accumulate less than 25 µg Se/g dry weight from their environment and will die in increased Se concentrations (White et al., 2004). Plants that take up higher amounts of Se in to their plant tissues are called Se accumulators and those that take up around 1% or more of plant dry weight are hyperaccumulators (Pilon-Smits and Quinn, 2010). The plant species, Brassicaceae (*Stanleya pinnata*), studied by Freeman et al. (2010) is a hyperaccumlator of Se and was found in seleniferous soil west of Fort Collins, CO. Uptake of Se occurs preferentially over sulfate by Se-accumulators such as *A. bisulcatus*, rice, and Indian mustard (Terry, 2000). However, the

presence of sulfate in soils inhibits Se accumulation by some plants. On the other hand, the shoot accumulation of Se is affected only slightly by increasing salt levels for some plants while for others low levels of salinity can stimulate Se accumulation according to a in a study performed in Fresno, CA by Banuelos et al. (1996).

Pilon-Smits et al. (1999) analyzed twenty aquatic plants for SeO_4 and SeO_3 volatilization and accumulation. Several plants showed volatilization and accumulation rates per unit surface area that were comparable to the Indian mustard [*Brassic juncea* (L.)], which was at that time the best known terrestrial plant for Se phytoremediation. A key limitation with this study is that the performance of the plants in the presence of a saline environment is unknown. Salt grass was tested but did not perform well against the other plant species for volatilization rates. The ratio of shoot/root Se concentrations of SeO_3 for salt grass were the second highest of any of the other twenty plants. This shows that the salt grass can translocate fairly well. However, Se accumulation into plant tissue is not a sole solution to the Se problem in the LARV because the plants die and their biomass in then reincorporated into the surround soil. Plant biomass and total organic carbon in the soil affect rates of heterotrophic chemical reduction in the riparian corridor and the hyporheic zone. This is probably the major mechanism by which dissolved Se will be removed from groundwater that makes its way to the river.

2.7.2 Reduced Fertilizer Application

It is known that "U.S. farmers seem to apply excessive N (based on ex-post evaluations) even though N fertilizer increases the variance of yields" (Babcock, 1992). Other studies confirm that over-application of N fertilizer is common, exceeding the requirement the crop needs (Burwell et al., 1976; Scharf et al., 2005). Burwell et al. (2005) describes how excess N in the Missouri Valley loess near Treynor, Iowa can cause the pollution of streams when care is not taken to apply only the amount of fertilizer the crop needs. It is important to balance the

potential for reducing fertilizer application to lower nitrate accumulation with maintaining crop yields. In the LARV, farmers also tend to over-apply fertilizer so there is potential to lower application rates to fields to discourage the build-up of NO_3 in groundwater and streams.

2.7.3 Increased Irrigation Efficiency

Sprinkler (center-pivot), drip or trickle, and improved surface irrigation were considered in regard to their potential to achieve efficient irrigation application. Sprinkler irrigation is a method of irrigation application where water is distributed through a system of pipes and sprayed into the air through sprinklers so that small water drops travel to the ground (FAO, 2015). Drip or trickle irrigation "applies the water through small emitters to the soil surface, usually at or near the plant to be irrigated" (Hoffman et al., 2007). Surface, or flood, irrigation is where water is delivered to the field by a ditch, pipe, or other means and flows by gravity to water crops (Irrigation Techniques, 2014). Surge irrigation is a method of surface irrigation application where "flow is applied to furrows or borders intermittently during a single irrigation set to increase uniformity and infiltration" (Hoffman et al., 2007), and to decrease tailwater runoff.

Irrigation application efficiency is "the ratio of the volume of water which is beneficially used to the volume of irrigation water applied" (Hoffman et al., 2007). Examples of "beneficial uses include crop use, salt leaching, frost protection, crop cooling, and pesticide or fertilizer applications" while non-beneficial uses include "excessive deep percolation, surface runoff, weed ET, wind drift (in part), and spray evaporation" (Hoffman et al., 2007). As long as beneficial use is met by irrigation, increased application efficiency is generally advantageous because it reduces tailwater runoff and deep percolation below the root zone. Minimizing deep percolation is particularly desirable because it lowers excess flows that dissolve and mobilize undesirable solutes that accumulate in groundwater and make their way back to the stream system.

Irrigation application efficiency generally is substantially increased by the use of sprinkler and drip irrigation since water is applied at slower rates for longer periods of time. Sprinklers can be spaced uniformly and apply water at a lower rate than the soil infiltration rate; center-pivot systems can attain an efficiency of 75%-90% (Solomon, 2007). However, the use of sprinklers, like other methods of increasing application efficiency, in the LARV is problematic due to Colorado water rights. In order to use sprinklers, return flows to the Arkansas River are impacted and must be augmented in order to fulfill the Kansas-Colorado Arkansas River Compact. Sprinklers can also cause foliar damage to certain crops sensitive to saline water (Hoffman et al., 2007). Drip irrigation can be expensive for closely spaced crops and cannot be used for pasture and grains since they cannot be economically irrigated (Hoffman et al., 2007).

Potential irrigation application efficiencies of flood and surge irrigation are much lower than sprinkler irrigation. The mean application efficiency for surface irrigation events measured by Gates et al (2012) in the USR was about 72% in contrast to sprinkler irrigation events which had an average of about 77% in the USR; but, these values are likely biased on the high side due to more efficient irrigators participating in the study. These application efficiencies in the LARV are similar to those reported in Howell (2003) for graded furrow irrigation (65%) and center pivot sprinklers with spray heads without end guns (90%). The maximum attainable application efficiencies are 75% and 95%, respectively, according to Howell (2003). Maximum application efficiencies are achieved by minimizing deep percolation and tailwater runoff losses within the given constraints. Deep percolation occurs when more water infiltrates into the soil than can be stored for use by the crop. The excess water percolates down past the root zone into the deeper vadose zone and eventually to the water table. Tailwater runoff is water that runs off the end of the field in excess of what can be infiltrated into the soil (Gates et al., 2012). A minimum

amount of deep percolation is needed to leach salts from the soil profile that have accumulated due to extraction of pure water by ET. Not only is it possible to reduce the amount of application water to a field by changing the irrigation type but also by improving the management to reduce tailwater runoff and deep percolation. Better management is achieved by attending to the application of water as carefully as possible so little to no water is wasted and teaching all workers to do the same. Combinations of increased management and a change in irrigation type can be used to appropriately reduce in irrigation applications. Specifically for flood irrigation, surface irrigation efficiency can be improved by leveling the land, reducing the length of run, altering the set size to increase the rate of application, monitoring soil moisture to better schedule irrigation events and other methods.

2.7.4 Canal Sealing

Traditional methods to reduce seepage include reinforced or unreinforced concrete, fluid-applied membranes, and buried geomembranes, and compacted earth. Concrete has excellent durability (40-60 years) and 70% long-term effectives; the exposed geomembrane also has a durability of 20-40 years and a 90% effectiveness but is prone to weathering or mechanical damage including animal traffic, construction equipment, and vandalism; and the concrete with the geomembrane underliner has an effectiveness of about 95% and durability of 40-60 years since only the concrete cover has to be maintained (Swihart and Haynes, 1999). Materials needed for a compacted earth canal sealing method often tend not to be readily available (Swihart and Haynes, 1999).

Traditional canal lining methods have a high cost per area for construction and maintenance compared to the use of sealants to reduce seepage. Therefore, a granular form of linear anionic polyacrylamide (LA-PAM) was researched by the Desert Research Institute (DRI), CSU, and the U.S. Bureau of Reclamation for canal sealing (Susfalk et al., 2008). LA-PAM is a

less permanent and cheaper alternative for implementation in the LARV. It has been successfully applied using simple or automated fertilizer spreaders mounted on a boat that travels along the canal (Susfalk et al., 2008; Martin, 2014). A disadvantage is that the LA-PAM must be reapplied each year. The ecotoxicological perspective is being investigated through field experiments for LA-PAM where the highest concentrations lie in the canal sediments (Young et al., 2007). However, LA-PAM is not recommended for biologically sensitive canals. Results of the Susfalk et al. (2008) study included the estimation of reduced canal seepage rates for the Rocky Ford Highline Canal, Catlin Canal, and Ft. Lyon Canal within the USR and some other canals located in areas of the LARV outside the USR. The Rocky Ford Highline Canal had LA-PAM applied to 4 km (2.5 mi) in 2006, resulting in a 59% pretreatment seepage and between 56 to 115 days a 67% estimated seepage reduction. The Catlin Canal had two applications of LA-PAM applied to 3.9 km (2.4 mi) in 2006 and 2007 resulting in respective seepage reduction of 87% and 76%.

2.7.5 Lease Fallowing

In response to the loss of irrigation water in agriculture in the LARV due to farmers selling their water rights to cities and others (buy-and-dry), rotational lease fallowing has been studied as a means to allow farmers can make temporary water transfers while still retaining their irrigation water rights. Rotational fallowing could entail a group of agricultural water right holders to lease with a municipality a long-term agreement and rotate the fallowing of irrigated fields (Pritchett et al., 2008). The criteria used for the selection of fields for lease fallowing include that temporary water transfers must be approved by the State Engineer of Colorado and the same field can be fallowed for only three out of ten years as defined by C.R.S. 37-92-309 (2013).

Criteria used by Morway et al. (2013) in modeling lease-fallowing scenarios in the LARV are that applied irrigation is removed from fallowed fields and potential ET on the fields is changed from crops to a grass cover; fields fallowed do not receive pumped groundwater; and a crop hierarchy is followed that first fallows corn fields, then hayfields, and lastly alfalfa fields.

Lease-fallowing aids in reducing the return loads of Se to the Arkansas River since less water and fertilizer are applied on the landscape. This serves to decrease the amount of Se leached from surficial and weathered shale and lowers the inhibition of the chemical reduction of SeO_4 by the presence of NO_3 derived from fertilizer.

Chapter 3: Methods

3.1 Collection and Analysis of Stream Water and Sediment Samples

Representative cross sections along the Arkansas River and its tributaries were selected to sample for Se, U, and major dissolved ion concentrations and other water quality parameters. Measurement locations (Figure 3-1) were selected to represent the varying width of the riparian buffer zone and the changing geometric cross-sections along the river reach within the USR. Table 3-1 describes the locations in relation to the nearest road, nearest town, or landmark within the watershed, and the approximate width of the stream cross section. Photographs of each cross-section are provided in Appendix A.

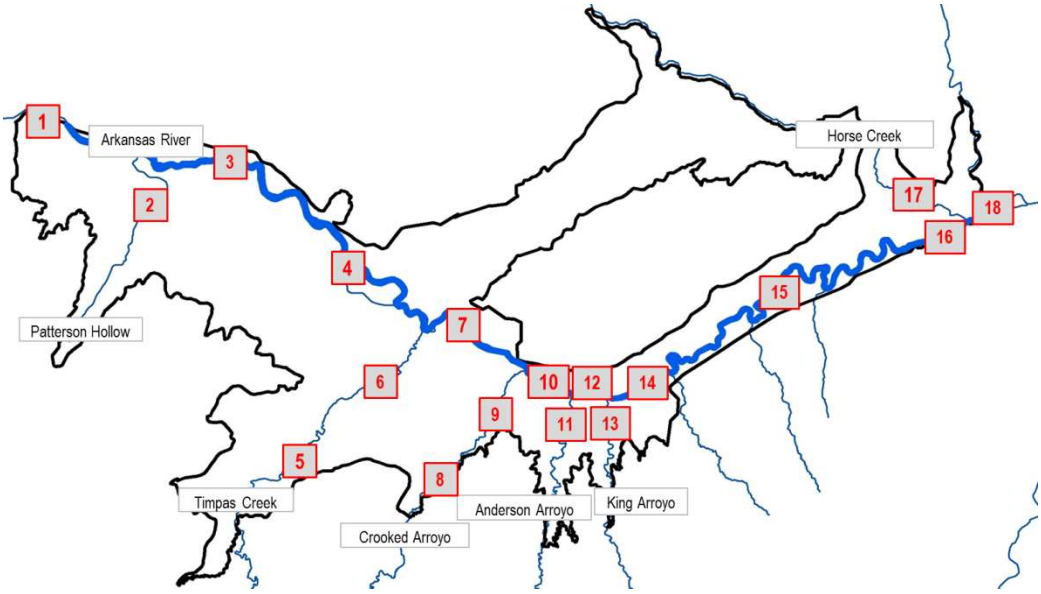

Figure 3-1. Stream measurement locations in the USR for March 2013-March 2014

Table 3-1. Locations and characteristics of measurement locations on the Arkansas River and its tributaries

Location	Near By Road	Description	Approximate Width (m)
1	Highway 207	Arkansas River north of Manzanola	62.5
2	CR* HH.5; CR 16	Patterson Hollow near Rocky Ford Canal	4.3
3	Highway 71	Arkansas River in between Manzanola and Rocky Ford	72.8
4	CR 21	Arkansas River north of Rocky Ford	75.3
5	Highway 10	Timpas Creek south of Rocky Ford	7.3
6	Highway 50	Timpas Creek just west of Swink	8.8
7	CR 24.5	Arkansas River at Swink	69.5
8	Highway 10	Crooked Arroyo between Swink and La Junta	4.6
9	Highway 50	Crooked Arroyo near the La Junta Walmart	4.0
10		Arkansas River between Crooked Arroyo and Anderson Arroyo approaching from south side	31.1
11	Highway 50	Anderson Creek north of Anderson St. in La Junta	3.0
12	Highway 109	Arkansas River at La Junta gauging station	54.3
14		Arkansas River downstream of King Arroyo	36.6
15		Arkansas River at Bent's Fort	44.5
16		Arkansas River near Jones Ditch	3.0
17	Highway 194	Horse Creek between Las Animas and La Junta	4.6
18	Highway 50	Arkansas River at the Las Animas gage station	36.6

***CR County Road**

3.1.1 Field Sampling and Measurements

Four trips were made from March 2013 to March 2014 to collect water samples, make in-situ measurements of water quality parameters, and collect sediment samples from selected stream location in the USR. Table 3-2 indicates when each measurement location was sampled for each trip. In March 2013, samples were taken and other measurements made at nine locations along the Arkansas River and at seven locations within five tributaries. In June, the number of Arkansas River sampling locations was increased to nine, and seven locations were sampled within tributaries.

Table 3-2. Locations measured for all trips during March 2013 – March 2014. An X indicates the location was sampled.

	Location																
Trips	1	**2**	3	4	**5**	**6**	7	**8**	**9**	10	**11**	12	14	15	16	**17**	18
Mar-13	X	**X**	X	X	**X**	**X**	X	**X**	**X**		**X**	X		X	X	**X**	X
Jun-13	X	**X**	X	X	**X**	**X**	X	**X**	**X**	X	**X**	X	X	X		**X**	X
Aug-13													X	X		**X**	X
Mar-14	X	**X**				**X**	X		**X**			X				**X**	X

Location 13 in King Arroyo was visited but never sampled from March 2013 to March 2014 due to inaccessibility of the channel location near the railroad and due to backed up water. The data for the majority of the flow and other water parameters for King Arroyo were provided by the La Junta Waste Water Treatment Plant and are provided in Appendix A (Table A-1 on page A-20). Location 16 was sampled only once, in March 2013, due to its location in exposed shale; however, the location was replaced by a more important location to inform the stream solute transport model for the region. Location 16 is in the Arkansas River downstream of the Jones Ditch diversion. Measurements were made there in March 2013; however, since it does not inform a location in the solute transport model, it was removed from further consideration. During the June 2013 and following sampling events, flow measurements were made at each location using an Acoustic Doppler Velocimeter (ADV). In August 2013, only four locations were measured due to low flows. In March 2014, water samples for chlorophyll a (Chla) were gathered at eight locations for use in estimating algae concentrations. The water Chla samples were collected by filtering the composite cross-sectional water sample, storing the filter in aluminum foil to prevent any further light exposure, and keeping the filters on ice. In April 2014, stream cross sections were topographically surveyed at the eight locations sampled and measured in March 2014. Surveys were not conducted at all locations due to limited time and funds. Rough sketches were made at all cross-sections during each sampling trip.

The procedure for data collection at each location included three stages: a safety check, cross-section establishment, and sampling and measurement. Safety checks are of primary concern and were conducted upon first arrival to a site and continued until the end. Key safety issues usually arise in selecting the parking location, accessing the site, and conducting sampling and measurement. Next, a cross-section was established at the site by determining the flow direction, avoiding sand bars, and aligning the cross-section perpendicular to the flow direction using a rope/tape measure stretched across the channel with 10-20 taped intervals. The intervals were created for the various measurements taken including the ADV which required 10-20 locations along the cross-section, sediment samples which were taken at four locations, water samples which were taken at eight locations, and the in-situ measurements which were taken at five to ten locations. Each interval composes an area slice of the water column which is used to calculate the flow through the stream cross-section. The number of intervals used at each measurement location varied with each trip as necessary adjustments to the collection of data were realized. After the first sampling trip, it was decided that more intervals were needed for the ADV measurements to increase the accuracy. Notes were made on field log sheets which included date, time, sketch of the cross-sectional profile, and a rough map showing approximate location of measurements within the cross-section (and example is given at the end of Appendix A). Photographs were taken of each site for the March 2013 sampling trip and sporadically during sampling trips thereafter. A staff gage was placed in the stream near the cross-section and read at the beginning and end of a site investigation to see if any measureable change in the water level had occurred. The total width of the cross-section was measured, noting the wet-channel and dry channel portions in the cross-sectional profile sketch. For example, at the

location on the Arkansas River near Manzanola and Highway 207 (Location 1) flow did not extend across the entire channel bed for all but high flow periods (Figure 3-2).

Figure 3-2. Location 1, a cross-section on the Arkansas River near Manzanola (facing downstream). Blue arrows indicate where sediment samples were collected (April 2014).

3.1.1.1 Bank and Sediment Sampling

Sediment samples were collected from the right and left banks and from the channel bed across the entire cross-section even in dry areas. Both bank samples and bed samples were collected for all trips in 2013. For the first trip in March 2013, only one sample was collected on each bank. The amount of sediment did not always fill at least half of the tube (a sufficient sample), so two samples were collected on each bank for the following two trips in 2013. The two samples were then combined equally by weight for analysis in the lab. A sufficiently large sample was needed to provide the laboratory enough for both sediment analysis and for a 20-g sediment portion for sorption analysis. In 2014, no bank sediment samples were gathered. The four bed samples collected during each of the four sample trips were averaged equally by weight to create a single composite bed sample for the entire cross-section for analysis in the lab.

Sediment samples were collected at variable depths using about 0.30-m (1-ft) long plastic sleeves with a 0.025-m (2-in) diameter. A photograph of the sleeves and caps is shown in Figure 3-3. First, during most of the sampling events, equal intervals were set up along the cross section

for collecting the four samples. Then a sleeve was pushed down into the soil at least 0.075 m (3 in). Usually, 0.15 m (6 in) to 0.23 m (9 in) of sediment was enclosed by the sleeve. Next, the sleeve was capped on the top to create a suction. Finally, the sleeve and sediment were pulled out of the stream bed and capped on the other end. The same procedure was used for the bank taken from the channel bank.

Figure 3-3. The sleeves and caps used for collecting bed and bank sediment samples in the Arkansas River and its tributaries.

After the sediment samples were collected and brought back to the laboratory, they were air dried for a week, pounded with a hammer, and passed through a #30 sieve. If two bank samples were collected from one side of the stream, they were averaged equally by weight to form one sample.

3.1.1.2 Unfiltered Water Sampling

One cross-section averaged sample of water and suspended sediment was gathered using the DH48 4.5 lb sediment sampler, or the "fish" (Figure 3-4A), following guidelines in Edwards and Glysson (1999). The fish was lowered slowly into the water and allowed to fill with water while the sampler was moved up and down at a steady rate across the water column being sampled. The DH48 sampler cannot sample the suspended sediment within 3.5 inches above the streambed. One cross-section-averaged sample contained six to ten (16 oz.) site-specific bottles of water and suspended sediment gathered at equally-spaced intervals across the stream cross-section. The bottles were all poured into a churn and mixed together (Figure 3-4B).

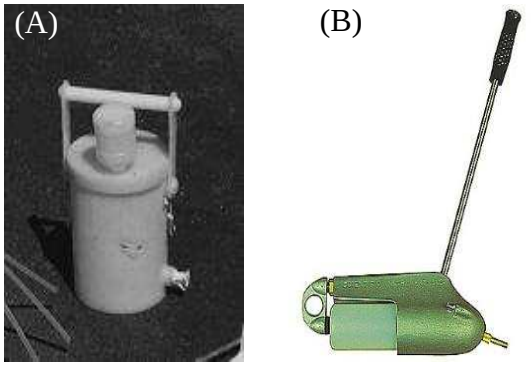

Figure 3-4. (A) A churn used for averaging the point suspended sediment samples into a cross-section averaged sample from http://pubs.usgs.gov/of/2000/ofr00-213/manual_eng/prepare.html#fig4. (B) DH48 sediment sampler used for shallow water and suspended sediment. Image from http://www.benmeadows.com/depth-integrated-sediment-samplers_36816467/

A peristaltic pump was used to pump water from the churn into two Nalgene sample bottles, one of 1-L Nalgene capacity and the other of 100-mL capacity, taking care not to induce air bubbles. The 1-L bottle was filled with extra sample for each site in case the other sample was lost or inadvertently opened throughout travel or shipping. Samples were immediately put on ice and ice new ice was purchased before traveling back to CSU. At CSU, samples were kept in a refrigerator to keep them cold until ready for shipment. Samplers were shipped to the appropriate laboratory with fresh ice and additional packaging if needed.

3.1.1.3 Filtered Water Sampling

Samples from the water column in the stream were pumped with a peristaltic pump though a disposable in-line 0.003-m^2 or 0.006-m^2 0.45-m capsule filter into 100-mL Nalgene bottles to analyze for total dissolved Se and SeO_3 at South Dakota Agricultural Laboratories (SDAL). Samples were pumped into a 250-mL bottle to analyze for N species and other solutes at Ward Laboratory in Nebraska, and into another 250-mL bottle to analyze for U at TestAmerica in Missouri. The SDAL and TestAmerica bottles had nitric acid preservative added to them. Example completed chain of custody forms and blank chain of custody forms are

shown at the end of Appendix A. Chain of custody forms detail the samples sent to the laboratory on a certain day and time. Once the samples were labeled, they were put on ice in a cooler with a temperature of less than 30°F. All 500-mL (~16 ounce) bottles used to collect the water and suspended sediment samples from the fish and the peristaltic pump were cleaned at each site by soaking them for 2 minutes each in a sequence of four buckets: a solution of approximately 0.0008-M HCl, a solution of approximately 0.008-M detergent, distilled water, and second bucket of distilled water. Each day all buckets were emptied and cleaned for the following day of data collection.

3.1.1.4 Chla Sampling

Chla samples were gathered using the previously described method of collecting cross-section averaged water and suspended sediment samples using the fish, but using five 500-mL bottles. The water and suspended sediment were pumped from the churn using the peristaltic pump through a disposable in-line 0.003 or 0.006-m^2 0.45-m capsule filter. The water was filtered again through a 25-mm diameter glass fiber filter and the filter was folded over on itself to protect the organic material and to limit light exposure. Immediately, samples were wrapped in aluminum foil and were put on ice in a cooler to keep them dark and at a temperature less than 30°F.

3.1.1.5 Flow Measurements with ADVs

A FlowTracker handheld ADV and wading rod (Figure 3-5) were used to measure velocity and stage to estimate volumetric flow rate through the stream cross-section. During each trip the number of stations within the cross-sections was increased to add accuracy. After the first sampling flow measurements were taken at as many sampling locations as possible at each cross-section with a minimum of 10 stations along very narrow cross sections and at 15 stations for wider cross-sections. If the flow depth was below 0.3 m (1 ft) at a station, only one

velocity measurement was taken with the ADV at that station. If the depth was greater than 0.3 m (1 ft) velocity measurements were made at 20%, 40%, and 60% of the flow depth from the stream bed). Flow rate, *Q*, through the cross section was determined by integrating the velocity and flow area data using the FlowTracker software as detailed in the *FlowTracker Handheld Technical Manual* (SonTek/YSI Inc., 2007). Values of flow *Q* were multiplied by averaged measured Se concentrations to estimate in-stream loading rates through the cross section.

Figure 3-5. (A) A close up of the FlowTracker (www.sontek.com) and (B) the FlowTracker and wading rod being used to measure flow.

3.1.1.6 In-Situ Measurements of Water Properties

Water temperature, pH, electrical conductivity (EC) (as specific conductance at 25 ^{o}C), dissolved oxygen (DO), and oxidation-reduction potential (ORP) were measured in-situ using a YSI 600 QS Multiparameter Sampling System (YSI Incorporated Yellow Springs, OH) (Figure 3-6) in the streams for all sampling trips and at all sampling locations. The location of each in-situ measurement coincided with the location where a water sample was taken using the DH-48 sampler. Therefore, approximately six to ten in-situ measurements were made at each stream sampling site with two sets collected by walking across the cross-section twice. These measurements were averaged along the cross section and over the two sets of data.

Figure 3-6. An YSI 600 QS Multiparmeter Sampling System used for in-situ measurements of water properties.

3.1.1.7 Surveys of Stream Cross-Section Geometry

The eight sites sampled during the March 2014 trip were surveyed using TOPCON GR-5 radio transceivers, a TOPCON TESLA data collector, a fiber survey rod, and a TOPCON tripod. One transceiver was used as the transmitter or base unit, and the other was used as the receiver or rover (Figure 3-7A and B). The base unit was on a tripod and the rover was on the survey rod. Four tributary locations (Patterson Hollow, Timpas Creek, Crooked Arroyo, and Horse Creek) and four river locations (Manzanola, Swink, La Junta, and Las Animas) were surveyed for cross-sectional geometry in April 2014. The locations along the Arkansas River surveyed were the most upstream point in Manzanola (Location 1) the most downstream point in Las Animas

(Location 18) and two intermediate points near Swink and near La Junta (Locations 7 and 12, respectively).

Figure 3-7. Surveying equipment including (A) the base unit (left) and rover (right) and (B) the Tesla data collector (http://www.gim-international.com/news/id6214-Juniper_to_Manufacture_Topcon_Tesla.html).

The procedure followed for survey data collection is outlined in the TOPCON MAGNET manual for the equipment and in Field 1.0 Help, the help manual. First, antennas were attached to the GR-5 units before they were turned on. The base unit was setup first at a secure location near each cross-section. The TESLA data collector was programmed with a new job for the Arkansas River surveying and was connected to a specific pre-programmed Bluetooth number. The base was then prepared to collect static data by entering required information such as the base station code, point number, and base height. Finally, the TESLA was disconnected from the base station. At the first cross section, the rover antenna was attached and the GS-5 was connected to the surveying rod. The rover then was turned on, the TESLA connections were switched to the rover, and the rover was then also connected to its respective Bluetooth. Next,

the rover was used to survey the first cross-section and then the remainder of the cross-sections by the same procedure. Codes were used to detail the location along each cross-section to indicate the left bank or right bank, when water was encountered, and if the location corresponded to a bankfull location (flat at one side and on the other side sloped created by a higher flow volume). The rod height also was measured for each cross-section. Data were saved at each point along the way. The accuracy of the survey was within 0.12 ft for the vertical RMS and 0.03 ft for the horizontal RMS since the base was collecting data for less than one hour at each cross-section (Inter-Fluve, Inc., 2014). Accuracy increases the longer the base station is allowed to collect static data. Due to technical difficulties on a cloudy day, the accuracies for all sites were twice as large as expected. A benchmark was used to establish a reference point at three bridge locations: Crooked Arroyo at Highway 50, Arkansas River at the La Junta off Highway 109, and the Arkansas River at Las Animas off Highway 50. The benchmark near Crooked Arroyo was Colorado Department of Highways Station 273 10.6 with an elevation of 4119.09 ft. The benchmark near the La Junta bridge was a National Geodetic Survey point F 432 from 1985. Finally, the benchmark on the Las Animas Bridge was a Colorado Department of Highways benchmark with unknown station number and an elevation of 3912.87 ft. One difficulty encountered during the survey was maintaining the line of site between the rover and base station due to the elevation change in creeks and the river which added the inaccuracy. It is much easier to conduct surveys in the winter after vegetation dies, since vegetation blocks satellites.

3.1.2 Lab Analysis Summary

A bottle of unfiltered water and a bottle of filtered water from each sampled field site were sent to South Dakota Agricultural Laboratories (SDAL), Brookings, SD for total dissolved Se and SeO_3 analysis for the last two sampling trips. For the first two sampling trips only a

filtered water sample was sent for analysis. The difference between the total dissolved Se and SeO_3 in a filtered sample was assumed to be the SeO_4. The total recoverable Se was determined from each unfiltered water sample. Dissolved Se samples were analyzed using SM3500-Se-C Fluorometric Method. SeO_3 samples were analyzed with a spectrometer. Samples analyzed at SDAL had a passing duplicate, relative percent error of ±10% and quality control readings were considered passing with values ±5% of the known value. Another filtered water sample from each site was sent to TestAmerica Laboratories, St. Louis, MO for analysis of total dissolved U using inductively coupled plasma-mass spectrometry. The method used for analysis was 200.8 in USEPA (1994). A final bottle of collected water from each site was sent to Ward Laboratories, Inc., Kearney, NE for analysis of dissolved nitrogen (N) species, including NH_4, NO_2, and NO_3; ortho-P; total P; Na; K; Ca; Mg; SO_4; Cl; CO_3; HCO_3; and B. The method used for analysis was also 200.8 in USEPA (1994), ICP method.

Lab preparation of sediment samples for analysis of sorbed and residual Se (elemental and organic) analysis was performed in the USDA-ARS laboratory in Fort Collins, Colorado before sediment samples were sent off to SDAL for testing using method AOAC 996.16 (adapted). Sediment samples were analyzed to determine sorbed Se by grinding the soil, adding a K_2HPO_4 solution to drive off the sorbed Se, shaking, centrifuging, and extracting the supernatant solution as described in Bailey (2012). The only difference between the method used and that described in Bailey was the amount of soil shaken (approximately 20 g) and the amount of solution added (40 mL). Suspended sediment, bed sediment, and the supernatant solution extracted from sediment samples were sent to SDAL for analysis of total dissolved Se and dissolved SeO_3. The amount of total (tot.) sorbed Se + solid Se, sorbed SeO_4, sorbed SeO_3, and residual Se concentrations were calculated via the following equations:

$$Tot.Sorbed\ Se + Solid\ Se = \frac{Tot.Rec.Se\ (lab\ result)\left(\frac{\mu g}{L}\right)}{1000\ \frac{mL}{L}} x \frac{100\ mL\ of\ 0.1\ M\ K_2HPO_4\ *}{Dry\ Mass\ of\ Sample\ (g)}$$

$$Sorbed\ SeO_3 = \frac{SeO_3\ (lab\ result)\left(\frac{\mu g}{L}\right)}{1000\ \frac{mL}{L}} x \frac{100\ mL\ of\ 0.1\ M\ K_2HPO_4\ *}{Dry\ Mass\ of\ Sample\ (g)}$$

$$Sorbed\ SeO_4 = Total\ Sorbed\ Se + Solid\ Se\ \left(\frac{\mu g}{g}\right) - Sorbed\ SeO_3\left(\frac{\mu g}{g}\right)$$

$$Est.Precipitated\ \&\ Organic\ Se$$

$$= Soil, Total\ Se\ (lab\ result)\left(\frac{\mu g}{g}\right) - Total\ Sorbed + Solid\ Se\left(\frac{\mu g}{g}\right)$$

$$\%\ Precipitated + Organic\ Se = \frac{Est.Precipitated + Organic\ Se\left(\frac{\mu g}{g}\right)}{Soil, Total\ Se\ \left(\frac{\mu g}{g}\right)}$$

$$\%\ Sorbed\ Se = \frac{Total\ Sorbed + Solid\ Se\left(\frac{\mu g}{g}\right)}{Soil, Total\ Se\ \left(\frac{\mu g}{g}\right)}$$

* The amount of 0.1 M K_2HPO_4 varies based on the dry mass of the sample. Either 100 mL was used or 25 mL was used depending on the dry mass of the sample. If close to 5 g of sample was used then 25 mL of0.1 M K_2HPO_4 was used. If close to 20 g of sample was used then 100 mL of 0.1 M K_2HPO_4 was used.

The results from all laboratories were entered into a database and sorted to describe the speciation for Se and N in water and sediments at the sample locations within the Arkansas River and its tributaries, as summarized in Chapter 4. Summary data tables were created for all trips and were sorted based on location in the tributaries or in the Arkansas River and are shown in part in Appendix B.

3.2 Conceptual Model for Se Cycling in Surface Water

To develop the Se surface water conceptual model an extensive literature review was performed on Se cycling in surface water. The initial framework for the conceptual model was

based off the N cycle described in the Soil and Water Assessment Tool Theoretical Documentation Version 2009 (Neitsch, 2011) originally provided in the Enhanced Stream Water Quality Model, QUAL2E. Next, a review was conducted on the various processes that dictate the interaction between algae and aquatic plants and the cycling of all Se species. All significant processes were included in the conceptual model presented in Section 4.2.1.

The model used to encode the cycling of Se was the One-Dimensional Transport with Inflow and Storage (OTIS) a surface water chemical transport model. OTIS was chosen to simulate the dynamic reactive transport of Se, N, and other species in the Arkansas River and its tributaries. The OTIS model was originally developed by the United States Geological Survey (Runkel, 1998). OTIS-MULTI, a modified version of OTIS, can better analyze a larger river network and multiple interacting chemical solutes.

3.3 Groundwater Modeling: Description of BMPs and Implementation in MODLFOW-UZF and UZF-RT3D

The calibrated and tested models described in Section 2.6, MODFLOW-UZF and UZF-RT3D were used to rank remediation strategies in the USR of the LARV by testing various BMPs. The five previously introduced BMPs in Section 2.7 are reduced fertilizer loading (RF), enhanced riparian buffer zone along the Arkansas River and its tributaries (ERB), partial sealing of earthen canals (CS), fallowing of cultivated land (LF), and reduced irrigation (RI). These BMPs were assumed to be applied over the entire study region. The effect of decreasing the amount of irrigation water in the system as in the case for reduced irrigation, canal sealing, and lease fallowing will cause a decrease in the mass input of SeO_4 via canal seepage and irrigation water application, a decrease in the local and regional groundwater gradient which will cause the rate of groundwater discharge of Se mass loading to the river network to decrease, and the amount of O_2 and NO_3 entering the aquifer likely resulting in less Se oxidation from marine

shale and enhanced chemical reduction of SeO_4. The effect of decreasing the hydraulic gradient also will lengthen the amount of time it takes for groundwater to travel to the river, contributing to one long time frame expected for BMP implementation to fully affect Se mass loading (Bailey et al., 2015).

Reduced fertilizer and enhanced riparian buffer zones affect the reactions taking place in the system as well as crop and plant uptake and volatilization. Reduced fertilizer will decrease the mass and concentration of NO_3 in the soil and groundwater, which will decrease the amount of SeO_4 removed from marine shale, and increase the amount of SeO_4 to be reduced to SeO_3, a more sorbent species. Enhanced riparian buffer zones increase the denitrification of NO_3; and provide more organic carbon, thereby, increasing the reduction of SeO_4 in route to the river (Bailey et al., 2015).

The simulation time must be long enough to account for the long travel time of groundwater from the point of application (cultivated fields) to points of aquifer-stream interaction as estimated as 10-20 years. The 38 year simulation period is composed of repeating the 9.5-yr groundwater flow simulation period described in Morway et al. (2013) four times, with conditions at the end of each 9.5-yr period used as the initial conditions for the next period.

Research was performed to better understand processes such as plant uptake, volatilization, and rates of chemical reduction for modeling riparian buffer zones, irrigation methods for increased irrigation efficiency, methods of canal sealing, and criteria for lease fallowing a field. A more detailed description of each BMP will follow as well as how it was modeled in RT3D-AG.

In the LARV, farmers are known to often over-apply anhydrous ammonia fertilizer and manure. The fertilizer is typically applied twice each season with 40% of the application

occurring two weeks before planting, and the remaining 60% applied six weeks after planting (Bailey et al., 2015). The amount of fertilizer applied in the simulation is based on historical data on crop type from the Farm Service Agency in Rocky Ford for 2006-2009. The chemical reaction rate and base crop parameter values used in the UZF-RT3D model are the same used in the calibrated 2006-2009 model from Baily et al. (2014). The fertilizer application rate was dependent of the type of fertilizer and crop type. This information was obtained from Michael Bartolo at the Colorado State University Arkansas Valley Research Center (AVRC) near Rocky Ford as described in Bailey (2012a). The plant growth impacts of varying N application rates were not fully analyzed in this study. The BMP scenarios tested were a 10% (RF10), 20% (RF20) and 30% (RF30) reduction of N fertilizer across all irrigated fields in the USR.

In order to model enhanced riparian buffer zones, the base reaction rates for denitrification, SeO_4 reduction, SeO_3 reduction, and volatilization for each riparian cell were increased by a specified daily rate. The lumped reaction rates were not increased more than 40% because of uncertainty in vegetative growth in the riparian buffer zone and organic carbon enhancement. The nature of enhancement might include increasing the riparian area and/or altering the mix of native trees and/or grasses along of the Arkansas River and its tributaries to create a more Se immobilizing habitat. The scenarios tested included enhanced riparian buffer low (ERB low), medium (ERB med), and high (ERB high) using constant reduction in reaction rates for each scenario.

For the canal sealing BMP a granular linear anionic polyacrylamide was assumed to be applied to the flow along the entire length of all canals in the study region using the methods described in Susfalk et al. (2008). The parameter in the model adjusted for each canal sealing

BMP scenario was the canal conductance as discussed in Morway et al. (2013). The BMP scenarios tested were 40% (CS40), 60% (CS60), and 80% (CS80) canal seepage reduction.

Lease fallowing also known as fallowing-leasing allows the temporary transfer of water from agricultural water right owners to the municipality. There are several assumed criteria for the selection of fields that could be leased fallowed. These criteria include that temporary water transfers must be approved by the State Engineer, that each ten-year agreement cannot be approved for subsequent ten year periods (C.R.S. 37-92-309, 2013), and that a given field can only be fallowed three years out of a ten-year period. Lease fallowing benefits the farmers so that the water right is not lost permanently. In regards to modeling these scenarios, additional criteria were necessary. Fields selected for lease fallowing receive no irrigation water and were selected with priority given to fields planted to corn, hay, and alfalfa in that order (Morway et al., 2013). When a field was fallowed the potential ET rates were modified in one model to represent those for a naturally-vegetated area. The BMP lease-fallow scenarios were derived to reduce total irrigated land by 5% (LF5), 15% (LF15), and 25% (LF25) from baseline conditions for a contiguous three-year period out of ten.

Farmers in the LARV not only tend to over-apply fertilizer but tend to over-apply water as well. The over-application of water often leads to waterlogging, salinity, and associated reduced crop yields. To reduce irrigation, farmers can better manage their surface water application and/or can change their irrigation technology, for example, from flood irrigation to surge or sprinkler. The method of reducing the amount of water applied also is detailed in Morway et al. (2013). For each reduced irrigation BMP scenario, the irrigation water applied was reduced by 10% (RI10), 20% (RI20), or 30% (RI30).

Each type of BMP or combination of BMPs was defined for three levels of intensity: basic, intermediate, and aggressive as summarized in Table 3-3. Lease fallowing and reduced irrigation scenarios both modified the same input file so lease fallowing and reduced irrigation were not be modeled as part of the same scenario as detailed by the last four rows in Table 4. Combined scenarios consisting of three BMPs include irrigation reduction (or lease fallowing), canal sealing, and fertilizer reduction; whereas, for the four-BMP scenarios, included enhanced riparian buffer zones BMPs as well.

Table 3-3. Five individual BMP scenarios and four sets of combined BMPs simulated at three different levels of intensity.

BMPs	Basic	Intermediate	Aggressive
Reduced Fertilizer (RF)	10% reduction	20% reduction	30% reduction
Enhanced Riparian Buffer (ERB)	low	Med	high
Canal Sealing (CS)	40% reduction	60% reduction	80% reduction
Leasing Fallowing (LF)	5% more	15% more	25% more
Reduced Irrigation (RI)	10% reduction	20% reduction	30% reduction
3 LF Combination Scenarios	10% RF, 40% CS, 5% LF	20% RF, 60% CS, 15% LF	30% RF, 80% CS, 25% LF
3 RI Combination Scenarios	10% RF, 40% CS, 10% RI	20% RF, 60% CS, 20% RI	30% RF, 80% CS, 30% RI
4 LF Combination Scenarios	10% RF, low ERB, 40% CS, 5% LF	20% RF, med ERB, 60% CS, 15% LF	30% RF, high ERB, 80% CS, 25% LF
4 RI Combination Scenarios	10% RF, low ERB, 40% CS, 10% RI	20% RF, med ERB, 60% CS, 20% RI	30% RF, high ERB, 80% CS, 30% RI

Each simulation was run for 38 years and the results for each scenario were compared to the Baseline. For all BMPs the decrease in groundwater Se concentrations and decrease of mass loadings to the Arkansas River and its tributaries were calculated. Future work currently is in

progress linking a surface water model to the groundwater model so that resulting in-steam concentrations can be predicted.

Chapter 4 presents the results of the data collection, Se surface water cycling equations, and groundwater modeling of BMPs in the Lower Arkansas River. The statistical analysis of the various species of Se and NO_3 is discussed as well as the analysis of the data informing the partitioning of residual, sorbed, and dissolved Se species in the soil and water. The Se surface water reaction equations are described. Finally, the modeled BMP scenarios results are shown and described for predicting groundwater concentrations and mass loading to the Arkansas River.

Chapter 4: Results and Discussion

4.1 Analysis of Stream Water and Sediment Samples

4.1.1 Residual, Sorbed and Dissolved Se in Stream Banks and Sediments

Laboratory results from SDAL were analyzed for total recoverable Se, SeO_3, and dissolved Se. Full data tables showing the results of the determination of residual (precipitated and organic) and sorbed Se concentrations sorted into river land tributary locations and by sampling trip are presented in Appendix B (Table B-3 and B-4). A summary of the average concentrations for the river and tributaries, sorted for each sampling trip, is shown in Table 4-1.

Table 4-1. Averages of residual (precipitated and organic) and sorbed Se concentrations in the stream banks and bed sediments of the Arkansas River and the tributaries sorted for each sampling trip.

Stream	Sampling Trip	Location within the Cross-Section	Total Recoverable Se (µg/L)	Selenite (µg/L)	Se, Dissolved (µg/L)	Total Sorbed Se + Solid Se (µg/g)	Sorbed Selenite (µg/g)	Sorbed Selenate (µg/g)	Non-Sorbed Se (µg/g)	Soil, Total Se (µg/g)	Est. of Precipitated and Org. Se (µg/g)	% Precipitated and Org. Se	% Sorbed Se
River	Trip 1	Bed	11.16	6.80	11.59	0.06	0.03	0.02	0.06	0.28	0.23	79%	21%
	Trip 2		9.74	7.23		0.05	0.04	0.01		0.28	0.23	82%	18%
	Trip 3		14.30	4.76		0.07	0.02	0.05		0.26	0.19	72%	28%
	Trip 4		8.94	1.97		0.04	0.01	0.03		0.23	0.18	80%	20%
	Trip 1	Banks	44.05	20.72	40.85	0.22	0.10	0.12	0.20	1.03	0.81	78%	22%
	Trip 2		33.90	19.66		0.17	0.10	0.08		0.89	0.72	80%	20%
	Trip 3		44.47	17.95		0.22	0.09	0.13		1.01	0.79	78%	22%
	Trip 1	Stie Specific Bed	12.43	6.96	11.59	0.06	0.03	0.03	0.06	0.30	0.24	79%	21%
	Trip 2		9.98	7.58		0.05	0.04	0.01		0.26	0.21	81%	19%
Trib	Trip 1	Bed	58.58	34.90		0.29	0.17	0.12		1.23	0.94	76%	24%
	Trip 2		107.72	78.46		0.54	0.39	0.15		1.66	1.13	68%	32%
	Trip 3		10.40	3.06		0.05	0.02	0.04		0.29	0.24	82%	18%
	Trip 4		71.25	43.90		0.36	0.22	0.14		1.24	0.88	72%	28%
	Trip 1	Banks	69.14	37.59		0.35	0.19	0.16		1.60	1.26	80%	20%
	Trip 2		61.43	34.17		0.31	0.17	0.14		1.82	1.51	82%	18%
	Trip 3		28.50	8.96		0.14	0.04	0.10		0.62	0.48	77%	23%

The color scheme used in Table 4-1 shows red as the highest value in a column and blue as the lowest value. The concentration of total recoverable Se, SeO_3, and dissolved Se in µg/L (column

headings shaded in green) were determined by SDAL. The values in μg/g (column headings shaded in blue) for total sorbed Se + solid Se, sorbed SeO_3, and sorbed SeO_4 where calculated from the lab results. These calculated values were determined by using the amount of sediment shaken with the K_2HPO_4 solution and the amount of K_2HPO_4 solution, and were converted to units of μg/g as described in Section 3.1.3. Comparing the Arkansas River average data for bed sediment samples for any sampling trip to the tributary average data for bed sediments reveals that the amount of Se is much higher in the tributaries bed sediments except for Trip 3, which was an incomplete sampling. Also, the data reveal higher Se concentrations in the bank samples from the Arkansas River than in the bed sediments. Total recoverable Se concentrations in river bank samples are three to four times higher than those in the river bed sediment samples, perhaps indicating the effect of flows on downstream transport, in contrast to the outer banks where intermittent flows permit accumulation of sorbed and residual Se. Higher concentrations of Se in stream banks compared to bed sediments is not as clear in the tributaries on average. The tributary average bank sample concentrations of total recoverable Se vary from 28.5 μg/L for Trip 3 in August to 69.4 μg/L for Trip 1 in March. Average concentrations of total recoverable Se in tributary bed samples varies from 10.4 μg/L for Trip 3 in August to 107.7 μg/L for Trip 2 in June. It is noteworthy that Trip 3 resulted in the lowest Se concentrations for both the bank and bed samples from the tributaries. However, it is important to note that during Trip 1 in March 2013 and Trip 2 in June 2013 there were a total of 48 and 58 samples collected, respectively, compared to Trip 3 in August 2013 and Trip 4 in March 2014 where only 12 and 8 samples, respectively, were collected for analysis. This makes statistically significant differences impossible to establish. Site specific bed sediment samples were taken only for one location for Trip 1 and Trip 2. The analysis for dissolved Se was only performed for the sample

from one site for Trip 1 to test if dissolved Se was a large enough fraction that it warranted analysis in the future. However, there was only a 6% difference between the Total Recoverable Se and the Dissolved Se. Since the laboratory quality control error average is about 5%, a 6% difference is only 1% over the laboratory quality control error. Therefore, further analysis for Total Recoverable Se compared to Dissolved Se was not needed.

No conclusive seasonal trends could be detected in the bank and bed sediment data from the Arkansas River. The variability in the sample data for the tributaries is much larger. The differences for each trip for the tributary data are the following from Trip 1 to Trip 3 respectively: 4%, 14%, and 5%. No bank sediments were collected during Trip 4.

Figures 4-1 and 4-2 illustrate the distribution of concentrations of dissolved Se, SeO_3, and SeO_4 in the water column and of concentrations of sorbed SeO_3, sorbed SeO_4, and precipitated/organic Se in the bank and bed sediments of the Arkansas River and the tributaries for Trip 2. Similar diagrams for all sampling trips are presented in the Appendix B. Figures 4-1 and 4-2 show concentration percentages that do not vary much between the Arkansas River and the tributaries for the Se species in the water and in the bank sediments. However, a marked difference exists in the estimated percentages for precipitated and organic Se concentrations in the bed sediments. The percentage point differences between precipitated and organic Se concentrations in the river and those in the tributaries for Trips 1 through 4 are 4, 15, 10, and 8, respectively.

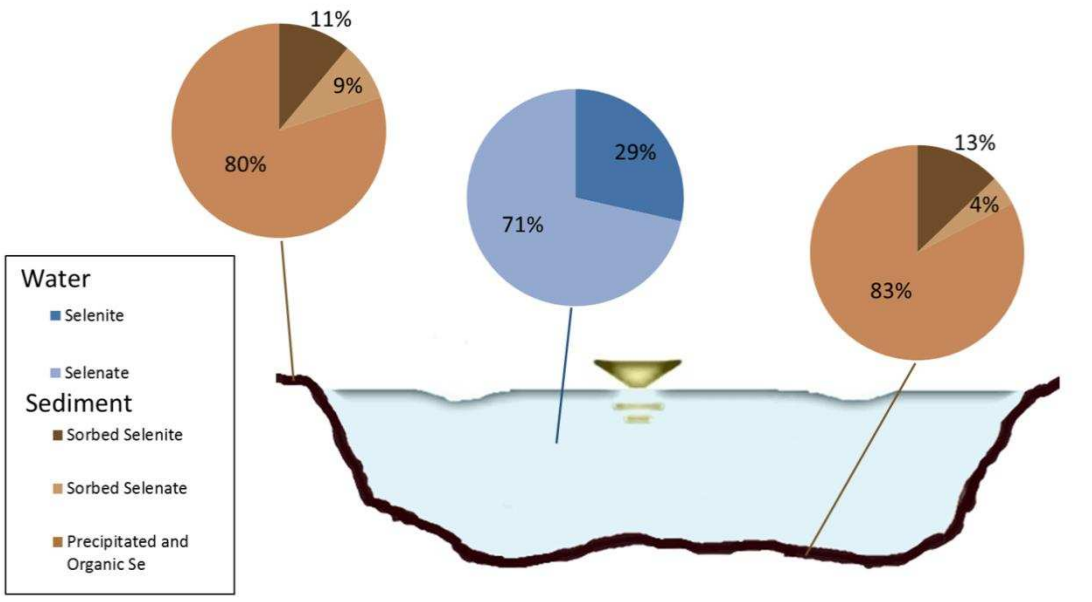

Figure 4-1. Percentages of dissolved Se species in the water and of sorbed Se species compared to residual Se in the bank and bed sediments for samples from the Arkansas River for Trip 2.

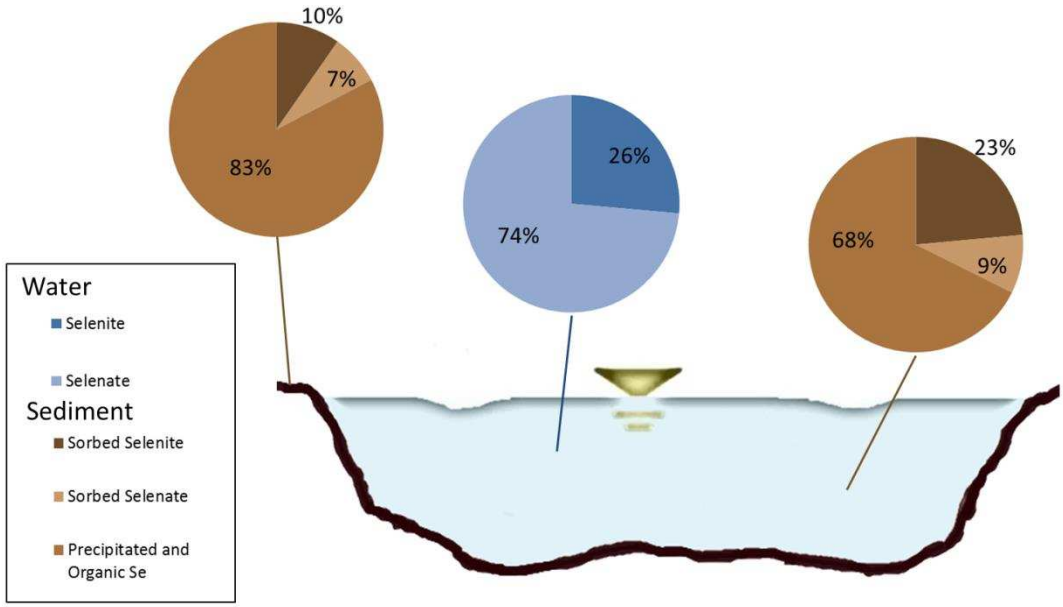

Figure 4-2. Percentages of dissolved Se species in the water and of sorbed Se species compared to residual Se in the bank and bed sediments for samples from the tributaries for Trip 2.

Samples for total recoverable Se were collected only during the last two sampling trips. Thus, the amount of suspended Se and Se sorbed to sediments in the water column could be determined for these sampling trips and are presented in Table B-1. Some of the total recoverable Se concentrations are lower than the total Se (which is the dissolved Se since the samples were filtered in the field), especially for the tributaries. Considering the estimated error in the laboratory flourometric and ICP methods of analysis, discussed in Chapter 3, the difference between these two results is very small. Overall, the differences between the total recoverable Se and total Se indicate that the suspended and sediment-sorbed Se in the water column is negligible.

4.1.2 Database Compilation of Unfiltered and Filtered Water Measurements

Upon returning from the field to CSU, data collected with the ADV, the YSI probe, and all notes on the field sheets were downloaded and/or entered into the project database. All water samples were shipped to the appropriate laboratory for analysis. Reports of laboratory analysis were entered into the project database.

4.1.3 Chla Results

Only preliminary results were attained for the Chla water samples and are not reported here. Further details can be found in Section 5.1.

4.1.4 Flow Measurements with ADVs

At each cross-section for Trips 2 through 4, the flow rate was measured with a FlowTracker Handheld ADV, especially at locations where a permanent gauging station was not near enough to approximate flow at the cross-section. Gauging stations are operated either by the USGS or by the Colorado Division of Water Resources (CDWR). ADV measurements were downloaded after the field team returned to the office and were processed to calculate flow rate, Q, and Q values were compared to the gauging station measurement if applicable. Table 4-1b

provides a comparison of *Q* measured with the ADV and that measured at a nearby gauging station. The instrument estimated uncertainty shown in column 6 of Table 4-1b was calculated using the FlowTracker software as explained in Section 3.1.1.5. The percent difference in column 8 is that between the *Q* measured with the ADV (column 5) and that measured at the nearby gauging stations (column 7). Generally, the percent difference is higher for tributary sites compared to sites in the Arkansas River, except for Site No. 6 on Timpas Creek with an 8% difference. The average percent difference for the Arkansas River locations is 10%, and the average percent difference for all the tributary locations is about 37%. Percent differences were largest for low flow rates which are more difficult to measure accurately. All gage locations were within 200 m of sample locations where ADV measurements were made, with gage locations usually residing upstream of sample locations. If a sample location was chosen upstream of a gauging location, then the separation distance was between 100 m and 200 m.

Table 4-2. Summary of ADV measurements of *Q* compared to *Q* measured at nearby gauging stations.

Site No.	Location	Meas-ured Top Width (ft)	Aver-age Measu red Flow Depth (ft)	*Q* (cfs)	Instru ment Esti-mated Uncert-ainty	*Q* Measured at Nearby Gauging Station (cfs), Gauging Station Name	Percent Difference
1	Arkansas River North of Manzanola off of Hwy 207	224	1.36	598	±10%		
3	Arkansas River Between Manzanola and Rocky Ford (Hwy 71)	235	0.93	479	±12%		
4	Arkansas River North of Rocky Ford off County Road 21	192	1.84	714	±9%	699, Arkansas River Near Rocky Ford	-2
6	Downstream on Timpas Creek off of Hwy 50	31	2.09	40	±5%	44, Timpas Creek at Mouth Near Swink, CO	8
7	Arkansas River North of Swink off of County Road 24.5	160	1.90	687	±5%		
8	Downstream on Crooked Arroyo off of Hwy 50	9	1.66	8	±2%		
9	Upstream on Crooked Arroyo off of Hwy 10	11	1.02	13	±7%	20.9, Crooked Arroyo near Swink, Co	37
10	Arkansas River In Between Crooked and Anderson	112	2.15	602	±5%		
12	Arkansas River in La Junta off of Hwy 109	173	1.34	432	±11%	479, Arkansas River at La Junta	10
14	Arkansas River Downstream of King Arroyo	120	2.01	560	±15%		
15	Arkansas River at Bent's Fort	153	1.13	343	±7%		
16	Arkansas River just Upstream of Horse Creek						
17	Horse Creek	16	0.64	0.90	±58%	2.55, Horse Creek at Highway 194	65
18	Arkansas River at Las Animas off of Hwy 50	119	2.23	615	±9%	786, Arkansas River at Las Animas	22

Note: Patterson Hollow and Anderson Arroyo had too low a flows to measure, data were not recovered from Location 5, and King Arroyo was not accessible.

4.1.5 Pearson Correlation of Bank and Bed Sediment Concentrations, Stream Water Concentrations, and In-Situ Measurements of Water Properties

A preliminary statistical analysis was performed to examine the correlation among measured variables using only the data from 2013 (not including Trip 4) for the Arkansas River and the tributaries. Variables examined are concentrations of Na, K, Ca, Mg, Cl, B, U, SO_4-S,

HCO_3, CO_3, $CaCO_3$, $CaCO_3$, NH_4-N, NO_2-N, NO_3-N, ortho-phosphorus and total phosphorus (P); total Se (fluorometric method), total Se (ICP method), dissolved SeO_3, total recoverable Se (fluorometric); sorbed SeO_3; sorbed SeO_4; estimate of precipitated and organic Se, pH (measured in field with YSI), ORP (YSI), DO (YSI), EC (YSI), pH (measured at Ward Laboratories), Na adsorption ratio (SAR) (Ward), adjusted SAR (Ward), TDS (Ward), and EC (Ward). A conservative sample size of N=26 and a two-tailed test with significance level of p = 0.05 (0.025 testing significance in both directions) was employed. The associated statistically significant correlation coefficient value is 0.51. Table 4-3 summarizes the resulting calculated values of Pearson correlation (Pearson's Correlation Coefficient r, n.d.) for Se concentrations for both the Arkansas River and the tributary correlation data performed in Microsoft Excel. Statistically significant moderate correlation values (0.51 – 0.69) are highlighted in light green. Values indicating strong correlation (0.70 – 1.00) are highlighted in dark green.

Table 4-3. Pearson correlation table for Se concentrations in samples taken from both the Arkansas River and the tributaries.

	Total Dissolved Se (Fluorometric) (µg/L)	Dissolved SeO_3 (Fluorometric) (µg/L)	Sorbed SeO_3 (bed sediment) (µg/g)	Sorbed SeO_3 (bank sediment (avg)) (µg/g)	Sorbed SeO_4 (bed sediment) (µg/g)
Total Dissolved Se (Fluorometric) (µg/L)	-				
Dissolved SeO_3 (Fluorometric) (µg/L)	-0.18	-			
Sorbed SeO_3 (bed sediment) (µg/g)	0.17	0.09	-		
Sorbed SeO_3 (bank sediment (avg)) (µg/g)	-0.26	-0.10	0.35	-	
Sorbed SeO_4 (bed sediment) (µg/g)	0.39	-0.15	0.83	0.31	-
Sorbed SeO_4 (bank sediment (avg)) (µg/g)	0.15	-0.21	0.15	0.45	0.34
Estimated Precipitated and Organic Se (bed sediment) (µg/g)	0.26	0.03	0.90	0.37	0.90
Estimate Precipitated and Organic Se (bank sediment (avg)) (µg/g)	0.01	0.19	0.66	0.55	0.51

The results suggest some statistically significant strong relationships: in stream bed sediment sorbed SeO_3 (µg/g) is strongly correlated (0.83) to sorbed SeO_4 (µg/g) and (0.90) to precipitated and organic Se (µg/g); and sorbed SeO_4 (µg/g) in stream bed sediment is strongly correlated (0.90) to precipitated and organic Se (µg/g) in bed sediment. Also, sorbed SeO_3 (µg/g) in the bed and bank sediments, along with sorbed SeO_4 (µg/g) in the bed sediment, are weakly to moderately correlated with precipitated and organic Se (µg/g) in the bank sediment.

The sorbed SeO_3 concentration in the bed strongly correlates with the sorbed SeO_4 concentration in the bed since the laboratory-determined SeO_3 concentration was used to calculate the amount of SeO_4 by difference from the laboratory-determined total Se concentration. In other words, since total dissolved Se in the sample effluent was assumed to be composed primarily of SeO_4 and SeO_3, when the total Se concentration is relatively high, the

concentrations of SeO_4 and SeO_3 also are proportionally high. A possible reason for the strong correlation between the sorbed SeO_3 and SeO_4 in the bed sediments with the estimate of precipitated and organic Se in the bed is that bacteria use dissimilatory reduction of both SeO_4 and SeO_3 to produce elemental Se (Herbel et al., 2003; Steinberg and Oremland, 1990).

For nutrients and Se concentrations in the stream samples, significant statistical correlations were found between the concentration of NH_4-N (mg/L) and the concentration of NO_2-N (mg/L) in the water column with a correlation coefficient of 0.81; and between the concentration of NO_2-N (mg/L) and total dissolved Se concentration (µg/L) using the fluorometric method in the water column with a correlation coefficient of 0.71 (Table 4-4). More data are needed to substantiate these relationships. However, the results seem logical since NH_4 is oxidized to NO_2 in the nitrogen cycle and NO_3, which reduces to NO_2, is related to total dissolved Se due to the oxidation of selenide from surficial and subsurface shale by autotrophic reduction of NO_3 (Bailey et al 2012).

Table 4-4. Pearson correlation table for nutrient and Se concentrations in samples taken from both the Arkansas River and the tributaries.

	Ammonium, NH_4-N (WARD) (mg/L)	Nitrite, NO_2-N (WARD) (mg/L)	Nitrate NO_3-N (WARD) (mg/L)
Nitrite, NO_2-N (WARD) (mg/L)	0.81	-	
Nitrate NO3-N (WARD) (mg/L)	0.25	0.40	-
Ortho Phosphorus, P (WARD) (mg/L)	0.56	0.64	0.07
Total Phosphorus, P (WARD) (mg/L)	0.51	0.44	-0.27
Total Dissolved Selenium, Se (Fluorometric) (µg/L)	-0.06	0.14	0.71

When only analyzing concentrations derived from the Arkansas River samples alone, the only strong statistical correlation discovered is 0.80 between the sorbed SeO_4 in the bank sediments of the river and the estimate of precipitated and organic Se in the bank sediment average (µg/g) (Table 4-5).

Table 4-5. Pearson correlation table for Se concentrations in samples taken from only the Arkansas River.

	Sorbed Selenite, SeO_3 (bed sediment) (µg/g)	Sorbed Selenite, SeO_3 (bank sediment (avg)) (µg/g)	Sorbed Selenate, SeO_4 (bed sediment) (µg/g)	Sorbed Selenate, SeO_4 (bank sediment (avg)) (µg/g)
Sorbed SeO_3 (bank sediment (avg)) (µg/g)	0.30	-		
Sorbed SeO_4 (bed sediment) (µg/g)	-0.37	-0.54	-	
Sorbed SeO_4 (bank sediment (avg)) (µg/g)	-0.24	0.37	0.24	-
Estimate of Precipitated and Organic Se (bed sediment) (µg/g)	0.19	0.10	-0.17	-0.32
Estimate of Precipitated and Organic Se (bank sediment (avg)) (µg/g)	-0.23	0.32	0.03	0.80

The moderate inverse correlation between sorbed SeO_3 in the river bank sediment and sorbed SeO_4 in the river bed sediment may be due to the loss of SeO_4 to create SeO_3, although, not in the same location, but the bed and bank seemed to be more linked.

The greater number of significant correlations for the combined river and tributary data suggest that greater correlations are present in the tributary stream data. The influence of nitrate on Se in irrigated agricultural groundwater systems The strongest correlations exist in the concentrations in the bed sediments for the combined river and tributary data; however, for the Arkansas River data the strong correlation exists for samples from the bank sediments. A possible explanation is that microbial-mediated reactions are facilitated by lower flows and the finer bed sediments in the tributaries. In the Arkansas River, higher flows are more common and with larger-grained (predominantly sand) bed sediments, whereas flows along the banks are slower and more infrequent with finer-grained sediments present providing more potential for microbial-mediated reactions.

4.2 Surface Water Modeling

4.2.1 Se Surface Water Conceptual Model

The processes relating the different Se species in surface water are shown in Figure 4-3, as derived from a review of the literature. Se exists in nature in six forms: organic Se, SeO_4, SeO_3, elemental Se, selenide, and volatile Se. Algae and aquatic plants consume SeO_4 and SeO_3 in the water system. When algae and aquatic plants die they produce organic Se either in the form of SeMet or other organic Se. SeMet and other organic Se can settle into the channel bed or banks, mineralize into SeO_4, and volatilize. If mineralized into SeO_4, certain types of bacteria can continue to convert SeO_4 into SeO_3, or algae and aquatic plants can consume the SeO_4. Alternatively, SeO_4 can also be volatized. SeO_3 can also be converted to elemental Se, volatilized, or taken up by algae and aquatic plants. Elemental Se is usually converted to

selenide. Selenide exists in many forms and for this model is predominantly in the inorganic state as seleno-pyrite or as other Se-bearing species. Reactions are reversible although Figure 4-3 shows the more efficient direction. A Se module was added to the OTIS-MULTI model incorporating the formulas detailed in Section 4.2.2 which are used to describe the processes illustrated in Figure 4-3.

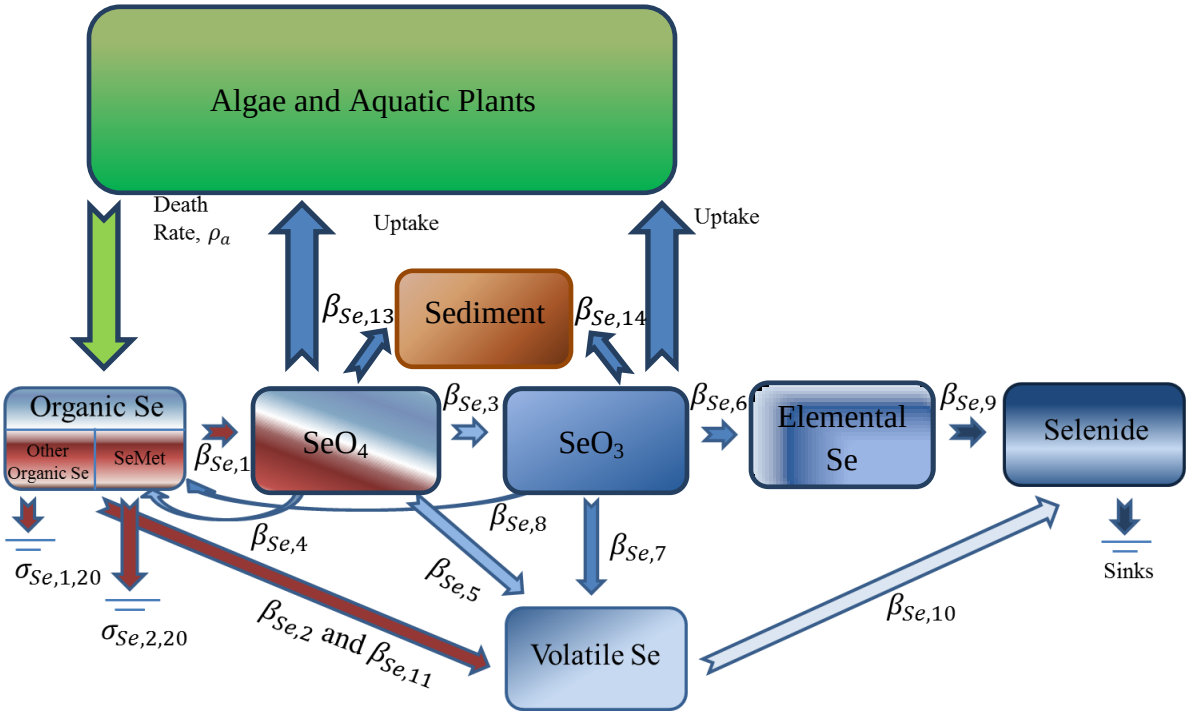

Figure 4-3. Se cycling in surface water where the dominant direction of reactions are shown but the reversible reaction are possible in some cases and may be different numerically.

The Se module is to be used to simulate the fate and transport of selenomethionine, other organic Se, SeO_4, SeO_3, elemental Se, selenide, and volatilized Se concentrations, accounting for sorption, chemical reduction, algal uptake, algal respiration, and volatilization. The next section outlines the equations for each Se species (organic Se, SeO_4, SeO_3, etc.) that were coded into OTIS-MULTI with all terms defined. Testing and implementation of the model will not be discussed since it is beyond the scope of study of this thesis.

4.2.2 Selenium Equations for OTIS-MULTI

Organic Selenium

The change (Δ) in dissolved organic Se—except selenomethionine (SeMet), also referred to as other organic Se—due to biochemical reactions over a river cell during a time step (Δt) is defined by the following equation:

$$\Delta C_{OthOrgSe_{str}} = \left[\left(\alpha_{Se,1} \cdot \rho_{a,1} \cdot C_{a\lg} \right) - \left(\sigma_{Set,Se1} \cdot C_{OthOrgSe_{str}} \right) - \left(\beta_{Se,1} \cdot C_{OthOrgSe_{str}} \right) - \left(\beta_{Se,2} \cdot C_{OthOrgSe_{str}} \right) \right] \cdot \Delta t \qquad (4)$$

This equation assumes the dominant reaction pathway and does not include a term for the reversible reaction because the oxidation processes are very slow compared to the reduction processes. The terms on the right side of the equation (starting from the left and moving to the right) represent the conversion of algal biomass Se to organic Se (which takes place when algae die); settling of organic Se; mineralization of organic Se to SeO_4; and volatilization of organic Se. The settling of organic Se term refers to processes such as the sorption of organic Se to sediment particles which settle out of the water column to the channel perimeter. The variables in Equation 1 are defined below (variables defined in italics were added to the QUAL2E model; the remaining terms were already present in the model):

$C_{OthOrgSe_{str}}$ = *average organic Se concentration at the beginning of the time step (mg Se/L)*

$\alpha_{Se,1}$ = *fraction of algal biomass that is Se (mg Se/mg alg biomass)*

$\rho_{a,1}$ = death rate of algae (T^{-1})

$C_{a\lg}$ = average algal biomass concentration at the beginning of the time step (mg/L)

$\sigma_{Set,Se,1}$ = *rate coefficient for other organic Se settling (T^{-1})*

$\beta_{Se,1}$ = *rate coefficient for the mineralization of other organic Se to SeO_4 (T^{-1})*

$\beta_{Se,2}$ = *rate coefficient for volatilization of other organic Se (T^{-1})*

<u>SeO_4</u>

The change in dissolved SeO_4 due to biochemical reactions over a river cell during Δt is defined by the following equation:

$$\Delta C_{SeO_{4str}} = \left[\left(\beta_{Se1}\cdot C_{OthOrgSe_{str}}\right) - \left(fr_{SeO_4}\cdot\alpha_{Se,1}\cdot\mu_a\cdot C_{alg}\right) - \left(\beta_{Se,3}\cdot C_{SeO_{4str}}\right) - \left(\beta_{Se,4}\cdot C_{SeO_{4str}}\right) - \left(\beta_{Se,5}\cdot C_{SeO_{4str}}\right) + \left(\beta_{Se,12}\cdot C_{SeMet_{str}}\right) - \left(\beta_{Se,13}\cdot C_{SeO_{4str}}\right)\right]\cdot\Delta t \quad (5)$$

This equation assumes the dominant reaction pathway and does not include a term for the reversible reaction because the oxidation processes are very slow compared to the reduction processes. The terms on the right side of the equation in order are the mineralization of other organic Se to SeO_4; the uptake of SeO_4 by algae; the chemical reduction of SeO_4 to SeO_3; the assimilation of SeO_4 to SeMet; the volatilization of SeO_4; and the mineralization of SeMet to SeO_4. The variables in this equation are defined below:

$C_{SeO_{4Str}}$ = *The average SeO_4 concentration at the beginning of the time step (mg Se/L)*

$\beta_{Se,3}$ = *The rate coefficient for the chemical reduction of SeO_4 to SeO_3 which is inhibited by O_2 and NO_3 (T^{-1})*

$\beta_{Se,4}$ = *The rate coefficient for the assimilation of SeO_4 to SeMet (T^{-1})*

$\beta_{Se,5}$ = *The rate coefficient for the volatilization of SeO_4 to species such as dimethylselenide also known as DMSe (T^{-1})*

$\beta_{Se,12}$ = *The rate coefficient for the mineralization of SeMet to SeO_4 (T^{-1})*

μ_a = *The local specific growth rate of algae (T^{-1})*

fr_{SeO_4} = *The fraction of algal Se uptake from the SeO_4 pool (unitless)*

$\beta_{Se,13}$ = *The rate coefficient for the sorption of SeO_4 to suspended or bed sediments (T^{-1})*

The fraction of algal Se uptake from the SeO_4 pool is characterized by the following equation and is calculated within the OTIS-MULTI code:

$$fr_{SeO_4} = \frac{f_{SeO_4} \cdot C_{SeO_4 Str}}{\left(f_{SeO_4} \cdot C_{SeO_4 Str} + \left(1 - f_{SeO_4}\right) \cdot C_{SeO_3 Str} \right)} \qquad (6)$$

wherein

f_{SeO_4} = *The preference factor for* SeO_4

The fraction of algal Se uptake from the SeO_4 pool SeO_4 addresses the requirement of aquatic plants for uptake of SeO_4 that must be fulfilled.

The local rate constant for transformation of SeO_4 to SeO_3 at 20°C, ($\beta_{Se,3}$), SeO_3 to elemental Se ($\beta_{Se,6}$) ,and elemental Se to selenide ($\beta_{Se,9}$) is calculated below:

$$\beta_{Se,n} = \beta_{Se,n,20} \cdot \left(1 - \exp\left[-0.6 C_{O_{2str}}\right]\right) \cdot \left(1 - \exp\left[-0.6 C_{NO_{3str}}\right]\right) \cdot 1.083^{Tw-20} \qquad (7)$$

Wherein n = 3, 6, or 9 and the variables are defined as follows:

$\beta_{Se,n,20}$ = *The rate coefficients* $\beta_{Se,3}$, $\beta_{Se,6}$, *and* $\beta_{Se,9}$ *at 20°C(*T^{-1}*)*

$C_{O_{2str}}$ = *The average dissolved oxygen concentration in the stream (mg* $O_2 L^{-1}$*)*

$C_{NO_{3str}}$ = *The average nitrate concentration (mg* NL^{-1}*)*

T_w = *The average water temperature for the time step (°C).*

$\beta_{Se,6}$ = *The rate coefficient for the chemical reduction of* SeO_3 *to elemental Se which is inhibited by* O_2 *and* NO_3 (T^{-1})

$\beta_{Se,9}$ = *The rate coefficient for the reduction of elemental Se to selenide which is inhibited by* O_2 *and* NO_3 (T^{-1}),

Therefore, the rate constants $\beta_{Se,3,}$ $\beta_{Se,6,}$ and $\beta_{Se,9}$ have corrections for oxygen limiting Se reactions, nitrate limiting Se reactions, and variance of temperature from 20°C.

<u>SeO_3</u>

The change in dissolved SeO_3 due to biochemical reactions over a river cell during Δt is modeled by the following equation:

$$\Delta C_{SeO_{3str}} = \left\{ \left[\beta_{Se,3} \cdot C_{SeO_{4str}} \right] - \left[\left(1 - fr_{SeO_{4str}} \right) \alpha_{Se,1} \cdot \mu_a \cdot C_{a\lg} \right] - \left[\beta_{Se,6} \cdot C_{SeO_{3str}} \right] - \left[\beta_{Se,7} \cdot C_{SeO_{3str}} \right] - \left[\beta_{Se,8} \cdot C_{SeO_{3str}} \right] - \left[\beta_{Se,14} \cdot C_{SeO_{3str}} \right] \right\} \cdot \Delta t \quad (8)$$

This equation assumes the dominant reaction pathway and does not include a term for the reversible reaction because the oxidation processes are very slow compared to the reduction processes. The terms on the right side of the equation in order are the chemical reduction of SeO_4; the uptake of SeO_4 by algae; the chemical reduction of SeO_4 to SeO_3; the volatilization of SeO_3, and the assimilation of SeO_3 to SeMet. In the uptake term, the remainder of algae's requirement of SeO_4 is taken up by SeO_3 which is why in Equation 5 the uptake of SeO_3 algae is characterized by a one minus the preference factor for SeO_4. The parameters and terms are characterized below:

$C_{SeO_{3Str}}$ = *The average SeO_3 concentration at the beginning of the time step (mg Se/L)*

$\beta_{Se,7}$ = *The rate coefficient for the volatilization of SeO_3 (T^{-1})*

$\beta_{Se,8}$ = *The rate coefficient for the assimilation of SeO_3 to SeMet (T^{-1})*

$\beta_{Se,14}$ = *The rate coefficient for the sorption of SeO_3 to suspended or bed sediments (T^{-1})*

<u>*Elemental Selenium*</u>

The change in dissolved elemental Se due to biochemical reactions over a river cell during Δt is modeled by the following equation:

$$\Delta C_{Se^0_{str}} = \left[\left(\beta_{Se,6} \cdot C_{SeO_{3str}} \right) - \left(\beta_{Se,9} \cdot C_{Se^0_{str}} \right) \right] \cdot \Delta t \quad (9)$$

This equation assumes the dominant reaction pathway and does not include a term for the reversible reaction because the oxidation processes are very slow compared to the reduction processes. The terms on the right side of the equation in order are the chemical reduction of SeO_3 to elemental Se and the reduction of elemental Se to selenide. A new rate coefficient and terms are characterized below:

$C_{Se^0_{str}}$ = *The average elemental Se concentration at the beginning of the time step (mg Se/L)*

<u>*Selenide*</u>

The change in dissolved selenide due to biochemical reactions over a river cell during Δt is represented by the following equation:

$$\Delta C_{Se^{-2}_{str}} = \left[\left(\beta_{Se,9} \cdot C_{Se^0_{str}}\right) + \left(\beta_{Se,10} \cdot C_{VolaSe_{str}}\right) - \left(Sink\right)\right] \cdot \Delta t \qquad (10)$$

This equation assumes the dominant reaction pathway and does not include a term for the reversible reaction because the oxidation processes are very slow compared to the reduction processes. The terms on the right side of the equation in order are the reduction of elemental Se to selenide and the conversion of volatile Se species to selenide. A new rate coefficient and terms are characterized below.

$C_{Se^{-2}_{str}}$ = *The average selenide concentration at the beginning of the time step (mg Se/L)*

$\beta_{Se,10}$ = *The rate coefficient for the conversion of volatile Se species to selenide (T^{-1}),*

<u>*Volatilized Selenium*</u>

The change in volatile Se due to biochemical reactions over a river cell during Δt is defined by the following equation:

$$\Delta C_{VolaSe_{str}} = \left[\left(\beta_{Se,2} \cdot C_{OthOrgSe_{str}}\right) + \left(\beta_{Se,5} \cdot C_{SeO_{4str}}\right) + \left(\beta_{Se,7} \cdot C_{SeO_{3str}}\right) + \left(\beta_{Se,11} \cdot C_{SeMet_{str}}\right) - \left(\beta_{Se,10} \cdot C_{VolaSe_{str}}\right)\right] \cdot \Delta t \qquad (11)$$

This equation assumes the dominant reaction pathway and does not include a term for the reversible reaction because the oxidation processes are very slow compared to the reduction processes. The terms on the right side of the equation in order are the volatilization of other organic Se, SeO_4, SeO_3, and SeMet as well as the conversion of volatile Se species to selenide. The new rate coefficient and terms are characterized below:

$C_{VolaSe_{str}}$ = *The average volatile Se concentration at the beginning of the time step (mg Se/L)*

$\beta_{Se,11}$ = *The rate coefficient for the volatilization of SeMet (T^{-1})*

<u>*Selenomethionine (SeMet)*</u>

The change in dissolved SeMet due to biochemical reactions over a river cell during Δt is defined by the following equation:

$$\Delta C_{SeMet_{str}} = \left[\left(\alpha_{Se,2}\cdot\rho_{a,1}\cdot C_{a\lg}\right)-\left(\sigma_{Set,Se2}\cdot C_{SeMet_{str}}\right)-\left(\beta_{Se,11}\cdot C_{SeMet_{str}}\right)-\left(\beta_{Se,12}\cdot C_{SeMet_{str}}\right)\right]\cdot\Delta t \qquad (12)$$

This equation assumes the dominant reaction pathway and does not include a term for the reversible reaction because the oxidation processes are very slow compared to the reduction processes. The terms on the right side of the equation in order are the conversion of algal biomass Se to SeMet (when algae die), settling of SeMet, the volatilization of SeMet, and mineralization of SeMet to SeO_4. The terms are defined below:

$C_{SeMet_{str}}$ = *The average SeMet concentration at the beginning of the time step (mg Se/L)*

$\alpha_{Se,2}$ = *The fraction of algal biomass that is Se (mg Se/mg alg biomass)*

$\sigma_{Set,Se,2}$ = *The rate coefficient for SeMet settling (T^{-1})*

4.3 Simulating the BMPs with MODFLOW-UZF and UZF-RT3D

4.3.1 Se Mass Loadings

The cumulative Se (as SeO_4) mass loadings to the Arkansas River and tributaries over the simulated time period are depicted in Figure 4-4 as red bars. The green bars depict Se mass transferred from the stream to the groundwater. It is apparent that the majority of the simulated mass entering the Arkansas River is along the segment upstream of Timpas Creek and Crooked Arroyo. These two tributaries also contribute a significant amount of Se mass to the river.

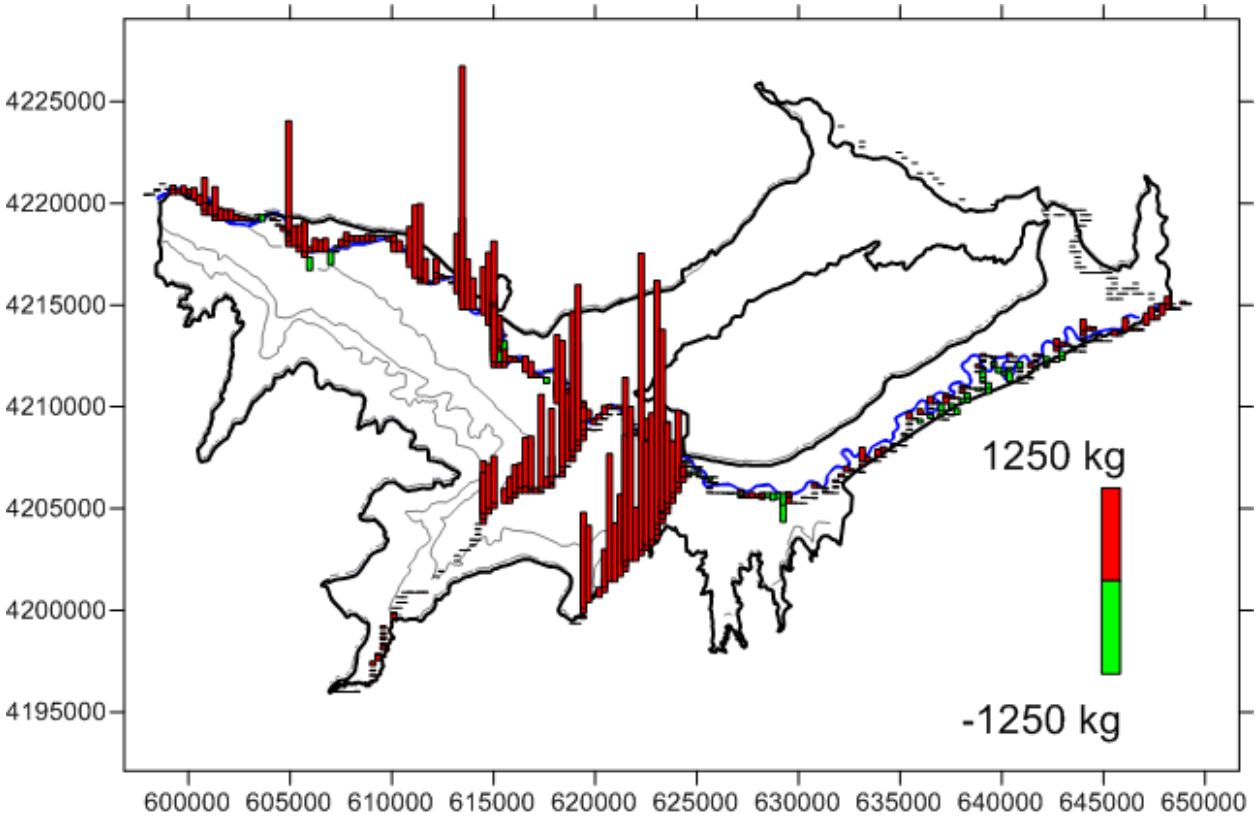

Figure 4-4. The spatial distribution of cumulative simulated Se mass loadings over the simulated time period for the Baseline scenario

A possible explanation for the high Se mass loadings transferred from the groundwater to the streams in the upstream region of the Arkansas River (Timpas Creek and Crooked Arroyo) is due to the large number of irrigated fields that bound these water bodies along with canals. Downstream of Crooked Arroyo, the irrigated fields near the Arkansas River are much narrower and fewer. There is also only one canal.

For all scenarios the spatial distribution of cumulative simulated Se mass loadings over the simulated time period were subtracted from the corresponding cumulative simulated Se mass loadings simulated under the Baseline scenario. An example of the cumulative Se mass loading results is shown in Figure 4-5 for the aggressive scenario for lease fallowing. However, the prospective decrease in total cumulative Se mass loading from the Baseline loading is the focus of this research. Therefore, all scenarios below will show the decrease in total cumulative Se mass loading from the Baseline scenario.

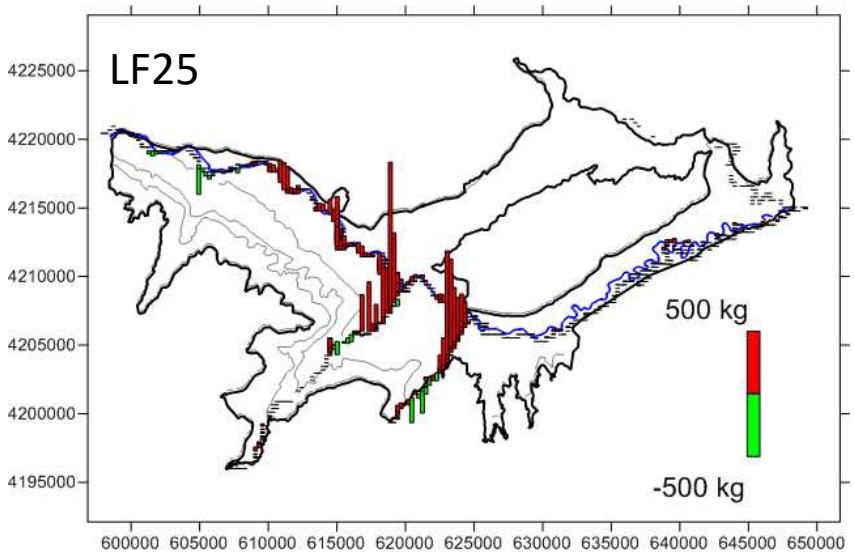

Figure 4-5. The spatial distribution of cumulative Se mass loading over the simulation time period for the LF25 BMP scenario.

A comparative example of the simulated impact of basic (LF5), intermediate (LF15), and aggressive (LF25) individual BMP scenarios is shown in Figure 4-6. Green bars indicate a decrease in total cumulative Se mass loading from the Baseline scenario, and red bars indicate an increase in Se mass loading (Bailey et al., 2014). Thus, the LF25 plot in Figure 4-6 was constructed by subtracting the loadings depicted in Figure 4-5 from those depicted in Figure 4.4 with positive results (or decreases from the baseline) being depicted with green bars and negative results (or increases from the baseline) being depicted with red bars. All other groups of individual scenarios are shown in Appendix C. As expected, Se mass loading is predicted to

substantially decrease with an increase in the number of fallowed fields due to an increase in the decreased application of water from LF5 to LF15 to LF25. The greatest mass load reduction to surface water is in the tributaries Timpas Creek and Crooked Arroyo.

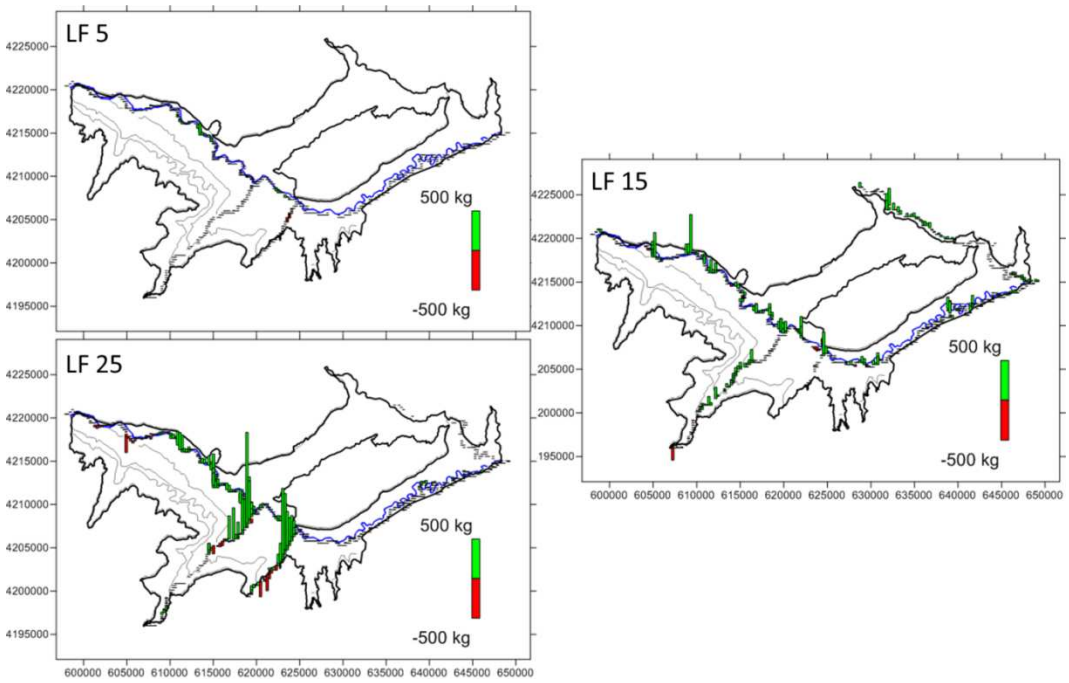

Figure 4-6. The spatial distribution of cumulative Se mass loading differences from the Baseline over the simulation time period for BMP scenarios LF5, LF15, and LF25.

Figure 4-7 illustrates results for another group of simulated combined BMP scenarios. The group consists of one scenario that is basic, one that is intermediate, and one that is aggressive. Each scenario combines four BMPs: reduced irrigation, canal sealing, reduced fertilizer, and enhanced riparian buffer zones all at the same level (basic, intermediate, aggressive). These combination BMP scenarios show a much greater amount of predicted mass load reduction upstream in Timpas Creek and Crooked Arroyo than the individual BMP scenarios. Predicted mass load reductions along the downstream segments of the Arkansas River are relatively small possibly due to the combination of scenarios applying less water to fewer fields in the downstream region. Also, the comparative difference in the predicted decrease in Se mass loading for the intermediate scenario compared to that for the aggressive scenario is not as

great as the difference compared to the basic scenario which may be due to less synchronization of scenarios at the basic level.

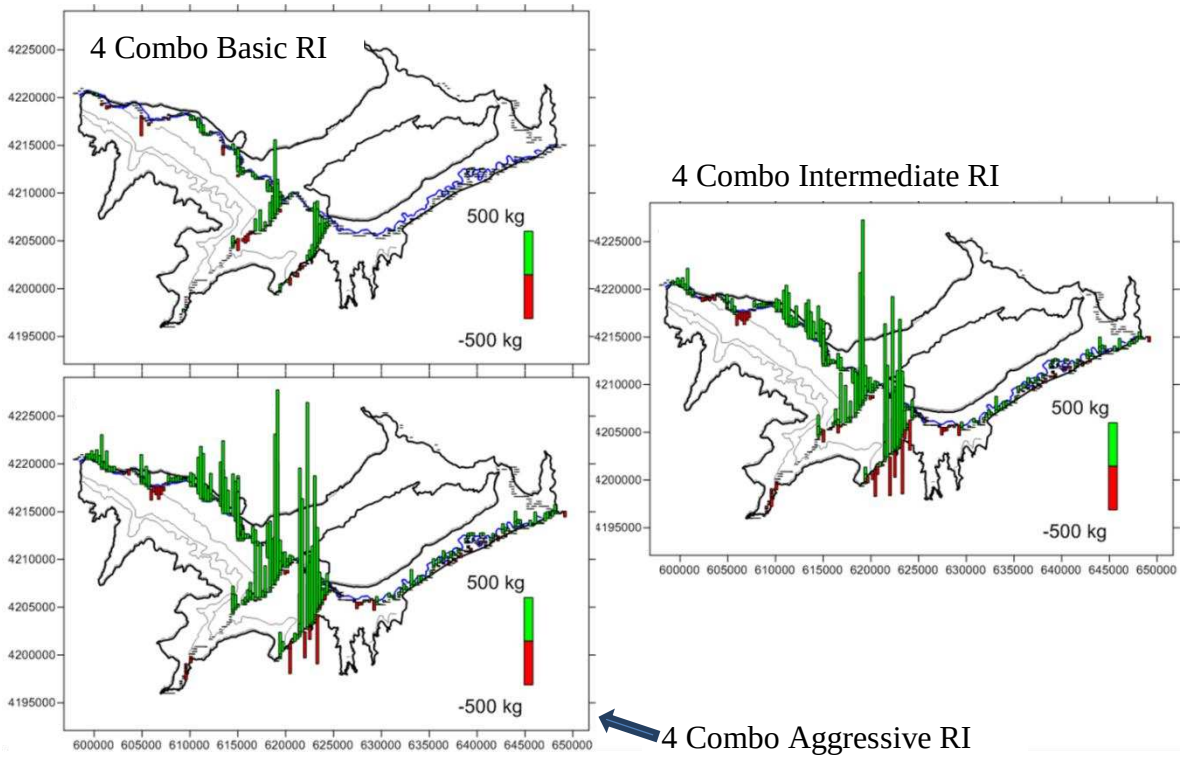

Figure 4-7. The spatial distribution of cumulative Se mass loading differences from the Baseline over the simulation period for basic, intermediate, and aggressive combined BMP scenarios.

Cumulative mass loading differences from the Baseline over the simulation period for all individual aggressive BMP scenarios and two combination scenarios are shown in Figure 4-8 along the Arkansas River and three tributaries. The spatially-varying simulated mass loadings exemplify low reductions in mass loading to the streams for the RF30 and ERB aggressive scenarios. The simulated reduction in Se mass loadings is high for the tributaries in all other scenarios plotted except RF30 and ERB high. This suggests that the reduction in fertilizer or increasing reactions in the riparian buffer is not as effective as decreasing the amount of water to decrease Se in the system. The simulated combination scenarios indicate the greatest decrease in Se mass loading to the streams due to multiple BMPs used in concert with one another.

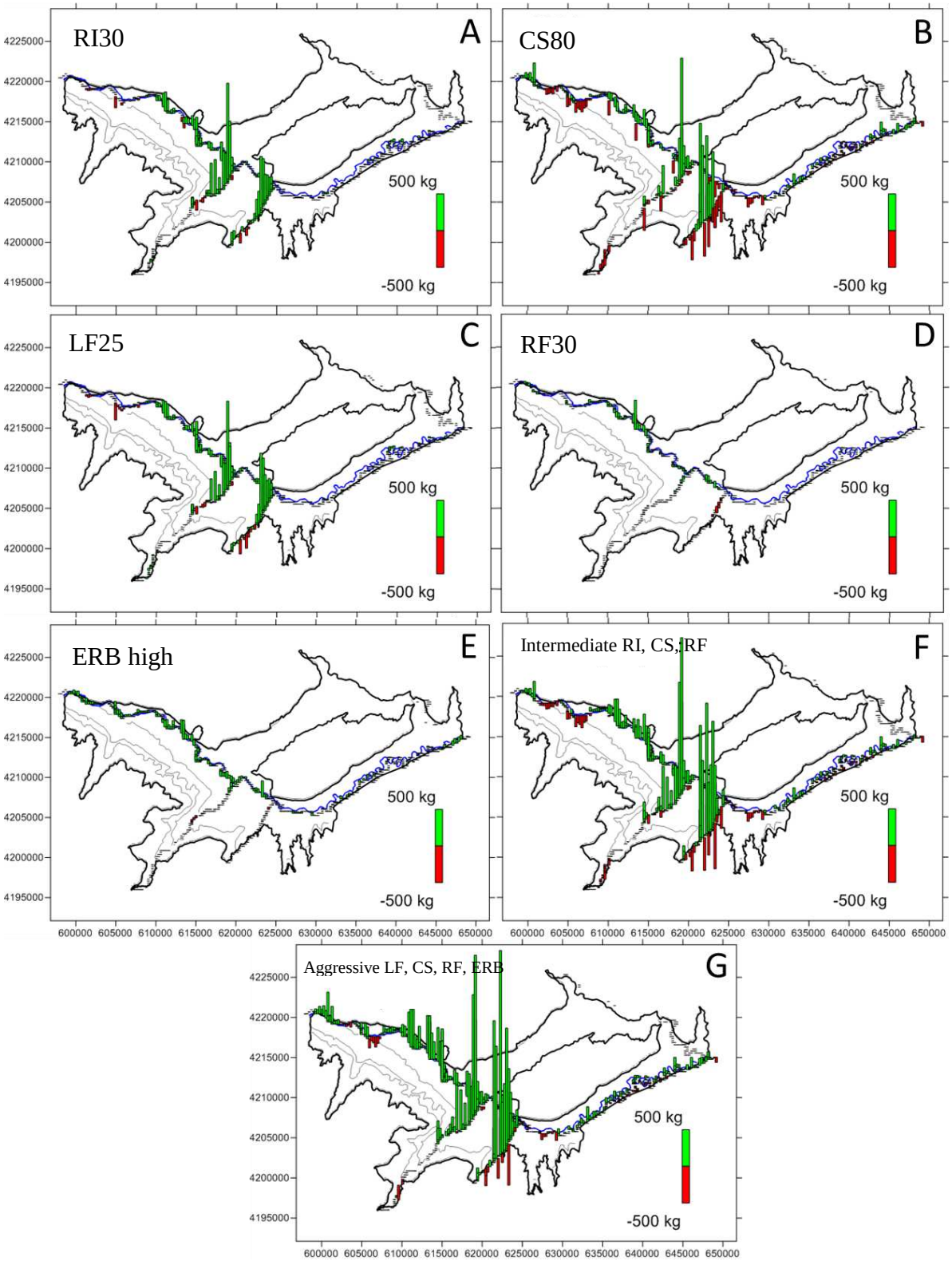

Figure 4-8. The spatial distribution of cumulative Se mass loading differences from the Baseline over the simulation period for all individual aggressive BMPs and for two combined BMPs involving a change in the amount of water applied

For the water-management BMPs (RI, LF, CS), the higher decrease in Se mass loading can be explained by the fact that the tributaries are predominantly fed by groundwater. Decreasing the application of groundwater to fields and transferred along the canals adds less water to the subsurface which causes the water table to lower and creates a smaller hydraulic gradient (Bailey et al., 2014). The two tributaries contributing the most Se mass to the Arkansas River are Timpas Creek and Crooked Arroyo. Timpas Creek and Crooked Arroyo are located near exposed shale bluffs and are surrounded on both sides by large amounts of irrigated fields. Horse Creek, located in northeast contributes much less Se mass, since it is located further from exposed shale bluffs and is not surrounded on both sides by irrigated fields.

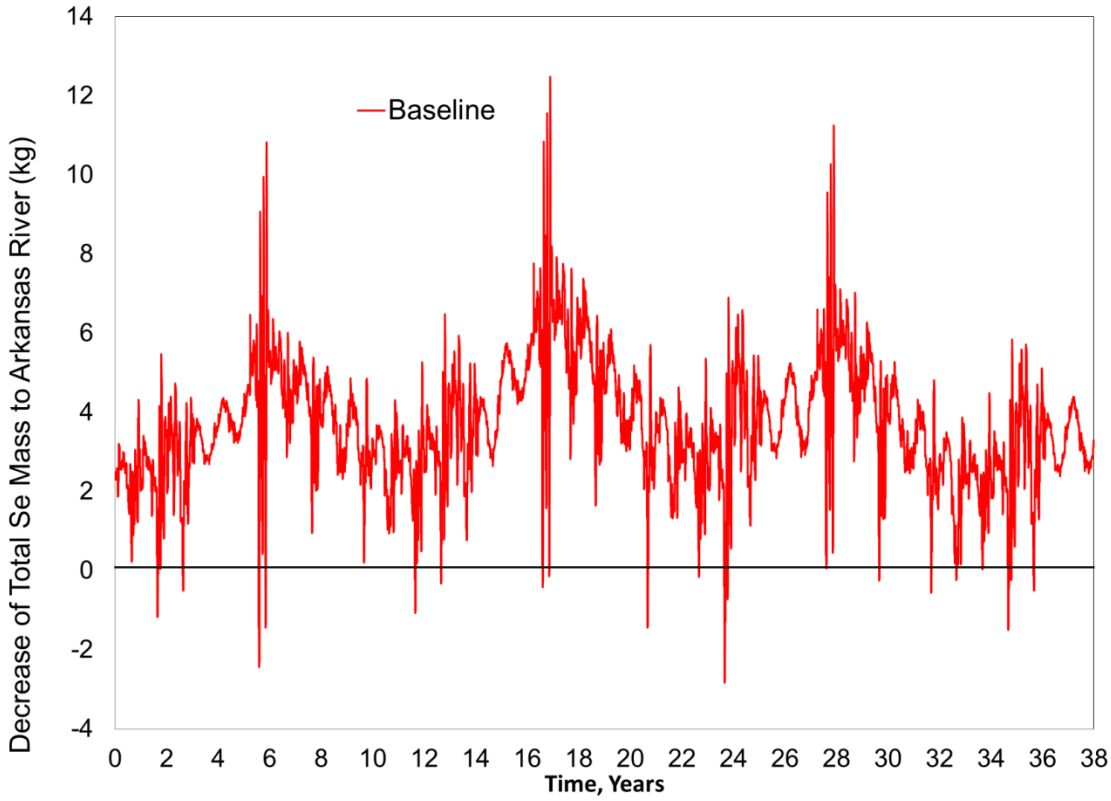

Figure 4-9. Baseline total Se mass to the Arkansas River in kg/day for the entire simulation time 38 years

The baseline time series of total Se mass loading to the Arkansas River are shown in Figure 4-9. A positive difference indicates a decrease in daily Se mass loading, and a negative difference indicates an increase in daily Se mass loading. The temporal variation is large ranging

from approximately -3 kg/day at approximately year 24 (meaning an increase of total Se mass) to the Arkansas River to a decrease of approximately 12 kg/day at approximately year 16. A cyclic nature is apparent in the output due to the existence of wet and dry years and the repetition of a simulated historic period of 11 years over the 38 year period. To show the magnitude of the Se mass loading reductions for all BMP scenarios, the differences between the Baseline and each scenario were calculated and are shown in Figure 4-10.

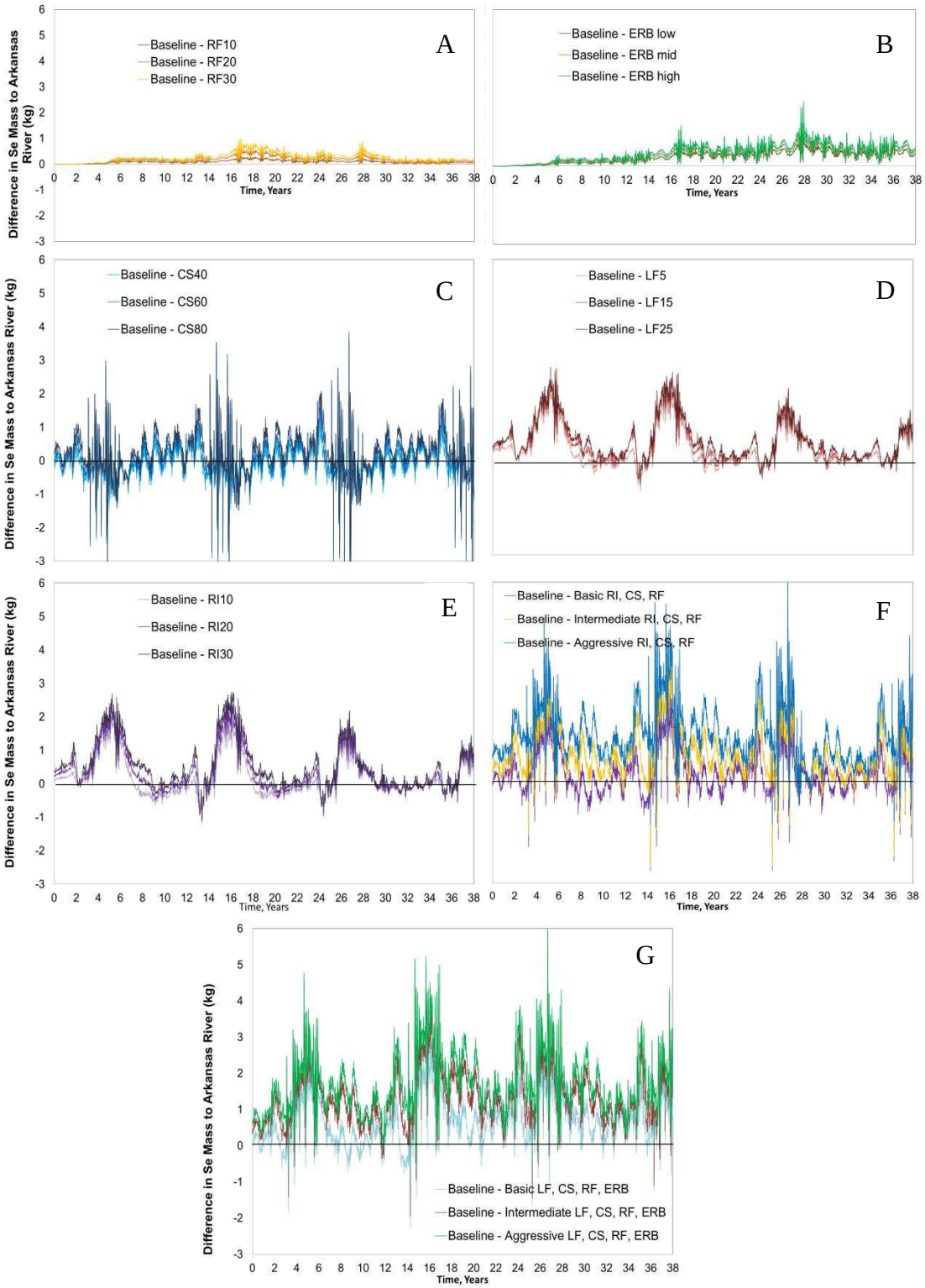

Figure 4-10. Time series of simulated differences in total Se mass to the Arkansas River and tributaries from the Baseline for (A) reduced irrigation (RI), (B) canal sealing (CS), (C) land fallowing (LF), (D) reduced fertilizer (RF), (E) enhanced riparian buffer zone (ERB), and (F-G) combination BMP scenarios. Scenario (F) implements RI, CS, and RF BMPs simultaneously while Scenario (G) implements LF, CS, RF, and ERB BMPs simultaneously.

Results for all five individual BMPs and two combinations are shown in Figure 4-10 with all the same scale so that the large simulated reductions in Se mass loading for the combination BMP scenarios can be compared to those simulated for the individual scenarios. The time series of Se mass loading reductions at the various levels of BMP scenarios (basic, intermediate, and aggressive) for lease fallowing and reduced irrigation are the same general shape. This is an expected result since both individual sets of scenarios limit the amount of water applied on irrigated fields and limits the water that consequently percolates below the root zone to the water table. The shape of the three levels of BMP scenarios for reduced fertilizer and enhanced riparian buffer zone are similar as well since both deal with altering chemical reactions within the system, especially within the N cycle. The reduced fertilizer scenarios decrease the amount of NO_3 in the system which lowers the oxidation of Se from the weathered, surficial, and bedrock shale forms. The idea behind implementing an enhanced riparian buffer is to plant more and different trees and grasses to increase plant volatilization of Se and to encourage the accumulation of organic matter which enhances heterotrophic reduction of SeO_4. This process results in less transport of mobile Se into the stream. The most unique set of results are the three levels of canal sealing scenarios. The predicted mass loading reductions for the canal sealing scenario oscillate from positive to negative much more frequently than for all other scenarios which makes the shape of the graph more similar to the Baseline. The timing of the increases in Se mass loading for the group of RI and LF scenarios are indicated by negative differences which reach a local minimum periodically in Year 13 and 24. This may be associated with the timing of water application and reduced seepage during wet years which decreases the Se mass loading from the canals to the aquifer (Bailey et al., 2014).

The simulated reduced irrigation and enhanced riparian buffer scenarios never result in increased mass loadings (negative differences). The lease fallowing and reduced irrigation scenarios generate slightly increased mass loadings but only by 1 to 2 kg/day whereas the simulated canal sealing scenarios result in about 3 kg/day increases much more frequently. The combination scenarios amplify the tendencies (the shape of the graph) for all BMPs, since they are conglomerated together in each set of combinations. The combinations of four BMPs result in larger simulated decreases in mass loadings than the combinations of three BMPs as expected.

Finally, the simulated total Se mass loading percent differences from the Baseline were computed for the 38-year simulation period to indicate the most effective BMPs for mitigation of Se loading to the stream network over the entire region. Using this measure, the most effective to least effective BMPs are reduced irrigation, enhanced riparian buffer zone, lease fallowing, reduced fertilizer, and canal sealing (Figure 4-11). The basic level three BMP combination scenarios perform slightly worse than the most effective individual BMPs, but basic level four BMP combination scenarios perform significantly better. Both the intermediate and aggressive BMP combination scenarios are much more effective at reducing Se than any individual BMP scenario. However, the feasibility of implementing all BMPs at once over the entire region would be low. It would seem more reasonable to target areas with high levels of Se in order to reduce difficulty and cost. Basic, intermediate, and aggressive BMP levels are tested to indicate the highest potential impact, providing an upper threshold for an improvement target.

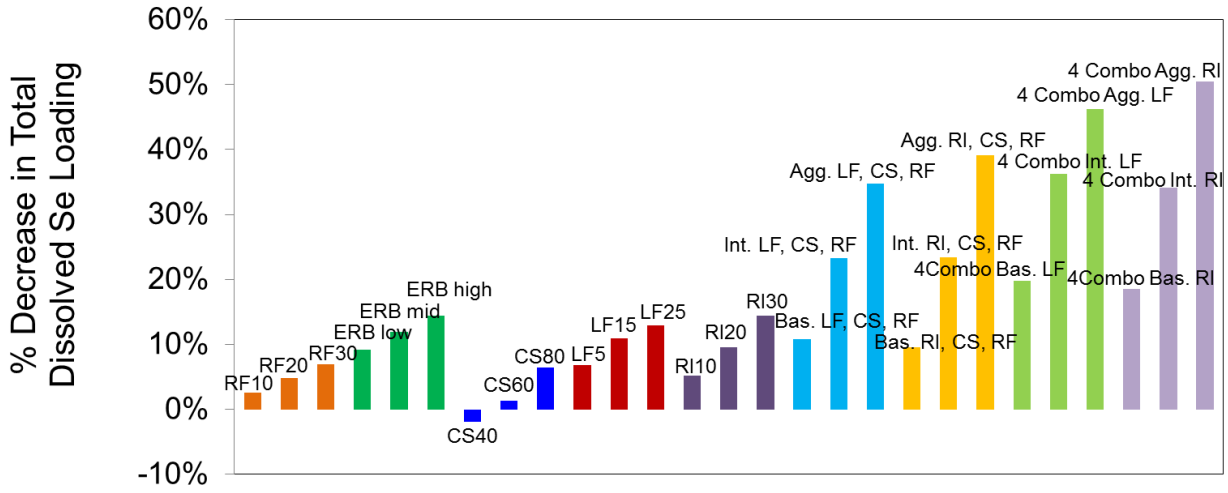

Figure 4-11. Percent decrease in simulated total dissolved Se mass loadings directly to the Arkansas River for individual and combined BMPs. Abbreviations for basic, intermediate, and aggressive are the following bas., int., and agg. respectively.

Most results were to be expected except the negative percent reduction in mass loading predicted for the CS40 BMP. This could be due to the depression of the water table due to less seepage to the water table combined with different de-percolation rates or an error in the calculations of the model.

The addition of comparison of the reduction in Se mass loadings from to both the tributaries and to the Arkansas River compared to reduction in Se mass loadings directly to the Arkansas River is provided in Figure 4-12. Horse Creek did not produce significant changes in Se mass loadings, and its results were excluded from the calculations. For individual scenarios, all three levels of BMP implementation for reduced irrigation, enhanced riparian buffer, and reduced irrigation resulted in smaller percent reduction in mass loading when including the contributions from the tributaries. Only canal sealing and lease fallowing scenarios resulted in greater reductions in Se mass loadings. The effects of incorporating the tributary contributions on the results for the combined BMPs could be either positive or negative. For the three BMP combination scenarios which included lease fallowing or reduced irrigation, the percent decrease in Se mass loadings was enhanced when contributions from the tributaries were included for all

six scenarios. However, the four BMP scenario combinations did not produce a consistent trend of higher or lower impacts across the three levels of management (basic, intermediate, or aggressive).

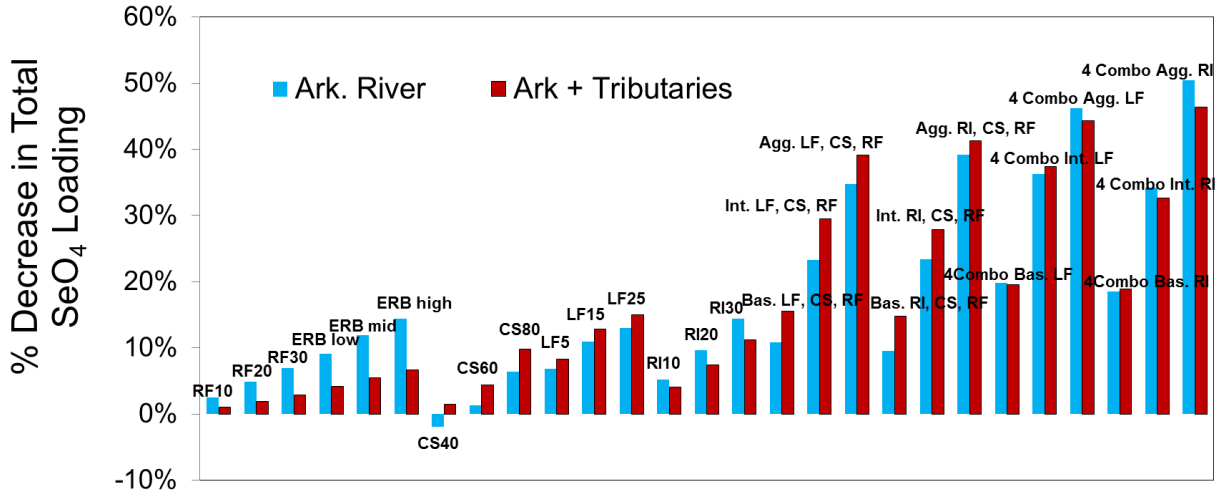

Figure 4-12. Percent decrease in total dissolved Se total mass loadings to the Arkansas River plus the tributaries (Crooked Arroyo and Timpas Creek) in red and directly to the Arkansas River alone in blue for individual and combined BMPs. Abbreviations for basic, intermediate, and aggressive are the following bas., int., and agg. respectively.

4.3.2 Se Groundwater Concentrations

Simulated groundwater concentrations were described for each canal command area in the USR (Figure 4-13). A canal command area is the land area made up of fields which are supplied irrigation water from a given canal.

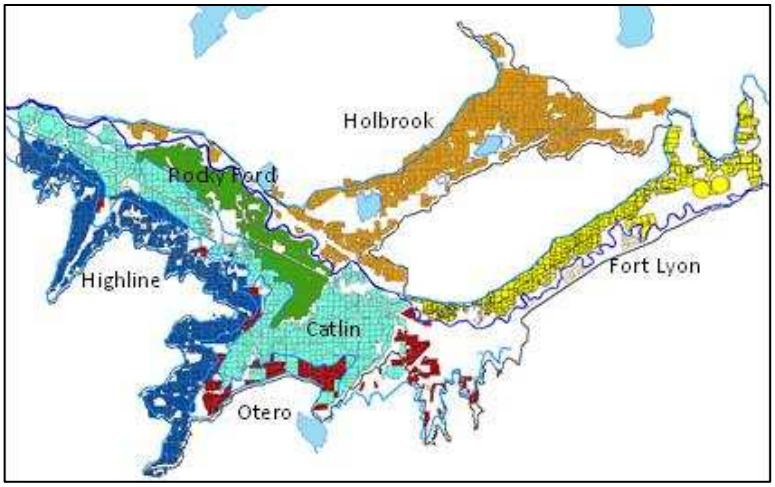

Figure 4-13. The canal command areas of the Upstream Study Region

The six canal command areas in the USR are supplied water by the following canals Rocky Ford Highline (Highline), Otero, Catlin, Rocky Ford, Fort Lyon, and Holbrook. The area not made up of irrigated fields that are supplied irrigation water under a given canal is referred to as the "outside region." Time series plots that show percent differences of average simulated C_{SeO_4} for each considered BMP from the respective average simulated baseline C_{SeO_4} values for each command area and the outside region are shown in Figure 4-14. The SeO_4 concentrations compared in these plots are those simulated in Layer 4 of the MODFLOW-UZF model because this is the geologic layer which corresponds to the elevation of the shallow saturated zone from 1999–2009 and is the layer in which most groundwater monitoring wells were drilled and field measurements were made for use in model calibration (Bailey et al., 2014). The positive percent differences indicate a decrease in average simulated C_{SeO_4} within a command area for a given scenario compared to the baseline. The results over the 38-year simulation are quite variable across the considered BMPs and command areas because the command areas vary in a number of ways including the number of fields that encompass them, the distance to canals, and shape. One reason for the patterns of temporal variability over the simulation period includes the weather variability over the 38 year simulation. The simulated groundwater concentrations

increase for many of the scenarios/command areas due to the overall mass of SeO_4 decreasing. The concentration has increased due to a lowering of the water table which is associated with lowering of water content in cultivated areas where applied irrigation or canal seepage volumes have been reduced (Bailey et al., 2015). The results for the ERB high or RF30 scenario are not more than 5% for any command area. A possible reason for the ERB high scenario could be due to the lack of effect of increased reaction rates of the riparian buffer zone for the cells near the Arkansas River and the tributaries. The interactions could be too far away to significantly decrease the C_{SeO_4} in the command areas. For RF30, the small effects on the decrease of the C_{SeO_4} could be due to the decrease of N fertilizer loading not being able to decrease the C_{NO_3} sufficiently to significantly affect Se transformation processes (e.g., SeO4 chemical reduction to SeO3) (Bailey et al., 2015).

The outside region made up of fields that do not receive irrigation water from any of the canals named in Figure 4-13 results in all positive results although some are small. The outside region's results are mostly positive because the area was affected by water management as shown by with the aggressive scenario showing decreases of average C_{SeO_4} up to 20%. The outside region is smaller compared to most of the command areas, is affected by the decrease of water in the system, and is affected by the reduction of N fertilizer/increase of reaction rates in the riparian zone. The results of for each command area will be discussed in approximate order from most effective in decreasing the average C_{SeO_4} to least effective: Fort Lyon, Holbrook, Rocky Ford Highline, Rocky Ford, Otero, and Catlin canals.

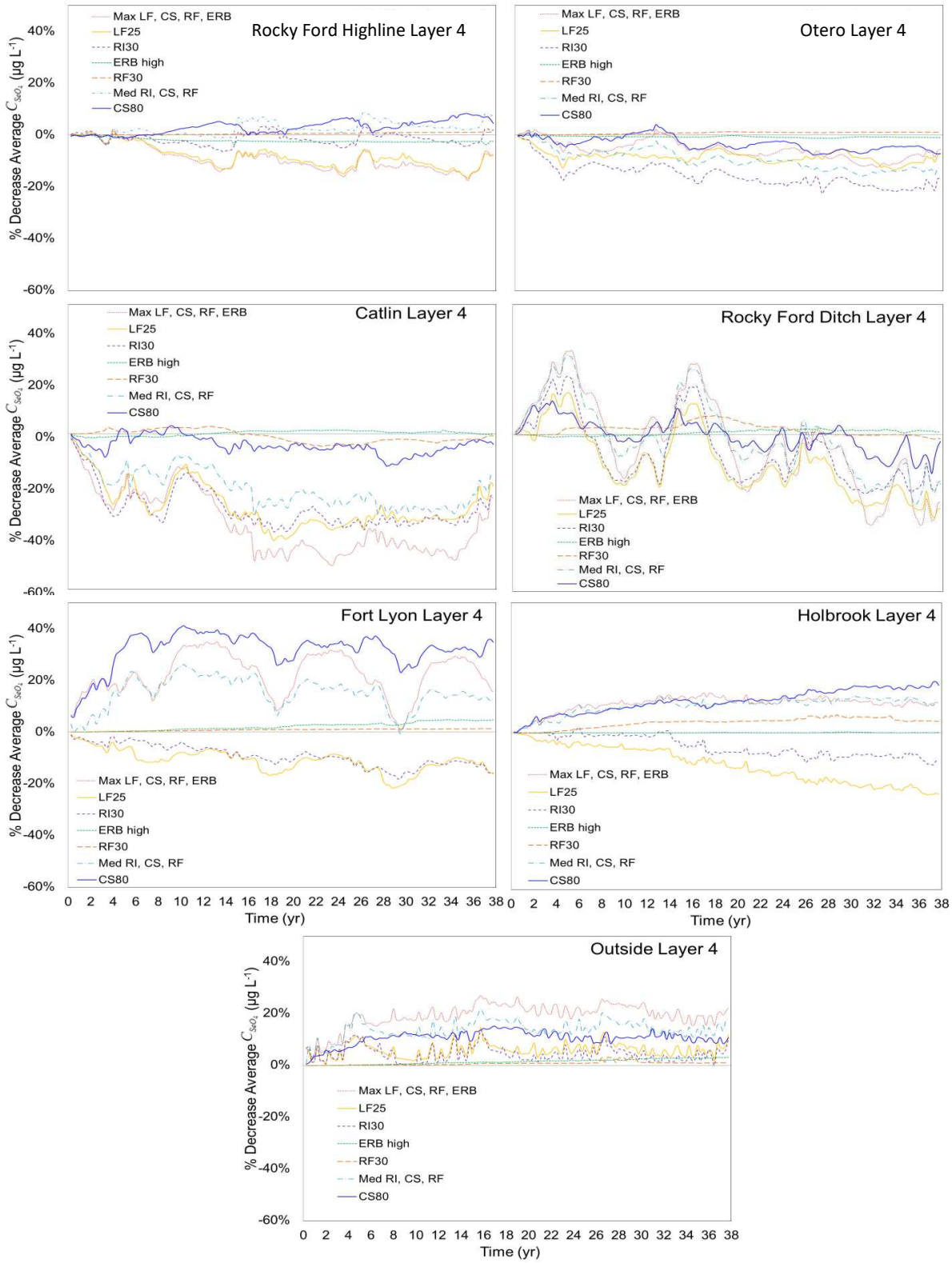

Figure 4-14. Time series percent decrease of average C_{SeO_4} concentrations for the Rocky Ford Highline Canal, Otero Canal, Catlin Canal, Rocky Ford Ditch, Fort Lyon Canal, Holbrook Canal, Outside region

The BMPs applied in the Fort Lyon command area decreased C_{SeO_4} in all but two BMP scenarios. Only the LF25 and RI30 BMPs were simulated to result in increased C_{SeO_4}. The percent differences in the Fort Lyon Canal region are the largest simulated, with the greatest percent differences found for the CS80 scenario. The simulated increased concentrations for the RI30 scenario may be explained by the decrease of applied water due to more efficient irrigation methods used which would lead to a decrease in the water percolating to the water table. The water table would then mostly likely drop along with the gradient to the river. The upflux from the unsaturated zone would also mostly likely decrease. However, since the loadings are relatively the same for different scenarios, the lessening of water applied has increased the concentration. The physical processes for the LF25 and CS80 scenarios would be similar to the reduced irrigation scenario discussed above except that lease fallowing would eliminate the water application on various fields selected for fallowing and canal sealing would decrease the seepage of water out the canal and into the ground surface. The difference for the CS80 scenario which decreased C_{SeO_4} could be that the gradient, although slowed, is not flowing over as much shale en route to the river. The shape of the fields in the Fort Lyon command area is very narrow and mostly borders the Arkansas River very closely, so it takes the groundwater much less time to reach the river than any other command area. Even including the results for the RI30 and LF25 scenarios, the highly beneficial results indicate it is most effective to implement BMPs in the Fort Lyon command area to decrease C_{SeO_4} concentrations in groundwater.

The Holbrook Canal command area results look similar to those for the Rocky Ford Highline Canal command area results, although greater decreases in C_{SeO_4} in groundwater are predicted for the Holbrook Canal. Only the LF25 and RI30 scenarios are predicted to result in increased C_{SeO_4} possibly due to the same reason discussed for the Fort Lyon command area. The

CS80 BMP is predicted to be the most effective in the Holbrook command area with a simulated decrease of about 20% in C_{SeO_4}. In this case, the reduced seepage is decreasing the C_{SeO_4} where the water table is expected to drop due to less seepage from the canals. However, other factors must be influencing the C_{SeO_4} to decrease instead of increase as in the lease fallowing and reduced irrigation scenarios previously described. In the Holbrook command area, the CS80 scenario resulted in a slowed gradient, but the slowed gradient is not leaching as much SeO_4 from shallow shale deposits. There are not as many shallow shale deposits surrounding the Holbrook command area.

Results for the Rocky Ford Highline Canal command area reveal a simulated increase in average C_{SeO_4} values for BMP scenarios LF25 and Aggressive (Max) LF, CS, RF, and ERB. The combination scenario Max LF, CS, RF, ERB resulted in the largest simulated increase in C_{SeO_4} and the combination scenario Intermediate (Med) RI, CS, and RF in the largest decrease.

The Max LF, CS, RF, and ERB scenario has the same basic shape as the LF25 scenario, while the Med RI, CS, and RF scenario and the RI30 scenario share the same shape as well. Therefore, the LF25 scenario is unable to overcome the drop of the water table and increase in SeO_4 loading while the RI30 scenario is able to decrease the C_{SeO_4}. One possible reason for this could be that the uneven application of water for the LF25 scenario is causing localized increases in the gradient which would cause increased leaching of SeO_4; while the RI30 scenario has water more uniformly applied on the fields in the command area, so the localized increases to the gradient are not causing increased leaching of SeO_4 from the shale bedrock.

The Rocky Ford canal command area results show simulated decrease in C_{SeO_4} early in the 38 year simulation. However, the final results at the end of the 38 year simulations are large

increases which are shown by its highly oscillatory graph. The location of the Rocky Ford Ditch is south of the upstream portion of the Arkansas River in the USR, and it borders the downstream most portion of Timpas Creek. The location of the command area influences its increase of C_{SeO_4} as does the lower water table elevations due to its link to the lowering of the water content in cultivated areas where applied irrigation happened or canal seepage volumes have been reduced (Bailey et al., 2015).

The results for the Otero Canal show mostly simulated increases in C_{SeO_4} in Layer 4 for the considered BMPs. The Otero Canal command area is the smallest of all the command regions, and its location is in the south of the study region with parts near Timpas Creek and Crooked Arroyo. Almost half of the fields in the Otero command are surrounded by shallow shale which increases the C_{SeO_4} compared to other command areas.

The results for Catlin Canal command area show the greatest simulated increases in C_{SeO_4} for most of the considered BMPs. The smallest increases in C_{SeO_4} were for RF30, CS80, and ERB high. The reason why canal sealing could be most effective compared to the other water management scenarios is due to less water percolating down to the water table along the canals and more water reaching the fields which offsets the percolation rate in each command area. The Catlin Canal command area borders the Otero Canal command area fields. The proximity of these canals to Timpas Creek, Crooked Arroyo, and surficial shale may explain why their results are mostly increases in the C_{SeO_4}.

The calculated percent decreases in C_{SeO_4} from the baseline for each command area and for the outside (non-irrigated) region are provided in a different form in Table 4-6. These percent decreases are for the final year of the simulated period for each BMP scenario from Figure 4-14.

Table 4-6. Percent decreases (from Baseline) for six command areas and the outside (non–irrigated land). The green and yellow are small positive or negative final percent differences corresponding to a decrease in the Se concentration percent difference. Red and orange cells are larger positive percent differences and correspond to an increase in the Se concentration percent decrease.

Scen.	Type	Rocky Ford Highline	Otero	Catlin	Rocky Ford Ditch	Fort Lyon	Holbrook	Outside
1	RF10	0.40%	0.40%	-0.10%	-0.60%	0.50%	0.90%	0.40%
2	RF20	0.80%	0.70%	-0.40%	-1.00%	0.90%	2.30%	0.70%
3	RF30	1.10%	1.10%	-0.80%	-1.40%	1.30%	4.40%	1.20%
4	ERB low	-2.50%	-1.20%	-0.50%	0.50%	3.20%	0.00%	1.90%
5	ERB mid	-2.50%	-1.10%	-0.20%	0.90%	4.00%	0.10%	2.60%
6	ERB high	-2.50%	-1.00%	0.00%	1.20%	4.70%	0.20%	3.20%
7	CS40	2.90%	-2.10%	-1.70%	3.30%	15.20%	8.80%	8.00%
8	CS60	3.60%	-4.30%	-2.80%	1.00%	23.00%	13.80%	10.70%
9	CS80	4.50%	-7.10%	-4.00%	-2.60%	34.70%	18.30%	10.80%
10	LF5	-2.10%	-4.20%	-7.70%	-14.50%	-6.60%	-18.10%	10.70%
11	LF15	-6.00%	-5.60%	-14.90%	-24.40%	-10.60%	-20.10%	11.20%
12	LF25	-7.90%	-7.40%	-20.10%	-28.40%	-16.20%	-23.50%	11.90%
13	RI10	3.10%	-5.00%	-5.10%	-9.50%	-7.30%	-5.10%	9.10%
14	RI20	3.40%	-11.80%	-14.40%	-14.30%	-11.30%	-8.00%	9.80%
15	RI30	1.90%	-17.50%	-23.60%	-18.80%	-15.90%	-10.40%	10.30%
16	Min LF, CS, RF	3.30%	-6.20%	-8.20%	-14.60%	6.40%	-2.60%	18.70%
17	Med LF, CS, RF	-2.20%	-5.00%	-17.40%	-22.00%	13.40%	4.00%	20.10%
18	Max LF, CS, RF	-5.10%	-4.40%	-25.90%	-27.30%	12.30%	11.40%	22.00%
19	Min RI, CS, RF	8.80%	-6.60%	-6.40%	-10.40%	6.60%	5.30%	17.30%
20	Med RI, CS, RF	7.20%	-12.90%	-16.50%	-17.80%	12.40%	11.60%	18.60%
21	Max RI, CS, RF	5.70%	-12.90%	-27.50%	-26.40%	14.20%	20.30%	20.30%
22	4Combo Min LF	1.10%	-7.40%	-8.00%	-13.90%	8.40%	-2.70%	19.10%
23	4 Combo Med LF	-8.20%	-7.50%	-20.90%	-25.10%	10.80%	1.30%	21.70%
24	4 Combo Max LF	-7.40%	-5.60%	-24.90%	-25.30%	15.30%	11.40%	22.50%
25	4Combo Min RI	6.90%	-7.70%	-6.40%	-9.50%	8.70%	5.30%	17.70%
26	4 Combo Med RI	5.30%	-14.20%	-16.00%	-16.70%	15.00%	11.60%	19.10%
27	4 Combo Max RI	3.60%	-14.20%	-26.60%	-23.70%	17.10%	20.30%	20.80%

Chapter 5 presents the conclusions of this research concerning Se cycling in the irrigated stream-aquifer system of the LARV, what the collected data suggest about the presence of Se in various forms, and which BMPs seem to be the most promising for bringing about improvement. Future research goals are also suggested.

Chapter 5: Summary, Conclusions, and Recommendations

Posing a risk to aquatic life and livestock, the Se problem is widespread in the LARV and may increase if unanswered. This research uses three main components to address the need to better describe and find solutions to the problem of Se pollution in the LARV: (1) collection of Se data in streams to characterize solute and sediment concentrations, (2) development of a conceptual model of in-stream Se reactions, and (3) application of existing calibrated groundwater models to explore alternative Se remediation strategies.

Collection of water and soil samples help characterize the extent of the problem and the partitioning of Se species in the dissolved, sorbed, and residual phases in the stream system. Four sample trips were made to the LARV where a total of seventeen locations were sampled in the Arkansas River and its tributaries. Of the sixteen locations, ten are sampling locations in the Arkansas River and six are in the tributaries. The statistical analysis performed on the data gathered from the field for Se and N species indicates the average for all the dissolved Se data is 11.9 μg/L with a range of 6.7 μg/L to 32 μg/L (ICP method). The average of the sorbed Se data is 0.19 μg/g, and the range is 0.04 μg/g to 0.54 μg/g. The residual Se (precipitated and organic Se) data have an average of 0.63 μg/g, and a range of 0.18 μg/g to 1.51 μg/g. The spatial variability within the stream system for the each event is summarized in Table 5-1 which was determined by sorting the data based on event (trip) and if collected in the Arkansas River or the tributaries.

Table 5-1. Spatial variability of dissolved Se concentrations in μg/L for each trip, the river, and tributary data.

Arkansas River				
	Trip 1	**Trip 2**	**Trip 3**	**Trip 4**
Average	12.26	7.07	11.67	13.53
Minimum	9.76	6.48	11.3	13
Maximum	13.8	8.75	12.2	14.1
Tributaries				
Average	14.35	9.12	11.2	17.48
Minimum	6.04	7.07	11.2	11.1
Maximum	20.7	11.7	11.2	21.1

The data compare well to the previous data gathered in the area which describe the dissolved Se concentrations in the river are approximately double to triple the Colorado chronic standard of 4.6 μg/L (Gates et al., 2009).

Moreover, some strong correlations were detected between Se and N species. Strong correlations exist mainly between sorbed and reduced Se species in the stream bed for the Arkansas River and tributary data; however, for the Arkansas River data alone, the strong correlation exists in data from samples taken in the stream banks. This may infer that conversions between Se species are more active in the bed of the river and the bed or banks of the tributaries. The Arkansas River and tributary data exhibit strong statistical correlations for the following pairs: the stream bed sediment sorbed SeO_3 (μg/g) and the sorbed SeO_4 (μg/g); the stream bed sediment sorbed SeO_3 (μg/g) and the precipitated and organic Se (μg/g); and sorbed SeO_4 (μg/g) in stream bed sediment to precipitated and organic Se (μg/g) in bed sediment. When only analyzing concentrations derived from the Arkansas River samples alone, the only strong statistical correlation discovered is 0.80 between the sorbed SeO_4 in the bank sediments of the river and the estimate of precipitated and organic Se in the bank sediment average (μg/g). Thus, it seems that the tributaries reveal a higher statistical correlation in the bed than does the

Arkansas River. More data are needed to better establish the magnitude, variability, and inter-relationships of Se species in the water column, bed sediments, and banks of the stream system.

Results of the sorbed and residual Se analysis highlight the need for comprehensive studies to better characterize the seasonal variability. It is apparent that Se concentrations are typically higher in the tributaries than in the Arkansas River in both the bed and the banks. Sampled Se in the Arkansas River is higher in sediments of the river banks than in the river bed. However, in the tributaries the higher amounts of Se are found in the bed than in the banks on average.

The OTIS-MULTI stream solute reaction model has been successfully updated with a Se module detailing the cycling of Se in surface water. The various components of Se cycling modeled in OTIS-MULTI are described further below. Algae and aquatic plants consume SeO_4 and SeO_3 in the water system. When algae and aquatic plants die they produce organic Se either in the form of SeMet or other organic Se. SeMet and other organic Se can settle into the channel bed or banks, mineralize into SeO_4, and volatilize. If mineralized into SeO_4, certain types of bacteria can continue to convert SeO_4 into SeO_3, or algae and aquatic plants can consume the SeO_4. Alternatively, SeO_4 can also be volatized. SeO_3 can also be converted to elemental Se, volatilized, or taken up by algae and aquatic plants. Elemental Se is usually converted to selenide. Selenide exists in many forms and for this model is predominantly in the inorganic state as seleno-pyrite or as other Se-bearing species. The performance of the revised model is not addressed in this thesis but remains to be validated and tested for the LARV.

The MODFLOW-UZF and UZF-RT3D models, calibrated and tested against baseline data for the USR, were applied to evaluate the effectiveness of alternative BMPs to reduce groundwater Se concentrations and Se mass loading to the stream system. The scenarios tested

included the following individual scenarios: reduced fertilizer (RF10, RF20, RF30), lease fallowing (LF5, LF10, LF15), reduced irrigation (RI10, RI20, RI30), canal sealing (CS40, CS60, CS80), and enhanced riparian buffer zone (ERB low, ERB mid, ERB high). The combination scenarios tested included Basic LF, CS, RF; Intermediate LF, CS, RF; Aggressive LF, CS, RF; Basic RI, CS, RF, Intermediate RI, CS, RF; Aggressive RF, CS, RF; 4 Combo Basic LF, 4 Combo Intermediate LF; 4 Combo Aggressive LF; 4 Combo Basic RI, 4 Combo Intermediate RI; and 4 Combo Aggressive RI. In total, twenty-seven scenarios were tested. The three most effective scenarios out of all scenarios were 4 Combo Aggressive RI (50.4%), 4 Combo Aggressive LF (46.2%), and Aggressive RI, CS, RF (39.2%) (Table 5-1). The three most effective individual scenarios are RI 30 and ERB both at 14.4% and LF25 at 13.0%. The least effective individual scenarios were CS40 (-1.9%), CS60 (1.3%), and RI10 (2.5%). Using Table 4-6, the most effective at reducing the average SeO_4 concentration occurred for the CS80 in the USR. The least effective at reducing the average SeO4 concentration of groundwater was LF15 for the entire region.

Further sampling of Se species in the LARV would better define seasonality and spatial variability of Se cycling. Where possible, the thickness of stream bed sediments should be measured. Samples for sorbed and reduced Se should be taken at greater depths to better understand the total Se sequestered and the potential for re-entrainment under higher flows or oxidation states. Attendant data on DO and NO_3 concentrations should continue to be gathered to allow further exploration of the effects of redox reactions on Se cycling in the water column and sediments.

The OTIS-MULTI model, revised to incorporate the Se reaction equations, must be calibrated and tested using past dissolved Se data along with the data presented here on both Se

and algae in the waters and sediments of the LARV stream network. A sensitivity analysis should be performed to determine which parameters of the model are most influential on simulated Se concentrations, so these parameters can be prioritized for refinement. Further investigation of the sediment and water interactions, especially sorption, reduction, settling, and re-entrainment, should be undertaken so that the cyclic water column-sediment interaction can be better represented in OTIS-MULTI.

Several of the considered BMPs need to be studied further. The reason why the simulated CS40 BMP results indicated an increase in Se mass loading to the river should be examined. Modeling of the ERB scenarios should be improved by exploring how to better parameterize the impacts of altered plant mixes, organic matter composition, and size of the riparian corridor on reactions (sorption, chemical reduction, and volatilization). Rather than assuming uniform BMP implementation over the LARV, BMPs should be defined and simulated to target "hotspots" of Se sourcing and transport to achieve more cost-effective remediation action.

An ultimate aim of the research in the LARV is to create, test, and apply a comprehensive regional-scale groundwater-surface water flow and reactive transport model that links OTIS-MULTI-QUAL2E, along with the SFR module in MODFLOW, with the newly-developed MODFLOW-UZF-RT3D groundwater model. This interconnected model will account for Se and NO_3 cycling and transport in agricultural groundwater systems, will simulate daily mass transfer of chemical species between the aquifer and the stream network, and will account for the consequent reactive transport within the stream network. This allows for prediction of the spatial and temporal distribution of Se and NO_3 concentrations in the aquifer and within the Arkansas River and its tributaries. Moreover, accounting for mass transport in both groundwater and

surface water, as well as the interaction between these zones, will enable exploration of the potential effect of alternative BMPs in lowering concentrations toward compliance with regulatory standards and performance goals.

References

Babcock, B. A. (1992). The effects of uncertainty on optimal nitrogen applications. *Review of Agricultural Economics, 14*(2), 271-280.

Bailey, R. (2012). Regional selenium cycling in an irrigated agricultural groundwater system: conceptualization, modeling, and mitigation. Colorado State University. Dissertation.

Bailey, R. T., Gates, T. K., & Ahmadi, M. (2014). Simulating reactive transport of seleium coupled with nitrogen in a regional-scale irrigated groundwater system. *J. Hydrol., 515*, 29-46.

Bailey, R., Hunter, W. J., & Gates, T. (2012). The influence of nitrate on selenium in irrigated agricultural groundwater systems. *J. of Environ. Qual.*, 783-792.

Bailey, R., Morway, E., Niswonger, R., & Gates, T. (2013). Modeling variably saturated multispecies reactive groundwater solute transport with MODFLOW-UZF and RT3D. *Groundwater, 51*(5), 752-761.

Bailey, R., Romero, E., & Gates, T. (2015). Assessing best management practices for remediation of selenium loading in groundwater to streams in an irrigated region. *J. of Hydro.*, 341–359.

Banuelos, G., Zayed, A., Terry, N., Wu, L., & Akohoue, S. (1996). Accumulation of selenium by different plant species grown under increasing sodium and calcium chloride salinity. *Plant Soil*, 49-59.

Barceloux, D. (1999). Selenium. *J Toxicol Clin Toxicol, 37*(2), 145-72.

BarYosef, B., & Meek, D. (1987). Selenium sorption by kaolinite and montmorillonite. *Soil Sci.*, 11-19.

Benson, S. (1990). Influence of nitrate on the mobility and reduction kinetics of selenium in groundwater systems. In W. Frankenberger Jr., & R. Engberg (Eds.), *Enviromental Chemistry of Selenium* (pp. 437-457). New York, New York, USA: Marcel Dekker.

Beytut, E., Karatas, F., & Beytut, E. (2002). Lambs with white muscle disease and selenium content of soil and meadow hay in the region of Kars, Turkey. *Vet. J., 163*, 214-7.

Birkinshaw, S., & Ewen, J. (2000). Nitrogen transformation component for SHETRAN catchment nitrate transport modelling. *Journal of Hydrology*, 1-17.

Bowie, G. L., Sanders, J. G., Riedel, G., & Gilmour, C. C. (1996). Assessing selenium cycling and accumulation in aquatic ecosystems. *Water, Air, and Soil Pollution, 90*, 93-104.

Brendle, D. (2002). *Evaluation of possible alternatives to lower the high water table of St. Charles Mesa, Pueblo County, Colorado.* Water-Resources Investigations Report 01-4190.

Burkhalter, J., & Gates, T. (2005). Agroecological impacts from salinization and waterlogging in an irrigated river valley. *J. Irrig. Drain. Eng., 131*(2), 197-209.

Burkhalter, J., & Gates, T. (2006). Evaluating regional solutions to salinization and waterlogging in an Irrigated River Valley. *J. Irrig. Drain. Eng., 132*(1), 21-30.

Burwell, R. E., Schuman, G. E., Saxton, K. E., & Heinemann, H. G. (1976). Nitrogen in subsurface discharge from agricultural watersheds. *Journal of Environmental Quality, 5*(3), 325-329.

Chapman, P. M. (2010). *Ecological Assessment of Selenium in the Aquatic Environment.* United State of America: SETAC Press.

Chau, Y., Wong, P., & Silverberg, B. (1976). Methylation of selenium in the aquatic environment. *Science*, 1130-1131.

Depth-Integrating Samplers. (2009). Retrieved from Rickly Hydrological Company: http://www.rickly.com/ss/depth-integrating-samplers.htm

Doherty, J. (2002). *Manual for PEST, fifth ed.* Watermark Numerical Computing.

Edwards, T. K., & Glysson, G. D. (1999). *Field Methods for Measurment of Fluvial Sediment.* U.S. Geological Survey, Reston, Virginia.

Elhaddad, A., & Gacia, L. (2008). Surface energy balance-based model for estimating evapotranspiration taking into account spatial variability in weather. *J. Irrig. Drain. Eng.*

Fan, T. W.-M., Teh, S. J., Hilton, D. E., & Hagashi, R. M. (2002). Selenium biotransformations into proteinaceous forms by foodweb organisms of selenium-laden drainage waters in California. *Aquatic Toxicology, 57*, 65-84.

Fernandez-Martinez, A. a. (2009). Selenium environmental cycling and bioavailability: a structural chemist point of view. *Environ. Sci. Biotechnol., 8*, 81-110.

Fio, J. F., & Deverel, S. (1991). Selenium mobility and distribution in irrigated and nonirrigated alluvial soils. *Soil Sci. Soc. Am. J., 55*, 1313-1320.

Fordyce, F. (2007). Selenium geochemistry and health. *Ambio, 36*, 94-97.

Frankenberger Jr., W. T., & Arshad, M. (2001). Bioremediation of selenium-contaminated sediments and water. *BioFactors*, 241-254.

Freeman, J. L., Tamaoki, M., Stushnoff, C., Quinn, C. F., Cappa, J. J., & Devonshire, J. (2010). Molecular mechanisms of selenium tolerance and hyperaccumulation in stanleya pinnata. *Plant Physiology, 153*, 1630-1652.

Gates, T. K., Cody, B. M., Donnelly, J. P., Herting, A. W., Bailey, R. T., & Mueller Price, J. (2009). Assessing selenium contamination in the irrigated stream-aquifer system of the Arkansas River, Colorado. *J. Environ. Qual.*, 2344-2356.

Gates, T., Burkhalter, J., Labadie, J., Valliant, J., & Broner, I. (2002). Appraising options to reduce shallow groundwater tables and enhance flow conditions over regional scales in an irrigated alluvial aquifer. *Journal of Hydrology, 495*, 216-237.

Gates, T., Garcia, L., Hemphill, R., Morway, E., & Elhaddad, A. (2012). *Irrigation practices, water consumption, & return flows in Colorado's lower Arkansas River valley: field and model investigations.* Technical Completion Report No. 221, Colorado Water Institute; Technical Report No. TR12-10, Colorado Agricultural Experiment Station.

Goff, K., Lewis, M., Person, M., & Konikow, L. (1998). Simulated effects of irrigation on salinity in the Arkansas River Valley in Colorado. *Ground Water, 36*(1), 76–86.

Gupta, U. C., & Gupta, S. C. (2000). Selenium in soils and crops, its deficiencies in livestock and humans: implications for management. *Commun. Soil Sci. Plant Anal., 31*(11-14), 1791-1807.

Hamer, C., Halbert, B., Webster, M., & Scharer, J. (2012). Assessment of model adequacy and parameter identifiability for predicting contaminant transport in the Beverlodge Lake area. In *Water Pollution XI* (pp. 164-159). Canada.

Hamilton, S. J. (2004). Review of selenium toxicity in the aquatic food chain. *Sci. of the Total Environ., 326*(1-3), 1-31.

Hamilton, S., Buhl, K., & Lamothe, P. (2002). *Selenium and other trace elements in water, sediment, aquatic plants, aquatic invertebrates, and fish from streams in southeastern Idaho near phosphate mining operations: June 2000.* USGS Western U.S. Phosphate Project.

Herbel, M. J. (2003). Reduction of elemental selenium to selenide: experiments with anoxic sediments and bacteria that respire se-oxyanions. *Geomicrobiology Journal, 20*, 587–602.

Hodson, P. V. (1988). The effect of metal metabolism on uptake, disposition and toxicity in fish. *Aquatic Toxicology*, 3-18.

Hoffman, D., Ohlendorf, H., & Aldrich, T. (1988). Selenium teratogenesis in natural populations of aquatic birds in Central California. *Arch. Environ. Contam. Toxicol., 17*, 519 –525.

Hoffman, G. J., Evans, R. G., Jensen, M. E., Martin, D. L., & Elliott, R. L. (2007). Design and operation of farm irrigation systems. *Am. Soc. Agric. Biol. Engineers*.

Howell, T. A. (2003). Irrigation efficiency. In *Encyclopedia of water science* (pp. 467-472). New York: Marcel Dekker, Inc.

Inter-Fluve. (2014). *RTK Survey Protocol*. Retrieved from http://www.interfluve.com/

Irrigation Techniques. (2014, March 17). Retrieved from USGS (U.S. Geological Survey): http://water.usgs.gov/edu/irmethods.html

Ivahnenko, T., Ortiz, R., & Stogner, R. S. (2013). *Characterization of streamflow, water quality, and instantaneous dissolved solids, selenium, and uranium loads in selected reaches of the Arkansas River, southeastern Colorado, 2009-2010.* U.S. Geological Survey.

Janda, J. M., & Fleming, R. W. (1978). Effect of selenate toxicity on soil mycoflora. *Journal of Environmental Science and Health Part A*, 697-706.

Ježek, P., Škarpa, P., Lošák, T., Hlušek, J., Jůzl, M., & Elzner, P. (2012). Selenium – An important antioxidant in crops biofortification. (P. M. El-Missiry, Ed.) *Antioxidant Enzyme*.

Ji, Z.-G. (2008). *Hydrodynamics and water quality: modeling rivers, lakes, and estuaries.* New Jersey: John Wiley & Sons, Inc.

Johnsson, H., Bergstrom, L., Jansson, P., & Paustian, K. (1987). Simulated nitrogen dynamics and losses in a layered agricultural soil. *Agriculture, Ecosystems & Environment, 18*(4), 333-356.

Julien, P. Y. (2010). *Erosion and Sedimentation.* Cambridge: Cambridge University Press.

Kabata-Pendias, A., & Mukherjee, A. B. (2007). *Trace elements from soil to human.* Springer.

Karlson, U., & Frankenberger Jr., W. (1988). Determination of Gaseous Selenium-75 Evolved from Soil. *Soil Sci. Soc. Am. J.* , 678-681.

Konikow, L., & Person, M. (1985). Assessment of long-term salinity changes in an. *irrigated stream-aquifer system. Water Resour. Res., 21*(11), 1611–1624.

Kulp, T. R., & Pratt, L. M. (2004). Speciation and weathering of selenium in Upper Cretaceous chalk and shale from South Dakota and Wyoming, USA. *Geochimica et Cosmochimica Acta, 68*(18), 3687-3701.

Lemly, D. A. (1999). Selenium transport and bioaccumulation in aquatic ecosystmes: A proposal for water quality criteria based on hydrological units. *Ecotoxicol. Environ. Saf., 42*, 150-156.

Levander, O., & Burk, R. (2006). Update of human dietary standards for selenium. In *Selenium: Its Molecular Biology and Role in Human Health.*

Lindauer, I. E. (1983). A comparison of the plant communities of the South Platte and Arkansas River drainages in eastern Colorado. *The Southwestern Naturalist*, 249-259.

Losi, M., & Frankenberger Jr., W. (1997). Bioremediation of selenium in soil and water. *Soil Science*, 692-702.

Losi, M., & Frankenberger Jr., W. (1998). Microbial oxidation and solubilization of precipitated elemental selenium in soil. *J. Environ. Qual.*, 836-843.

Maher, W., Roach, A., Doblin, M., Fan, T., & Foster, S. (2010). Environmental Sources, Speciation, and Partitioning of Selenium. In P. M. Chapman, *Ecological Assessment of Selenium in the Aquatic Environment* (pp. 64-68). Pensacola: Society fo Environemental Toxicology and Chemistry (SETAC).

Martin, C. (2013). *Uncertainty in measuring seepage from earthen irrigation canals using the inflow-outlfow method and in evaluating the effectiveness of polyacrylamide applications for seepage reduction.* Fort Collins, Colorado: M.S. Thesis, Dept. of Civil and Env. Eng. Colorado State University.

Martin, C. A., & Gates, T. K. (2014). Uncertainty of canal seepage losses estimated using flowing water balance with acoustic Doppler devices. *Journal of Hydrology*, 746–761.

Minaev, V., Timoshenkov, S., & Kalugin, V. (2005). Structural and phase transformations in condensed selenium. *J. Optoelectron. Adv. Mater., 7*, 1717-1741.

Mirbagheri, S., Tanji, K., & Rajaee, T. (2008). Selenium transport and transformation modelling in soil columns and ground water contamination prediction. *Hydrological Processes*, 2475-2483.

Morway, E. D., Gates, T. K., & Niswonger, R. G. (2013). Appraising options to reduce shallow groundwater tables and enhance flow conditions over regional scales in an irrigated alluvial aquifer system. *Journal of Hydrology, 495*, 216-237.

Neitsch, S., Arnold, J., & Kiniry, J. (2011). *Texas Water Resources Institute Technical Report No. 406.* College Station, Texas: Texas A&M Univeristy System.

Niemann, J., Lehman, B., Gates, T., Hallberg, N., & Elhaddad, A. (2011). Impact of shallow groundwater on evapotranspiration losses from uncultivated land in an irrigated river valley. *J. Irrig. Drain. Eng.*, 201-512.

Niswonger, R. G., Panday, S., & Ibaraki, M. (2011). *MODFLOW-NWT, a Newton formulation for MODFLOW-2005.* U.S. Geological Survey Techniques and Methods 6–A37.

Niswonger, R. G., Prudic, D. E., & Regan, R. S. (2006). *Documentation of the unsaturated-zone flow (UZF1) package for modeling unsaturated flow between the land surface and the water table with MODFLOW-2005.* US Department of the Interior, US Geological Survey.

Ohlendorf, H. M., Hoffman, D. J., Saiki, M. K., & Aldrich, T. W. (1986). Embryonic mortality and abnormalities of aquatic birds: apparent impacts of selenium from irrigation drainwater. *Sci. Total Environ., 52,* 49 –63.

Oremland, R. S., Steinberg, N. A., Maest, A. S., Miller, L. G., & Hollibaugh, J. T. (1990). Measurement of in situ rates of selenate removal by dissimilatory bacterial reduction in sediments. *Environ. Sci. Technol.,* 1157-1164.

Osmundson, B. C., May, T. W., & Osmundson, D. B. (2000). Selenium concentrations in the Colorado pikeminnow (Ptychocheilus lucius): relationship with flows in the upper Colorado River. *Arch. Environ. Contam. Toxicol., 38,* 479-485.

Pearson's Correlation Coefficient r (Critical Value). (n.d.). Retrieved 2014, from Statistics in Psychology and Pedagogy: psystat.at.ua/Articles/Table_Pearson.PDF

Periodic Table-Selenium. (2014). Retrieved from Royal Society of Chemistry: http://www.rsc.org/periodic-table/element/34/selenium

Person, M., & Konikow, L. (1986). Recalibration and predictive reliability of a solute transport model of an irrigated stream-aquifer system. *J. Hydrol., 87*(1-2), 145-165.

Pilon-Smits, E. A., & Quinn, C. F. (2010). Selenium metabolism in plants. In R. Hell, & R.-R. Mendel (Eds.), *Cell Biology of Metals and Nutrients* (pp. 225-241).

Pilon-Smits, E., de Souza, M., Amini, A., Bravo, R., Payabyab, S., & Terry, N. (1999). Selenium volatilization and accumulation by twenty aquatic plants species. *J. of Environ. Qual.,* 1011-1018.

Poeter, E. P., Hill, M. C., Banta, E. R., Mehl, S., & Christensen, S. (2005). *Ucode_2005 and six other computer codes for universal sensitivity analysis, calibration, and uncertainty evaluation: US geological survey techniques and methods 6-A11*. US Geological Survey.

Presser, T., Piper, D., Bird, K., Skorupa, J., Hamilton, S., Detwiler, J., et al. (2004). Ch. 11 The phosphoria formation: A model for forecasting global selenium sources to the environment. *Handbook of Exploration and Environmental Geochemistry*, 299-319.

Presser, T., Sylvester, M., & Low, W. (1994). Bioaccumulation of selenium from natural geologic sources in western states and its potential consequences,". *Environ. Management, 18*(3), 423-436.

Pritchett, J., Thorvaldson, J., & Frasier, M. (2008). Water as a crop: limited irrigation and water leasing in Colorado. *Review of Agricultural Economics, 30*, 435–444.

Rajabli, J. N., Mirbagheri, S. A., Hasani, A. H., & Javid, A. H. (2013). Two-dimensional finite differences model for selenium transport and transformation in soil column and ground water contamination prediction (Case study: Gonbad-e Kavous site). *European Journal of Experimental Biology*, 291-300.

Runkel, R. (1998). *One-Dimensional Transport with Inflow and Storage (OTIS): A solute transport model for streams and rivers.* U.S. Geological Survey Water-Resources Investigations Report 98-4018, 73 p.

Scharf, P. C., Kitchen, N. R., Sudduth, K. A., Davis, J. G., Hubbard, V. C., & Lory, J. A. (2005). Field-scale variability in optimal nitrogen fertilizer rate for corn. *Agronomy Journal, 97*(2), 452.

Seby, F., Potin-Gautier, M., Giffaut, E., Borge, G., & Donard, O. (2001). A critical review of thermodynamic data for selenium species at 25°C. *Chem. Geol., 174*, 173-194.

Shanafield, M., Pohll, G., & Susfalk, R. (2010). Use of heat-based vertical fluxes to approximate total flux in simple channels. *Water Resour. Res.*

Solomon, K. H., El-Gindy, A., & Ibatullin, S. R. (2007). Planning and System Selection. In G. J. Hoffman, R. G. Evans, M. E. Jensen, D. L. Martin, & R. L. Elliott, *Design and Operation of Farm Irrigation Systems* (pp. 57-75). American Society of Agricultural and Biological Engineers.

SonTek/YSI Incorporated. (2007). *FlowTracker Handheld Technical Manual Firmware Version 3.3 Software Version 2.20 featuring SmartQC.*

Sorensen, E. M., Cumbie, P. M., Bauer, T. L., Bell, J. S., & Harlan, C. W. (1984). Histopathological, hematological, condition-factor, and organ weight changes associated with selenium accumulation in fish from Belews Lake, North Carolina. *Arch. Environ. Contam. Toxicol.*, 153-162.

Steinberg, N. A., & Oremland, R. S. (1990). Dissimilatory selenate reduction potentials in a diversity of sediment types. *Appl. Environ. Microbiol., 56*, 3550-3557.

Stephens, D. W., Waddell, B., Peltz, L. A., & Miller, J. B. (1992). *Detailed study of selenium and selected elements in water bottom sediment, and biota associated with irrigation drainage in the middle Green River basin.* Salt Lake City, Utah: U.S. Geological Survey Water-Resources Investigations Report 92-4084.

Susfalk, R., Sada, D., Martin, C., Young, M., Gates, T., Rosamond, C., et al. (2008). *Evaluation of linear anionic polyacrylamide (LA-PAM) application to water delivery canals for seepage reduction.* DHS Publication No. 41245.

Swihart, J., & Haynes, J. (1999). *Canal-lining demonstration project.* U.S. Department of the Interior. Denver: Bureau of Reclamation.

Terry, N., Zayed, A., de Souza, M., & Tarun, A. (2000). Selenium in higher plants. *Annu. Rev. Plant Physiol. Plant Mol. Biol*, 401-432.

Thompson-Eagle, E., & Frankenberger Jr., W. (1991). Selenium biomethylation in an alkaline, saline environment. *Water Reseach*, 231-240.

USEPA. (1994). *Method 200.8—Determination of trace elements in waters and wastes by inductively coupled plasma-mass spectometry. Revision 5.4.*

USEPA. (2016). *Ground Water and Drinking Water: Table of Regulated Drinking Water Contaminants*. Retrieved 10 23, 2016, from EPA US Environmental Protection Agency: https://www.epa.gov/ground-water-and-drinking-water/table-regulated-drinking-water-contaminants

USHHS. (2003). *Toxicological Profile for Selenium.* United States Department for Health and Human Services.

Weres, O., Bowman, H. R., Goldstein, A., Smith, E. C., Tsao, L., & Harnden, W. (1990). The effect of nitrate and organic matter upon mobility of selenium in groundwater and in a water treatment process. *Water, Air, and Soil Pollution*, 251-272.

Williams, K. T., & Byers, H. G. (1935). Occurrence of selenium in the Colorado River. *Industrial and Engineering Chemistry*, 431-432.

Wu, L., & Huang, Z.-Z. (1991). Selenium accumulation and selenium tolerance of salt grass from soils with elevated concentrations of selenium and salinity. *Ecotoxicology and Environmental Safety*, 267-282.

Yeh, G., & Tripathi, V. (1989). A critical evaluation of recent developments in hydrogeochemical transport models of reactive multichemical components. *Water Resources Research, 25*(1), 93–108.

Young, M. H., Tappen, J. J., Miller, G. C., Carroll, S., & Susfalk, R. B. (2007). *Risk characterization: using linear anionic polyacrylamide (LA-PAM) to reduce water seepage from unlined water delivery canal systems.* DHS Publication No. 41226.

Zalislanski, P., & Zavarin, M. (1996). Nature and rates of selenium transformations: A laboratory study of kesterson reservoir soils. *Soil Sci. Soc. Am. J.*, 791-800.

Appendix A: Field Sample Locations and Field Notes

Location 1: Arkansas River north of Manzanola off of Highway 207 (Surface Water Location Point Number 164)

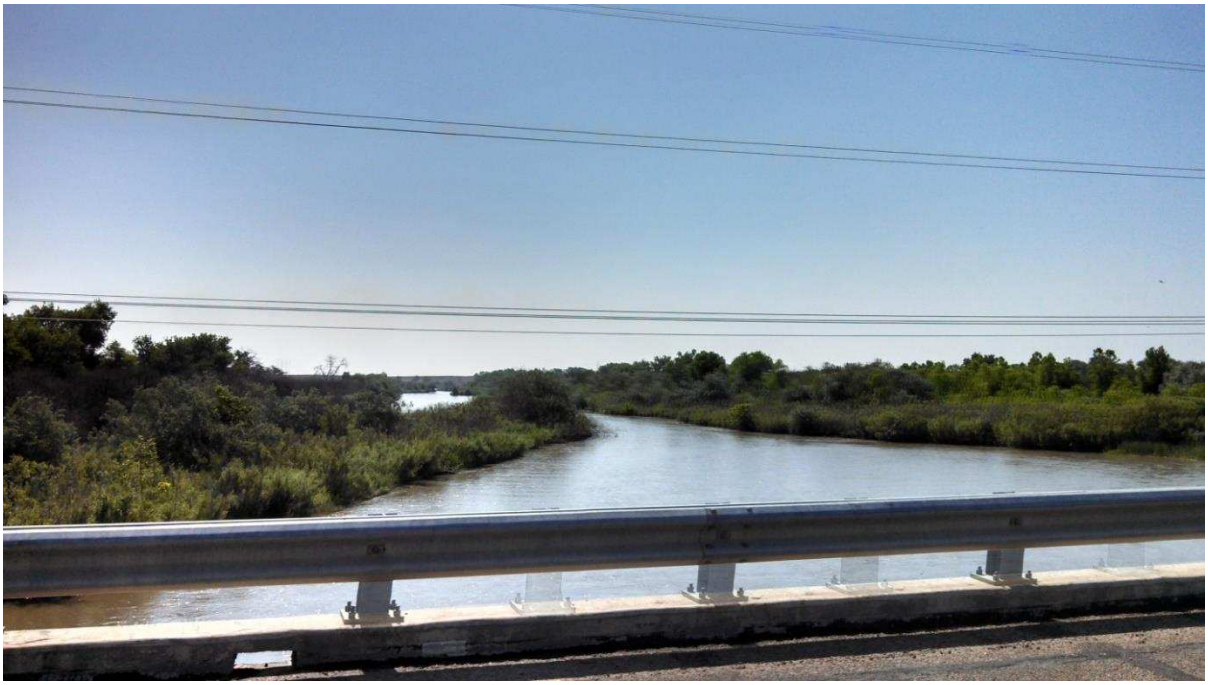

June 2013

Location 2: Patterson Hollow at the intersection of County Road HH.5 and County Road 16 near the Rocky Ford Highline Canal

March 2013

Location 3: Arkansas River in between Manzanola and Rocky Ford off of Highway 71 (Surface Water Location Point Number 141)

March 2013

Location 4: Arkansas River north of Rocky Ford off of County Road 21 (Surface Water Location Point 12)

March 2013

Location 5: Timpas Creek off of Highway 10 south of Rocky Ford (Surface Water Location Point 54)

March 2013

Location 6: Timpas Creek off of Highway 50 just west of Swink (Surface Water Location Point 62)

March 2013

March 2013

Location 7: Arkansas River at Swink off of County Road 24.5 (Surface Water Location 127)

March 2013

Location 8: Crooked Arroyo off of Highway 10 between Swink and La Junta (Surface Water Location 73)

Location 9: Crooked Arroyo off of Highway 50 near the La Junta Walmart (Surface Water Location 74)

August 2013

Location 10: Arkansas River just upstream of Anderson Arroyo approaching from the south bank

August 2013

Location 11: Anderson Creek north of Highway 50 and Anderson St. in La Junta (Surface Water Location 75)

March 2013

Location 12: Arkansas River at the La Junta Gauging Station off of Highway 109 (Surface Water Location 95)

March 2013

Location 14: Arkansas River Downstream of King Arroyo

August 2013

August 2013

Location 15: Arkansas River at Bent's Fort (Surface Water Location 162)

March 2013

Location 16: Arkansas River near Jones Ditch

March 2013

Location 17: Horse Creek off of Highway 194 between Las Animas and La Junta (Surface Water Point 207)

March 2013

Location 18: Arkansas River at the Las Animas gauge station off of Highway 50 (Surface Water Point 201)

August 2013

Table A-1. La Junta Wastewater Treatment Plant-King Arroyo Effluent Discharge Information in June 2013

Day of June	FLOW (MGD Daily)	PH S.U.	TEMP DEG C	RO RAW Se, PD µg/L	RO Conc. Se, PD µg/L	RO Finished Se, PD µg/L	Plant Inf. Se, PD µg/L	Plant Eff Se, PD µg/L	Combined Se., PD µg/L	Nh3 N Ammonia mg/L	NO3/NO2 as N mg/L	PHOS TL Wet mg/L
4	0.736	7.33	18.4	12.4	27.0	2.2	6.2	6.4	18.9			
13	0.760	7.49	18.0							0.43	0.39	0.6
17	0.875	7.54	18.7									
18	0.828	7.43	19.1									
19	0.824	7.01	20.8									

Sample Blank Chain of Custody

Colorado State University
Department of Civil Engineering
1372 Campus Delivery
Fort Collins, CO 80526-1372

COC # - (Year-Month-Day)

CHAIN OF CUSTODY RECORD
Arkansas River Assessment
Lower Basin

Sample Collector(s): Title: Telephone No. E-mail address:

Field ID No.	Date	Est. Time	Sample Type (GW or SW)	Lab ID No.	Type of Analysis	Comments

I hereby certify that I received, properly handled, and disposed of these samples as noted belc

Relinquished by: (Signature)	Date/Time	Received by: (Signature)
Relinquished by: (Signature)	Date/Time	Received by: (Signature)
Relinquished by: (Signature)	Date/Time	Received for Laboratory by: (Signature)

Disposition of Unused Portion of Sample:

Dispose X Retain for _____ days

Return _____ Other _____

F = Field filtered to 0.45 μm
P = Field preserved with nitric acid to pH < 2
U = Unfiltered sample

Page 1 of 1

Sample Chain of Custody

Colorado State University
Department of Civil Engineering
1372 Campus Delivery
Fort Collins, CO 80526-1372

COC # - 20140324
(Year-Month-Day)

CHAIN OF CUSTODY RECORD
Arkansas River Assessment
Lower Basin

Sample Collector(s):	Title:	Telephone No.	E-mail address:
E. Romero	**Research Assist.**	**970-491-5387**	eromero1@engr.colostate.edu

Field ID No.	Date	Est. Time	Sample Type (GW or SW)	Lab ID No.	Type of Analysis	Comments
ARK 127	3/17/2014	20:45	**SW**		**Uranium**	**F, P**
ARK 95	3/17/2014	6:00	**SW**		**Uranium**	**F, P**
ARK 95-1	3/17/2014	7:45	**SW**		**Uranium**	**F, P**
ARK 164	3/18/2014	13:11	**SW**		**Uranium**	**F, P**
ARK 201	3/18/2014	13:56	**SW**		**Uranium**	**F, P**
Patt	3/18/2014	14:30	**SW**		**Uranium**	**F, P**
Horse	3/19/2014	15:11	**SW**		**Uranium**	**F, P**
BLK-1	3/19/2014	16:11	**SW**		**Uranium**	**F, P**
Timp-62	3/19/2014	16:59	**SW**		**Uranium**	**F, P**
Crook	3/19/2014	17:15	**SW**		**Uranium**	**F, P**

I hereby certify that I received, properly handled, and disposed of these samples as noted be

Relinquished by: (Signature)	Date/Time	Received by: (Signature)
Relinquished by: (Signature)	Date/Time	Received by: (Signature)
Relinquished by: (Signature)	Date/Time	Received for Laboratory by: (Signature)

Disposition of Unused Portion of Sample:

Dispose **X** Retain for _____ days

Return _____ Other _____

F = Field filtered to 0.45 μm
P = Field preserved with nitric acid to pH < 2
U = Unfiltered sample

Page 1 of 1

Cross-Section Example Pages

#164

* Hard access
* 1st sample near

Surface Location: Arkansas River near ~~near Well 15~~ near P-164 Date: 3/16/13

Sample Name: ARKUPPAT Arrival Time: 3:25

Technicians: ECR CMW CDW Departure Time: 3:45

Site Map

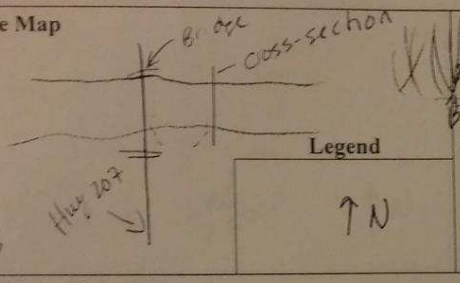

Cross Section

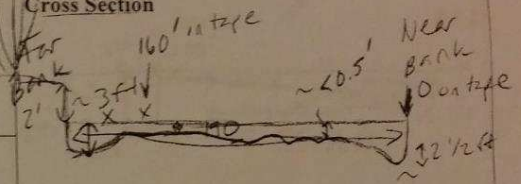

Water Sample Run A Staff Gage Height = 1.2'

	1	2	3	4	5	6
DO	10.49	9.88	9.63	9.47	9.44	9.56
Temp (C)	13.92	14.12	14.32	14.41	14.64	14.80
Cond (µS/cm)	1.181	1.183	1.113	1.171	1.177	1.225
pH	8.22	8.24	8.26	8.26	8.27	8.27
ORP (mV)	156.8	156.8	156.9	157.3	158.4	158.3

Water Sample Run B Staff Gage Height = 1.2' @ 160'

	1	2	3	4	5	6
DO	9.56	9.37	9.38	9.37	9.48	9.70
Temp (C)	14.14	14.35	14.48	14.59	14.72	14.82
Cond (µS/cm)	1.181	1.159	1.174	1.148	1.159	1.223
pH	8.28	8.29	8.28	8.39	8.28	8.28
ORP (mV)	157.3	156.6	158.1	157.7	157.1	158.6

Sediment/Soil Samples

	Initial Sample "A"		Duplicate Sample "B"	
	Recovered	Name	Recovered	Name
Near Bank				
1				
2				
3				
4				
Far Bank				

Notes
- well vegetated banks (at 100 m)
- good riparian zone

Cross-Section Example Pages

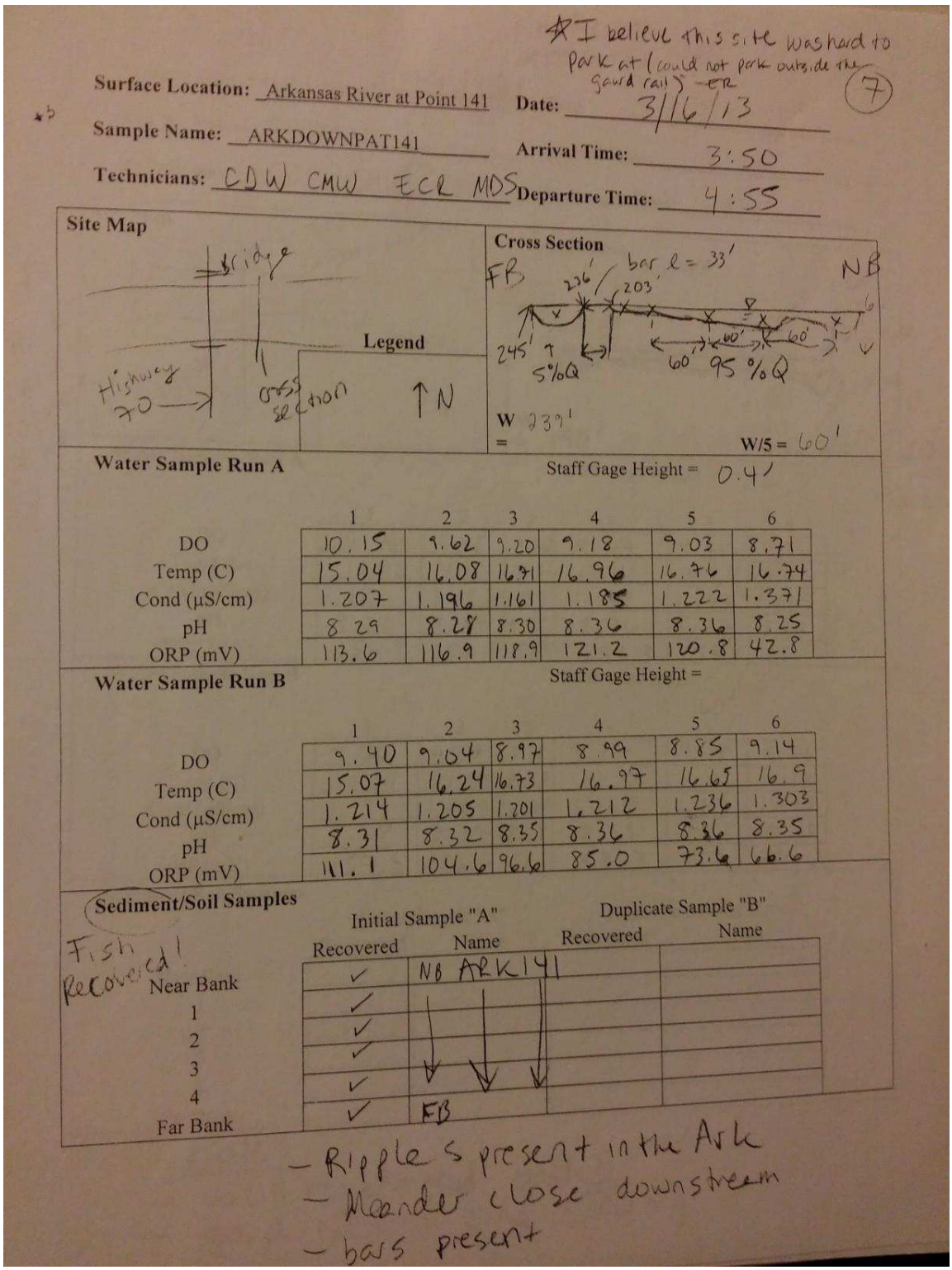

★I believe this site was hard to park at (could not park outside the guard rail) -ER

(7)

Surface Location: Arkansas River at Point 141 **Date:** 3/6/13

Sample Name: ARKDOWNPAT141 **Arrival Time:** 3:50

Technicians: CDW CMW ECR MDS **Departure Time:** 4:55

Site Map

Bridge

Legend

Highway 70 → Cross section ↑N

Cross Section

FB 226' bar ℓ = 33' 203' NB

245' 5%Q 60' 95 %Q 60' 60'

W 239' = W/5 = 60'

Water Sample Run A Staff Gage Height = 0.4'

	1	2	3	4	5	6
DO	10.15	9.62	9.20	9.18	9.03	8.71
Temp (C)	15.04	16.08	16.71	16.96	16.76	16.74
Cond (µS/cm)	1.207	1.196	1.161	1.185	1.222	1.371
pH	8.29	8.28	8.30	8.36	8.36	8.25
ORP (mV)	113.6	116.9	118.9	121.2	120.8	42.8

Water Sample Run B Staff Gage Height =

	1	2	3	4	5	6
DO	9.40	9.04	8.97	8.99	8.85	9.14
Temp (C)	15.07	16.24	16.73	16.97	16.65	16.9
Cond (µS/cm)	1.214	1.205	1.201	1.212	1.236	1.303
pH	8.31	8.32	8.35	8.36	8.36	8.35
ORP (mV)	111.1	104.6	96.6	85.0	73.6	66.6

Sediment/Soil Samples

Fish Recovered!

	Initial Sample "A" Recovered	Initial Sample "A" Name	Duplicate Sample "B" Recovered	Duplicate Sample "B" Name
Near Bank	✓	NB ARK141		
1	✓			
2	✓			
3	✓			
4	✓			
Far Bank	✓	FB		

- Ripples present in the Ark
- Meander close downstream
- bars present

Appendix B: Field Data Results

Table B-1. Se laboratory results

Location	Trip	Total Selenium, Se (Fluorometric)	Selenite, SeSO3 (Fluorometric)	Total Selenium, Se (ICP)	Total Recoverable Selenium, Se (Fluorometric)
		(ppb)	(ppb)	(ppb)	(ppb)
1	1	13.8	1.69	17	
	2	6.64	2.05	6.9	
	4	13	1.36		13.7
2	1	19	1.26	18	
	2	11.7	2.36	12	
	4	21.1	0.895		20.5
3	1	13.1	1.59	15	
	2	6.59	1.97	6.7	
4	1	12.6	1.7	12	
	2	6.61	2.15	7	
	2 Duplicate	6.1	1.5	7.6	
5	1	20.7	1.23	21	
	2	9.89	1.99	10	
6	1	20.7	1.6	29	
	2	10.5	2.07	9.4	
	4	18.5	1.55		17.6
7	1	12.8	0.845	25	
	2	7.14	1.88	7.2	
	4	13.4	1.25		14
8	1	6.04	*0.8*	7.7	
	2	7.38	2.14	8.6	
9	1	8.27	*0.8*	11	
	2	7.07	2	7.8	
9	4	19.2	1.14		19
10	2	6.85	2.48	6.9	
12	1	13.3	1.44	18	
	2	6.76	2.35	8	
	4	14.1	1.21		14.7
	4 Duplicate	13.9	1.31		14.5

Table B-1. Continued

Location	Trip	Total Selenium, Se (Fluorometric) (ppb)	Selenite, SeSO3 (Fluorometric) (ppb)	Total Selenium, Se (ICP) (ppb)	Total Recoverable Selenium, Se (Fluorometric) (ppb)
14	2	6.48	1.62	8.4	
	3	12.2	2.35		12.8
15	1	9.99	1.52	9.5	
	2	7.84	1.4	9.6	
	2 Duplicate	7.78	1.39	8.7	
	3	11.5	4.11		11.7
16	1	9.76	1.37	11	
17	1	11.4	2.25	21	
	2	8.17	3.37	11	
	3	11.2	2.66		11
	4	11.1	1.75		11.5
18	1	12.7	0.971	32	
	2	8.75	2.03	10	
	3	11.3	ND		11.4
	4	13.6	*0.8*		13.6

Note: The Selenite, SeO4 (Fluorometric) column has a detection limit of 0.8. The tests registering less than this value are indicated with italics.

Table B-2. Nitrogen, phosphorous, and uranium laboratory results

		Nitrogen			Phosphorous		Uranium
Location	Trip	Ammonium, NH4-N (WARD) (ppm)	Nitrite, NO_2-N (WARD) (ppm)	Nitrate NO_3-N (WARD) (ppm)	Dissolved Ortho Phosphorus, P (WARD) (ppm)	Total Dissolved Phosphorus, P (WARD) (ppm)	Uranium, U (ICP) (ppb)
1	1	*0.1*	*0.1*	1.2	0.01	0.38	16
	2	*0.1*	*0.1*	0.6	0.04	0.44	8.5
	4	*0.1*	*0.1*	1.8	0.06	0.05	13
2	1	*0.1*	0.2	2.9	0.02	0.36	54
	2	0.5	0.7	2.3	0.21	0.61	37
	4	*0.1*	*0.1*	3.8	0.1	0.04	48
3	1	*0.1*	*0.1*	1.1	0.01	0.37	17
	2	*0.1*	*0.1*	0.5	0.03	0.38	8.9
	2 Duplicate	*0.1*	*0.1*	0.5	0.04	0.41	

Table B-2. Continued

Location	Trip	Ammonium, NH4-N (WARD) (ppm)	Nitrite, NO_2-N (WARD) (ppm)	Nitrate NO_3-N (WARD) (ppm)	Dissolved Ortho Phosphorus, P (WARD) (ppm)	Total Dissolved Phosphorus, P (WARD) (ppm)	Uranium, U (ICP) (ppb)
4	1	*0.1*	*0.1*	1.1	0.01	0.35	20
	2	*0.1*	*0.1*	0.5	0.02	0.4	9
	2 Duplicate	*0.1*	*0.1*	0.5	0.04	0.41	8.8
5	1	*0.1*	0.2	1.8	0.08	0.23	43
	2	0.4	0.3	1.4	0.05	0.47	16
6	1	*0.1*	*0.1*	2.6	0.01	0.22	54
	2	0.6	0.3	1.7	0.04	0.45	16
	4	*0.1*	*0.1*	2.4	0.07	0.02	29
7	1	*0.1*	*0.1*	0.9	0.01	0.34	12
	2	*0.1*	*0.1*	0.5	0.08	0.42	9.3
	4	*0.1*	*0.1*	1.6	0.07	0.04	17
8	1	*0.1*	*0.1*	0.6	0.03	0.23	59
	2	0.4	0.3	1.1	0.27	0.65	14
9	1	*0.1*	*0.1*	0.9	0.04	0.28	60
	2	0.2	*0.1*	0.8	0.08	0.51	14
	4	*0.1*	*0.1*	1.3	0.08	0.08	40
10	2	*0.1*	*0.1*	0.6	0.04	0.42	9.9
12	1	*0.1*	*0.1*	1.2	0.01	0.28	35
	2	*0.1*	*0.1*	0.6	0.05	0.5	9.4
	4	*0.1*	*0.1*	1.9	0.06	0.03	23
	4 Duplicate	*0.1*	*0.1*	1.9	0.06	0.03	
14	2	*0.1*	*0.1*	0.6	0.05	0.53	10
	3	*0.1*	*0.1*	1.5	0.06	0.11	20
15	1	*0.1*	*0.1*	1.3	0.04	0.36	29
	2	*0.1*	*0.1*	1	0.09	0.51	15
	2 Duplicate	0.2	*0.01*	1	0.09	0.5	13
15	3	*0.1*	*0.1*	3.3	0.04	0.22	18
16	1	*0.1*	*0.1*	1	0.01	0.33	30
	2	0.2	*0.1*	1	0.05	0.07	
17	1	*0.1*	*0.1*	0.3	*0.01*	0.26	71
	2	*0.1*	*0.1*	0.4	0.09	0.41	35
	3	*0.1*	*0.1*	0.8	*0.01*	0.36	19
	4	*0.1*	*0.1*	0.1	0.07	0.07	42

Table B-2. Continued

Location	Trip	Ammonium, NH4-N (WARD) (ppm)	Nitrite, NO_2-N (WARD) (ppm)	Nitrate NO_3-N (WARD) (ppm)	Dissolved Ortho Phosphorus, P (WARD) (ppm)	Total Dissolved Phosphorus, P (WARD) (ppm)	Uranium, U (ICP) (ppb)
18	1	*0.1*	*0.1*	0.9	*0.01*	0.31	91
	2	*0.1*	*0.1*	1	0.08	0.47	8.7
	3	0.2	*0.1*	1	0.05	0.07	19
	4	*0.1*	*0.1*	1.1	0.07	0.07	35

Note: The Ammonium, NH4-N (WARD) as well as the Nitrite, NO2-N (WARD) columns have a detection limit of 0.1 so any italicized values are below the detection limit. The Ortho Phosphorus, P (WARD) column has a detection limit of 0.01. The tests registering less than 0.01 are indicated with italics.

Table B-3. All sorbed and residual (precipitated and organic Se) data for all trips sorted by sample point in the Arkansas River and by location

					SORBED SELENIUM DATA								PRECIPITATED AND ORGANIC SELENIUM DATA		
					Lab Results (Water from Soil)			**CALCULATIONS**				Lab Result	**CALCULATIONS**		
Index	**Location**	**Trip**	**Location Within Cross Section**	**Date Collected**	**Total Recoverable Se (µg/L)**	**Selenite (µg/L)**	**Se, Dissolved (SDAL) (µg/L)**	**Total Sorbed Se + Solid Se (µg/g)**	**Sorbed SeO_3 (µg/g)**	**Sorbed SeO_4 (µg/g)**	**Non-Sorbed Se (µg/g)**	**Soil, Total Se (µg/g)**	**Estimate of Precipitated and Organic Se (µg/g)**	**Percent Precipitated and Organic Se %**	**Percent Sorbed Se %**
1	1	1	RB	3/13/2013	62.00	28.40		**0.310**	**0.142**	**0.168**		1.600	1.290	81%	19%
2			BED		8.87	6.29		**0.044**	**0.031**	**0.013**		0.303	0.259	85%	15%
3	1	2	BED	6/19/2013	7.44	6.18		**0.037**	**0.031**	**0.006**		0.292	0.255	87%	13%
4			RB		41.50	25.20		**0.208**	**0.126**	**0.082**		1.280	1.073	84%	16%
5			LB		27.70	14.70		**0.139**	**0.074**	**0.065**		0.708	0.569	80%	20%
6	1	4	BED	3/17/2014	8.16	2.44		**0.041**	**0.012**	**0.029**		0.197	0.156	79%	21%
7	3	1	BED	3/16/2013	11.5	6.94		**0.057**	**0.035**	**0.023**		0.343	0.286	83%	17%
8			RB		23.3	6.54		**0.116**	**0.033**	**0.084**		0.727	0.611	84%	16%
9			LB		52.9	27.8		**0.263**	**0.138**	**0.125**		1.41	1.147	81%	19%
10	3	2	BED	6/19/2013	7.97	7.69		**0.040**	**0.038**	**0.001**		0.299	0.259	87%	13%
11			RB		40.90	29.80		**0.204**	**0.149**	**0.055**		0.944	0.740	78%	22%
12			LB		34.70	23.40		**0.173**	**0.117**	**0.056**		1.130	0.957	85%	15%
13	4	1	BED	3/16/2013	12.4	7.0	11.6	**0.062**	**0.035**	**0.027**	**0.058**	0.3035	0.242	80%	20%
14			LB		62.7	27.1	60.4	**0.315**	**0.136**	**0.179**	**0.304**	1.49	1.175	79%	21%
15			RB		22.4	7.81	21.3	**0.110**	**0.039**	**0.072**	**0.105**	0.563	0.453	80%	20%
16			BED1		12.1	6.4	11.4	**0.061**	**0.032**	**0.029**	**0.057**	0.278	0.217	78%	22%
17			BED2		10.7	5.59	9.77	**0.053**	**0.028**	**0.025**	**0.048**	0.356	0.303	85%	15%
18			BED3		12.6	7.85	11.9	**0.062**	**0.039**	**0.023**	**0.059**	0.239	0.177	74%	26%
19			BED4		14.3	7.98	13.3	**0.071**	**0.040**	**0.031**	**0.066**	0.341	0.270	79%	21%
20	4	2	BED	6/19/2013	7.60	6.04		**0.038**	**0.030**	**0.008**		0.257	0.219	85%	15%
21			RB		22.40	10.60		**0.112**	**0.053**	**0.059**		0.729	0.617	85%	15%
22			LB		11.20	7.60		**0.056**	**0.038**	**0.018**		0.261	0.205	79%	21%
23	7	1	BED	3/16/2013	11.1	5.85		**0.055**	**0.029**	**0.026**		0.289	0.234	81%	19%
24			RB		46.5	26.8		**0.233**	**0.134**	**0.099**		0.969	0.737	76%	24%
25		1	LB	3/16/2013	5	25	16.8	8.65	**0.084**	**0.043**	**0.041**	0.34	0.256	75%	25%

Table B-3. Continued

Index	Location	Trip	Location Within Cross Section	Date Collected	Total Recoverable Se (µg/L)	Selenite (µg/L)	Se, Dissolved (SDAL) (µg/L)	Total Sorbed Se + Solid Se (µg/g)	Sorbed SeO_3 (µg/g)	Sorbed SeO_4 (µg/g)	Non-Sorbed Se (µg/g)	Soil, Total Se (µg/g)	Estimate of Precipitated and Organic Se (µg/g)	Percent Precipitated and Organic Se %	Percent Sorbed Se %
26	7	2	BED	6/19/2013	7.73	6.00		**0.039**	**0.030**	**0.009**		0.163	0.124	76%	24%
27			BED2		7.70	5.97		**0.038**	**0.030**	**0.009**		0.273	0.235	86%	14%
28			RB		48.00	23.30		**0.240**	**0.117**	**0.124**		1.120	0.880	79%	21%
29			LB		61.30	31.40		**0.307**	**0.157**	**0.150**		1.450	1.143	79%	21%
30	7	4	BED 1	3/17/2014	8.37	2.22		**0.042**	**0.011**	**0.031**		0.226	0.184	81%	19%
31	10	2	BED	6/19/2013	10.1	7.48		**0.050**	**0.037**	**0.013**		0.328	0.278	85%	15%
32			RB		56.8	38.3		**0.284**	**0.192**	**0.093**		0.911	0.627	69%	31%
33			LB		40.2	24.3		**0.201**	**0.121**	**0.079**		0.635	0.434	68%	32%
34	12	1	BED	3/16/2013	9.62	6.85		**0.048**	**0.034**	**0.014**		0.289	0.241	84%	16%
35			RB		46	26.8		**0.230**	**0.134**	**0.096**		1.17	0.940	80%	20%
36			LB		40.8	15.2		**0.204**	**0.076**	**0.128**		0.811	0.607	75%	25%
37	12	2	BED	6/19/2013	10.1	7.95		**0.051**	**0.040**	**0.011**		0.328	0.278	85%	15%
38			BED2		10.2	7.49		**0.051**	**0.037**	**0.014**		0.199	0.148	74%	26%
39			BED3		12.3	9.52		**0.061**	**0.048**	**0.014**		0.297	0.236	79%	21%
40			BED4		9.72	7.33		**0.049**	**0.037**	**0.012**		0.279	0.230	83%	17%
41			RB		29.4	17.2		**0.147**	**0.086**	**0.061**		0.799	0.652	82%	18%
42			LB		20.6	9.92		**0.103**	**0.049**	**0.053**		0.355	0.252	71%	29%
43	12	4	BED	3/18/2014	7.71	1.47		**0.039**	**0.007**	**0.031**		0.210	0.171	82%	18%
44	14	2	BED	6/19/2013	9.5	7.15		**0.048**	**0.036**	**0.012**		0.289	0.241	84%	16%
45			RB		56.6	32.5		**0.283**	**0.163**	**0.121**		1.56	1.277	82%	18%
46			LB		7.27	ND		**0.036**	**N/A**	**N/A**		0.287	0.251	87%	13%
47	14	3	BED	8/21/2013	20	7.14		**0.100**	**0.036**	**0.064**		0.242	0.142	59%	41%
48			RB		35.9	11.5		**0.180**	**0.058**	**0.122**		0.957	0.778	81%	19%
49			LB		88.9	45.4		**0.445**	**0.227**	**0.218**		1.780	1.336	75%	25%
50	15	1	BED	3/16/2013	11.2	6.08		**0.056**	**0.030**	**0.026**		0.156	0.100	64%	36%
51			RB		49.9	14.5		**0.250**	**0.073**	**0.177**		1.39	1.140	82%	18%
52			LB		60	26.5		**0.299**	**0.132**	**0.167**		1.2	0.901	75%	25%
53	15	2	BED	6/19/2013	12.6	8.18		**0.063**	**0.041**	**0.022**		0.232	0.169	73%	27%
54			RB		25.8	12.3		**0.129**	**0.061**	**0.067**		0.817	0.688	84%	16%

Table B-3. Continued

In-dex	Lo-cation	Trip	Location Within Cross Section	Date Collected	Total Recoverable Se (µg/L)	Selen-ite (µg/L)	Se, Dissolved (SDAL) (µg/L)	Total Sorbed Se + Solid Se (µg/g)	Sorbed SeO_3 (µg/g)	Sorbed SeO_4 (µg/g)	Non-Sorbed Se (µg/g)	Soil, Total Se (µg/g)	Estimate of Precipitated and Organic Se (µg/g)	Percent Precipitated and Organic Se %	Percent Sorbed Se %
55	15	2	LB	6/19/2013	31.4	15.3		**0.157**	**0.077**	**0.081**		0.947	0.790	83%	17%
56	15	3	BED	8/21/2013	12.1	4.35		**0.061**	**0.022**	**0.039**		0.268	0.208	77%	23%
57			RB		56.9	21.4		**0.285**	**0.107**	**0.178**		1.700	1.416	83%	17%
58			LB		12.3	2.98		**0.061**	**0.015**	**0.047**		0.319	0.258	81%	19%
59	18	1	BED	3/16/2013	13.4	8.65		**0.067**	**0.043**	**0.024**		0.282	0.215	76%	24%
60			LB		42.3	28.8		**0.211**	**0.144**	**0.067**		0.644	0.433	67%	33%
61			RB		47	24.4		**0.235**	**0.122**	**0.113**		1.07	0.835	78%	22%
62	18	2	BED	6/19/2013	14.6	8.37		**0.073**	**0.042**	**0.031**		0.343	0.270	79%	21%
63			LB		37.4	13.8		**0.187**	**0.069**	**0.118**		1.35	1.163	86%	14%
64			RB		17.1	4.55		**0.086**	**0.023**	**0.063**		0.669	0.583	87%	13%
65	18	3	BED	8/21/2013	10.8	2.78		**0.054**	**0.014**	**0.040**		0.261	0.207	79%	21%
66			RB		60.3	24.5		**0.302**	**0.123**	**0.179**		0.986	0.685	69%	31%
67			LB		12.5	1.94		**0.063**	**0.010**	**0.053**		0.320	0.258	80%	20%
68	18	4	BED 1	3/18/2014	11.50	1.75		**0.058**	**0.009**	**0.049**		0.275	0.218	79%	21%

Table B-4. All sorbed and residual (precipitated and organic Se) data for all trips sorted by sample point in the tributaries and by location

					SORBED SELENIUM DATA						PRECIPITATED AND ORGANIC SELENIUM DATA		
					Lab Results (Water from Soil)		CALCULATIONS			Lab Result	CALCULATIONS		
In-dex	**Lo-cation**	**Trip**	**Location Within Cross Section**	**Date Collected**	**Total Recoverable Se (µg/L)**	**Selen-ite (µg/L)**	**Total Sorbed Se + Solid Se (µg/g)**	**Sorbed Selenite (µg/g)**	**Sorbed Selenate (µg/g)**	**Soil, Total Se (µg/g)**	**Estimate of Precipitated and Organic Se (µg/g)**	**Percent Precipitated and Organic Se %**	**Percent Sorbed Se %**
1	2	1	BED	3/16/2013	59.3	27.8	**0.298**	**0.140**	**0.158**	1.42	1.122	79%	21%
2			LB		59.8	3.04	**0.299**	**0.015**	**0.284**	0.828	0.529	64%	36%
3			RB		74.1	32.2	**0.367**	**0.159**	**0.207**	1.31	0.943	72%	28%
4	2	2	BED	6/19/2013	105.00	75.70	**0.525**	**0.379**	**0.147**	1.340	0.815	61%	39%
5			LB		38.80	19.50	**0.194**	**0.097**	**0.096**	1.870	1.676	90%	10%
6			RB		19.10	7.77	**0.095**	**0.039**	**0.057**	1.190	1.095	92%	8%
7	2	4	BED	3/19/2014	39.50	20.90	**0.197**	**0.104**	**0.093**	0.831	0.634	76%	24%
8	5	1	BED	3/16/2013	145	89.3	**0.725**	**0.447**	**0.279**	2.1	1.375	65%	35%
9			RB		24.9	8.8	**0.124**	**0.044**	**0.080**	1.01	0.886	88%	12%
10			LB		22.1	11.8	**0.111**	**0.059**	**0.052**	0.908	0.798	88%	12%
11	5	2	BED	6/19/2013	141.00	103.00	**0.704**	**0.514**	**0.190**	2.250	1.546	69%	31%
12			LB		65.60	40.20	**0.327**	**0.200**	**0.127**	2.050	1.723	84%	16%
13			RB		82.70	56.40	**0.413**	**0.282**	**0.131**	1.310	0.897	68%	32%
14	6	1	BED	3/16/2013	79.5	53.2	**0.399**	**0.267**	**0.132**	1.63	1.231	76%	24%
15			LB		53.4	24.2	**0.266**	**0.121**	**0.146**	1.62	1.354	84%	16%
16			RB		49.5	24.8	**0.248**	**0.124**	**0.124**	1.08	0.833	77%	23%
17		2	BED	6/19/2013	119.00	87.30	**0.594**	**0.435**	**0.158**	2.230	1.636	73%	27%
18			RB		47.00	11.30	**0.235**	**0.056**	**0.178**	1.320	1.085	82%	18%
19			LB		21.70	7.04	**0.109**	**0.035**	**0.073**	0.916	0.808	88%	12%
20		4	BED	3/17/2014	103.00	66.90	**0.516**	**0.335**	**0.181**	1.650	1.134	69%	31%

Table B-4. Continued

Index	Location	Trip	Location Within Cross Section	Date Collected	Total Recoverable Se (µg/L)	Selenite (µg/L)	Total Sorbed Se + Solid Se (µg/g)	Sorbed Selenite (µg/g)	Sorbed Selenate (µg/g)	Soil, Total Se (µg/g)	Estimate of Precipitated and Organic Se (µg/g)	Percent Precipitated and Organic Se %	Percent Sorbed Se %
21	8	1	BED	3/16/2013	69.1	42.5	**0.346**	**0.213**	**0.133**	1.64	1.295	79%	21%
22			LB		82.3	49.7	**0.412**	**0.249**	**0.163**	1.82	1.409	77%	23%
23			RB		88.3	19	**0.442**	**0.095**	**0.347**	1.61	1.169	73%	27%
24	8	2	BED	6/19/2013	44.60	22.30	**0.223**	**0.111**	**0.111**	0.798	0.575	72%	28%
25			LB		45.80	22.20	**0.229**	**0.111**	**0.118**	0.851	0.622	73%	27%
26			RB		60.90	27.60	**0.304**	**0.138**	**0.166**	1.420	1.116	79%	21%
27	9	1	BED	3/16/2013	78.6	47.3	**0.393**	**0.237**	**0.157**	1.76	1.367	78%	22%
28			RB		50	28.2	**0.251**	**0.141**	**0.109**	1.3	1.049	81%	19%
29			LB		72.7	46.9	**0.363**	**0.234**	**0.129**	1.5	1.137	76%	24%
30	9	2	BED	6/19/2013	118.00	79.30	**0.589**	**0.396**	**0.193**	1.930	1.341	69%	31%
31			RB		78.60	42.40	**0.393**	**0.212**	**0.181**	1.840	1.447	79%	21%
32			LB		146.00	109.00	**0.805**	**0.601**	**0.204**	2.390	1.585	66%	34%
33	9	4	BED	3/18/2014	168.00	123.00	**0.843**	**0.617**	**0.226**	2.600	1.757	68%	32%
34	11	1	BED	3/16/2013	50.9	29.8	**0.255**	**0.149**	**0.106**	1.32	1.065	81%	19%
35			LB		71.2	9.71	**0.355**	**0.048**	**0.307**	2.33	1.975	85%	15%
36			RB		56.3	36.9	**0.283**	**0.185**	**0.097**	1.28	0.997	78%	22%
37	11	2	BED	6/19/2013	164	123	**0.819**	**0.614**	**0.205**	3.16	2.341	74%	26%
38			RB		37.6	16.9	**0.188**	**0.085**	**0.104**	1.85	1.662	90%	10%
39			LB		120	63.5	**0.600**	**0.318**	**0.283**	5.14	4.540	88%	12%
40	16	1	BED	3/16/2013	15.5	6.82	**0.078**	**0.034**	**0.043**	0.318	0.240	76%	24%
41			LB		27.7	9.55	**0.139**	**0.048**	**0.091**	1	0.861	86%	14%
42			RB		26.6	10.3	**0.133**	**0.051**	**0.081**	0.911	0.778	85%	15%
43	17	1	BED	3/16/2013	67.7	44.5	**0.336**	**0.221**	**0.115**	0.951	0.615	65%	35%

Table B-4. Continued

Index	Location	Trip	Location Within Cross Section	Date Collected	Total Recoverable Se (µg/L)	Selenite (µg/L)	Total Sorbed Se + Solid Se (µg/g)	Sorbed Selenite (µg/g)	Sorbed Selenate (µg/g)	Soil, Total Se (µg/g)	Estimate of Precipitated and Organic Se (µg/g)	Percent Precipitated and Organic Se %	Percent Sorbed Se %
44	17	1	RB	3/16/2013	219	165	**1.097**	**0.827**	**0.271**	3.58	2.483	69%	31%
45			LB		119	86.8	**0.591**	**0.431**	**0.160**	2.81	2.219	79%	21%
46	17	2	BED	6/19/2013	130	112	**0.650**	**0.560**	**0.090**	2	1.350	68%	33%
47			LB		67.8	37.8	**0.339**	**0.189**	**0.150**	2.78	2.441	88%	12%
48			RB		28.4	16.8	**0.142**	**0.084**	**0.058**	0.592	0.450	76%	24%
49	17	3	BED	8/21/2013	10.4	3.06	**0.052**	**0.015**	**0.037**	0.287	0.235	82%	18%
50			RB		26.5	8.92	**0.133**	**0.045**	**0.088**	0.566	0.434	77%	23%
51			LB		30.5	9	**0.153**	**0.045**	**0.108**	0.674	0.522	77%	23%
52	17	4	BED 1	3/19/2014	234.00	157.00	**1.170**	**0.785**	**0.385**	2.340	1.170	50%	50%

Figure B-1. Trip 1 in the Arkansas River: percentages of dissolved Se species in the water and sorbed Se species compared to residual Se

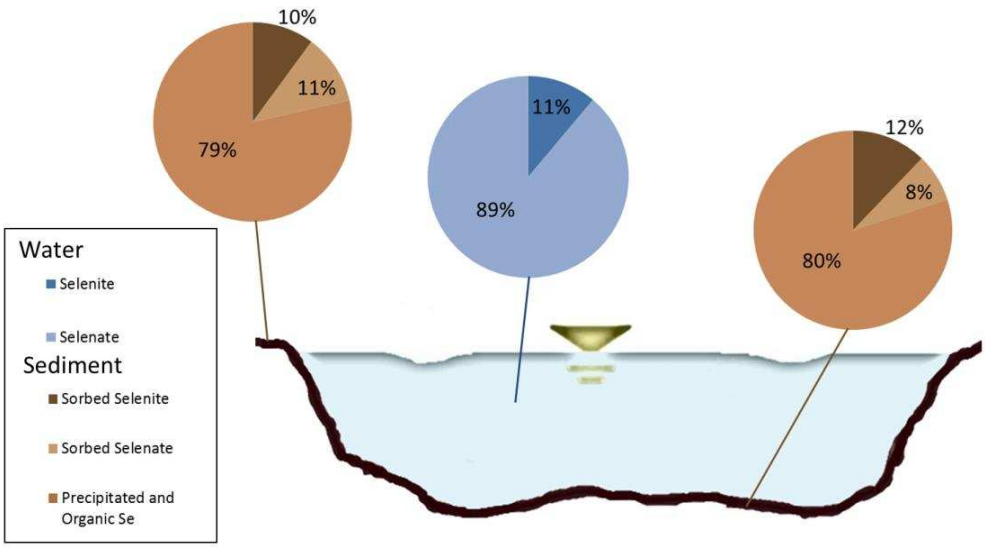

Figure B-2. Trip 1 in the Tributaries: percentages of dissolved Se species in the water and sorbed Se species

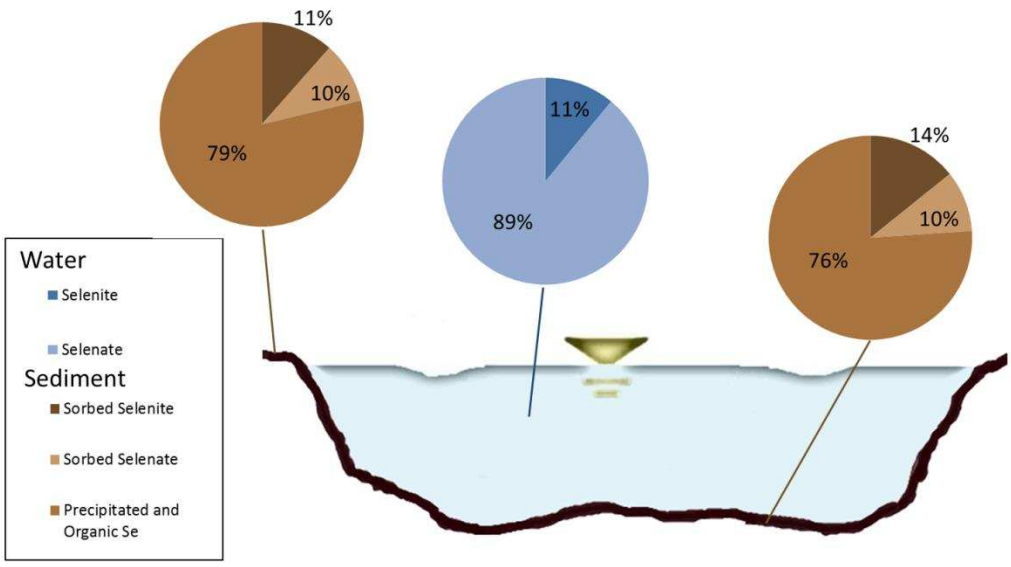

Figure B-3. Trip 2 in the Arkansas River: percentages of dissolved Se species in the water and sorbed Se species compared to residual Se

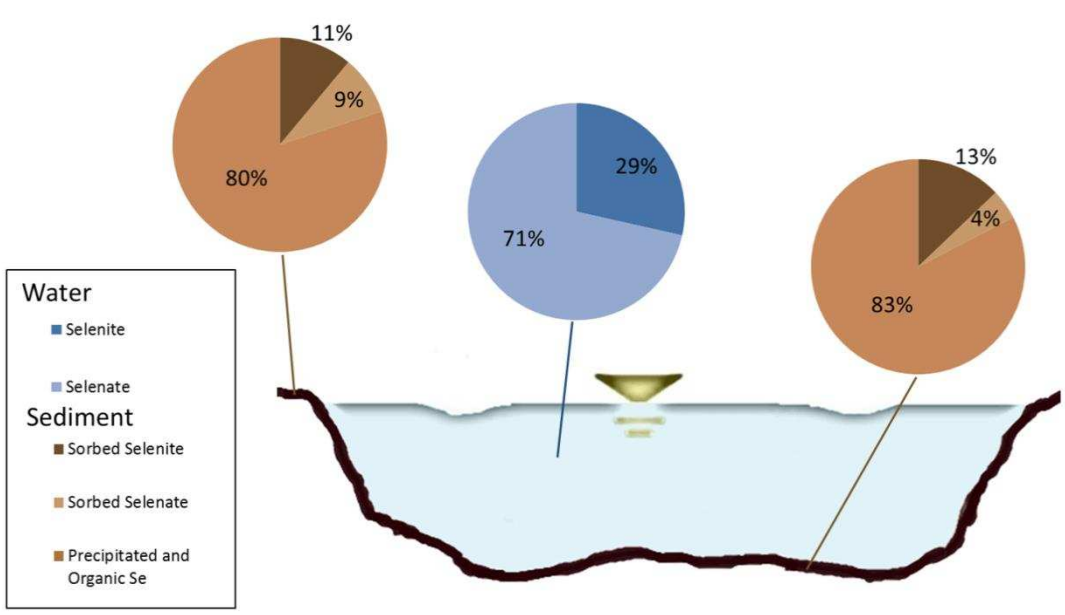

Figure B-4. Trip 2 in the Tributaries: percentages of dissolved Se species in the water and sorbed Se species compared to residual Se

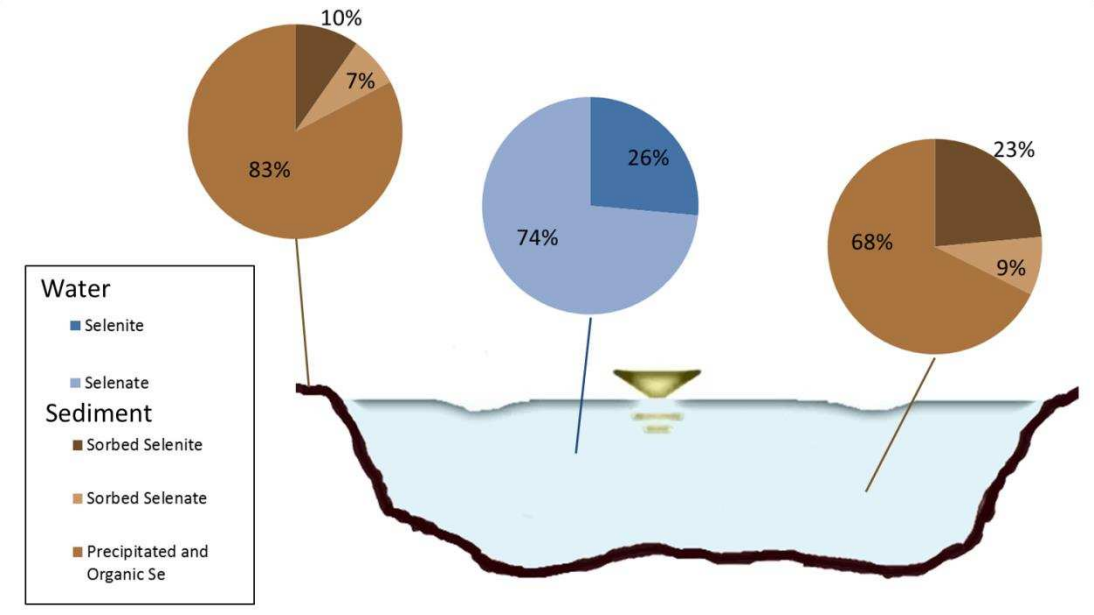

Figure B-5. Trip 3 in the Arkansas River: percentages of dissolved Se species in the water and sorbed Se species compared to residual Se

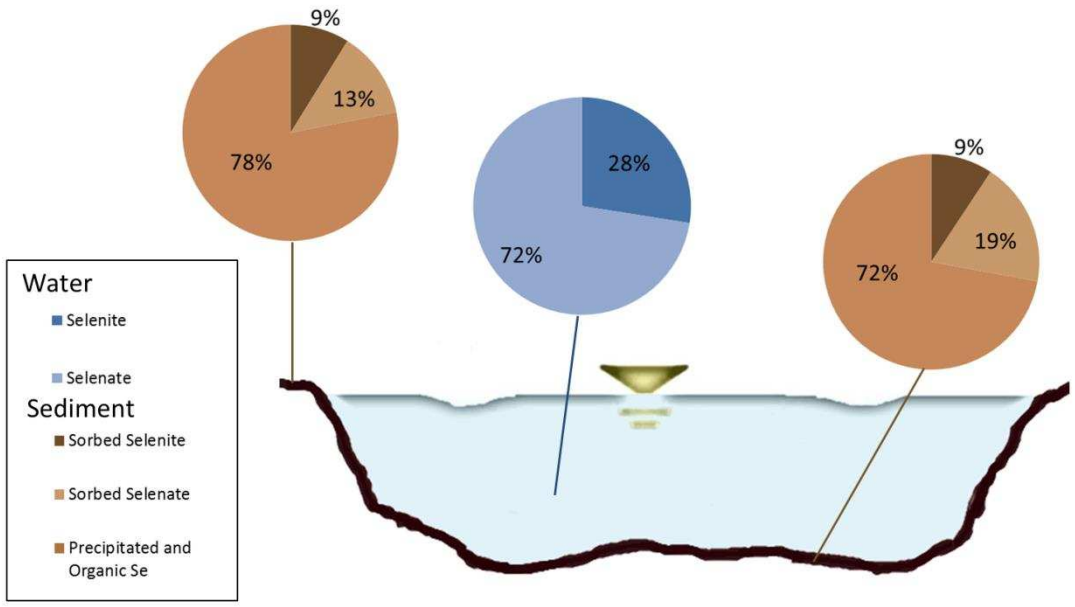

Figure B-6. Trip 3 in the Tributaries: percentages of dissolved Se species in the water and sorbed Se species compared to residual Se

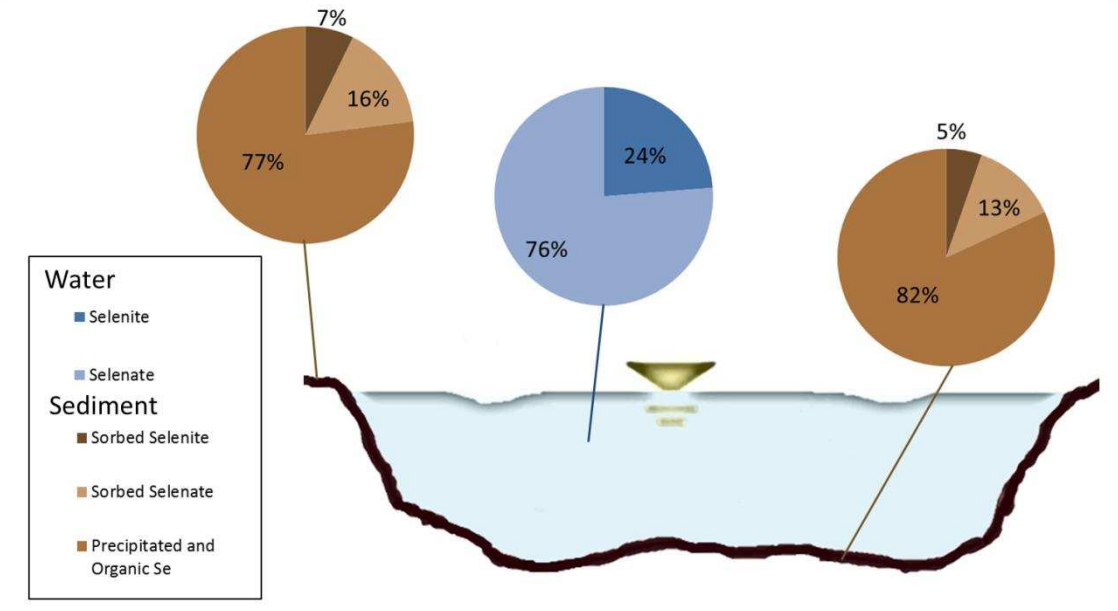

Figure B-7. Trip 4 in the Arkansas River: percentages of dissolved Se species in the water and sorbed Se species compared to residual Se

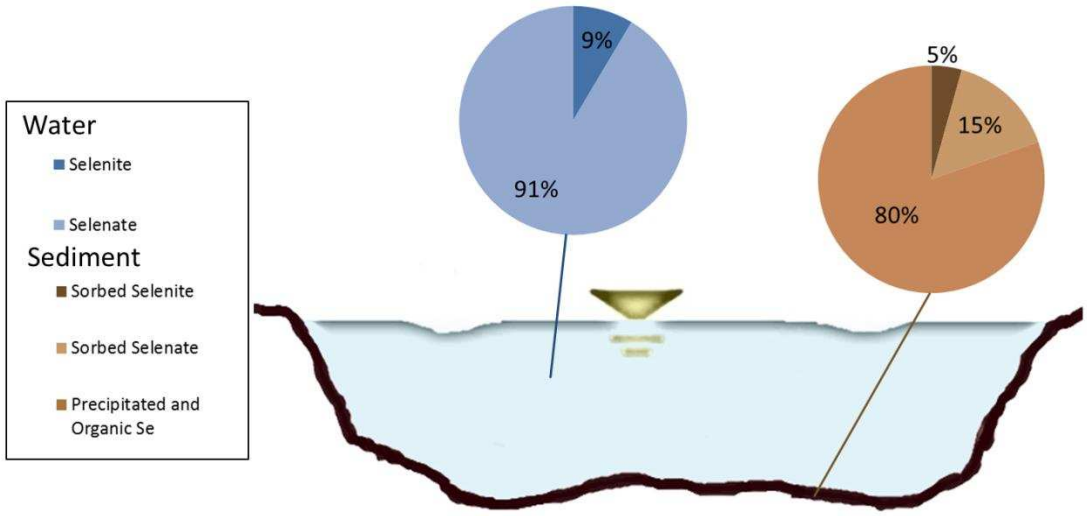

Figure B-8. Trip 4 in the Tributaries: percentages of dissolved Se species in the water and sorbed Se species compared to residual Se

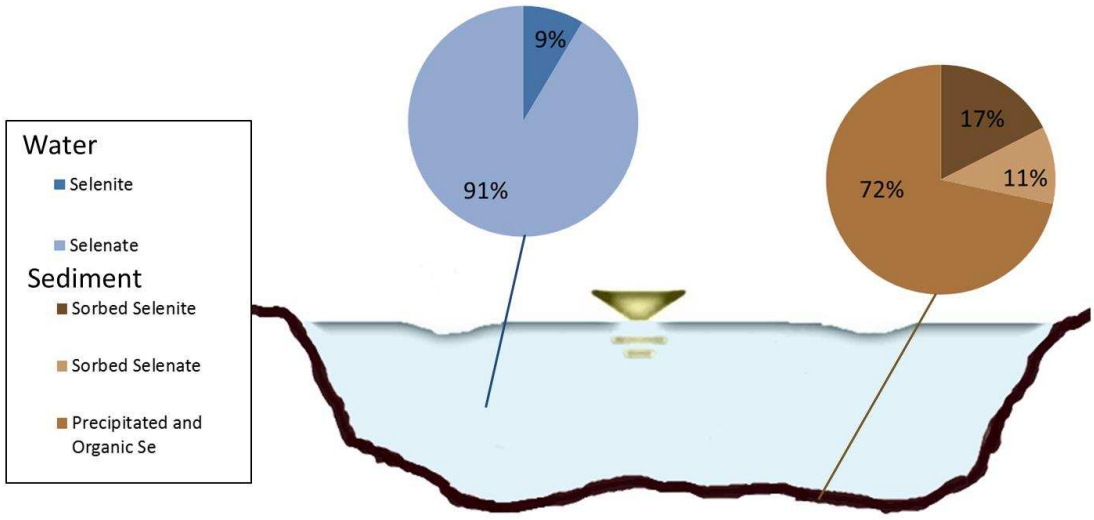

Appendix C: Additional Groundwater BMP Figures

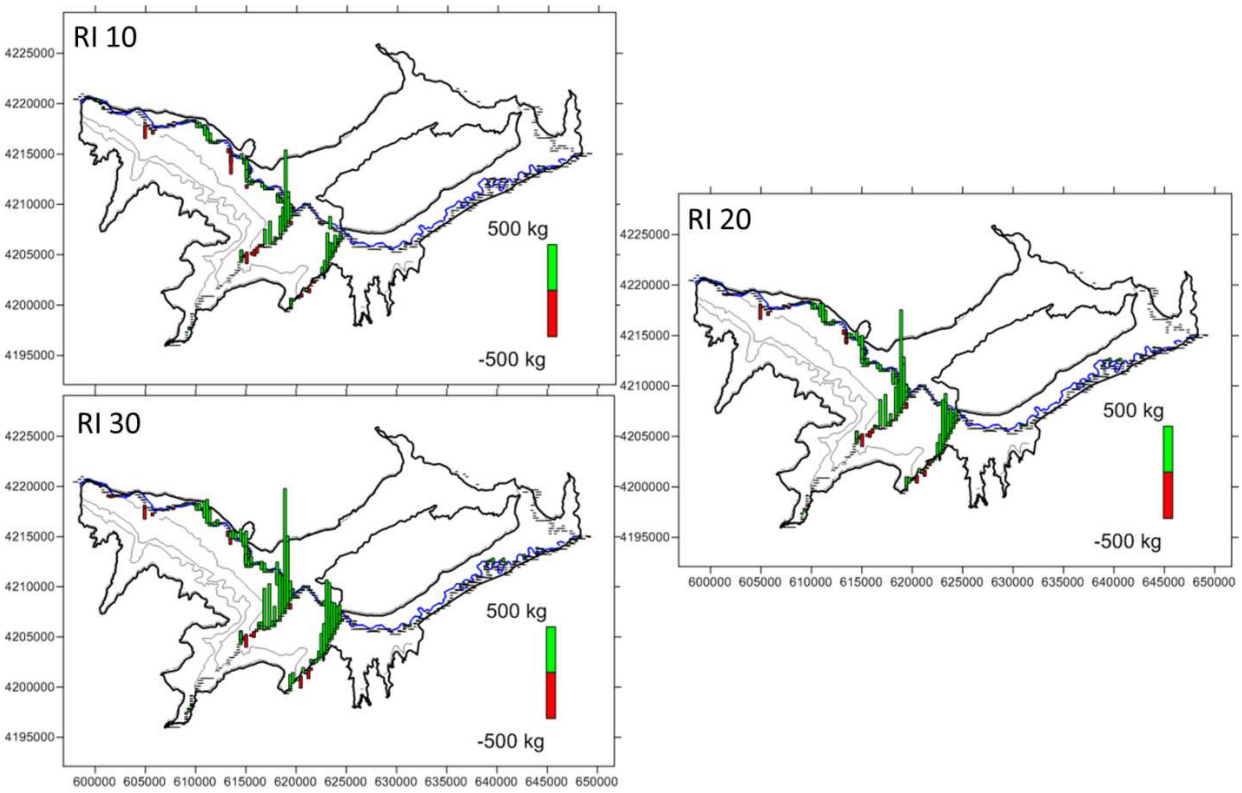

Figure C-1. The spatial distribution of temporally-averaged simulated Se mass loading differences from the Baseline for reduced irrigation scenarios

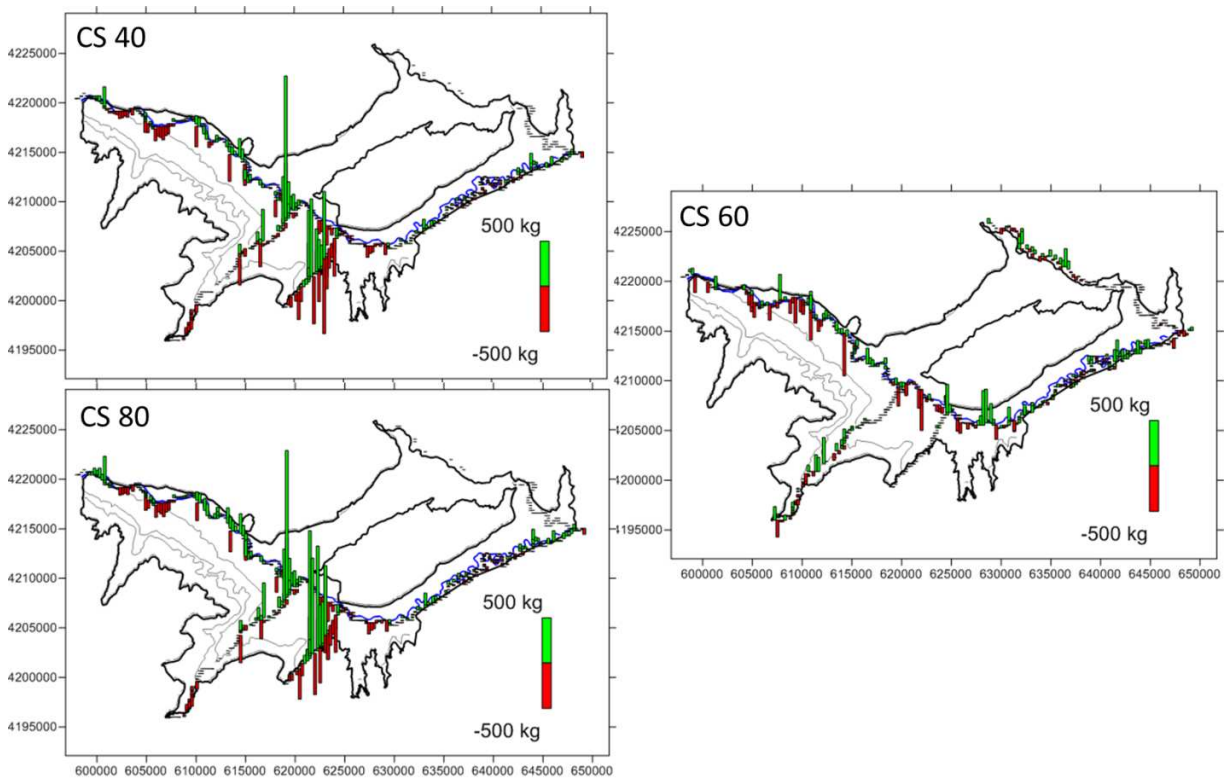

Figure C-2. The spatial distribution of temporally-averaged simulated Se mass loading differences from the Baseline for canal sealing scenarios

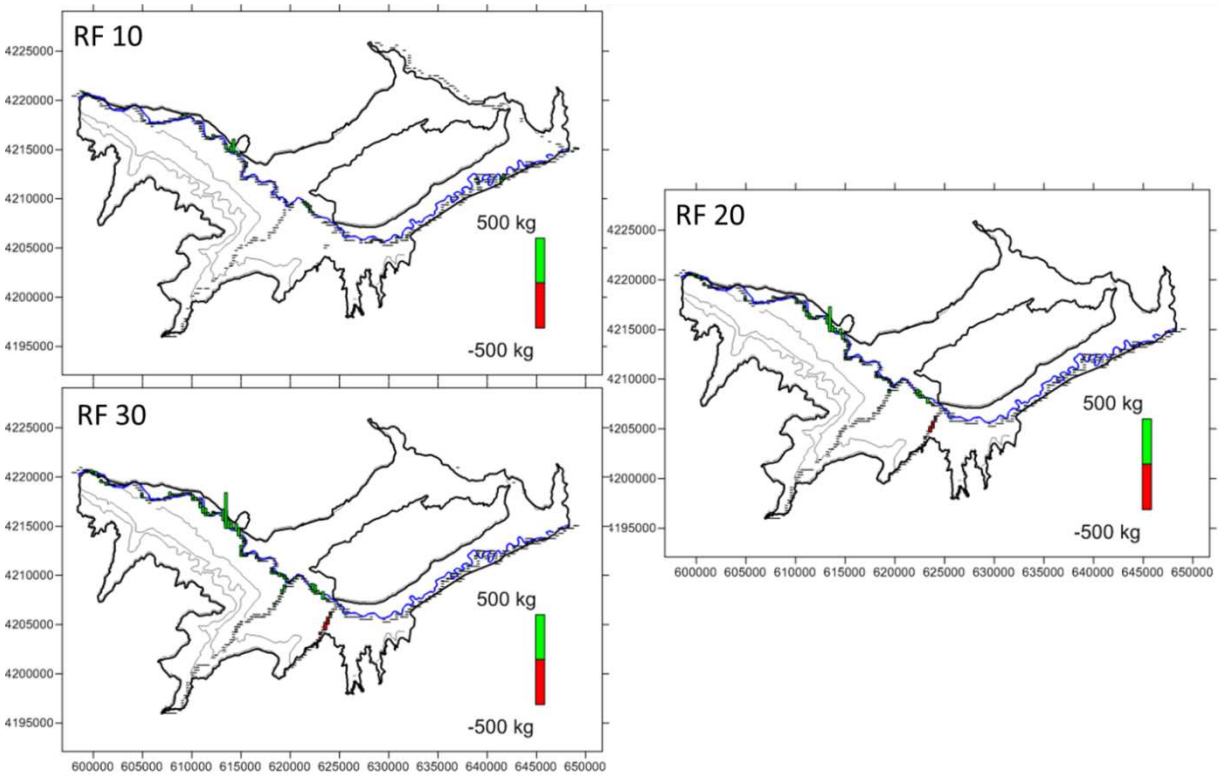

Figure C-3. The spatial distribution of temporally-averaged simulated Se mass loading differences from the Baseline for reduced fertilizer scenarios

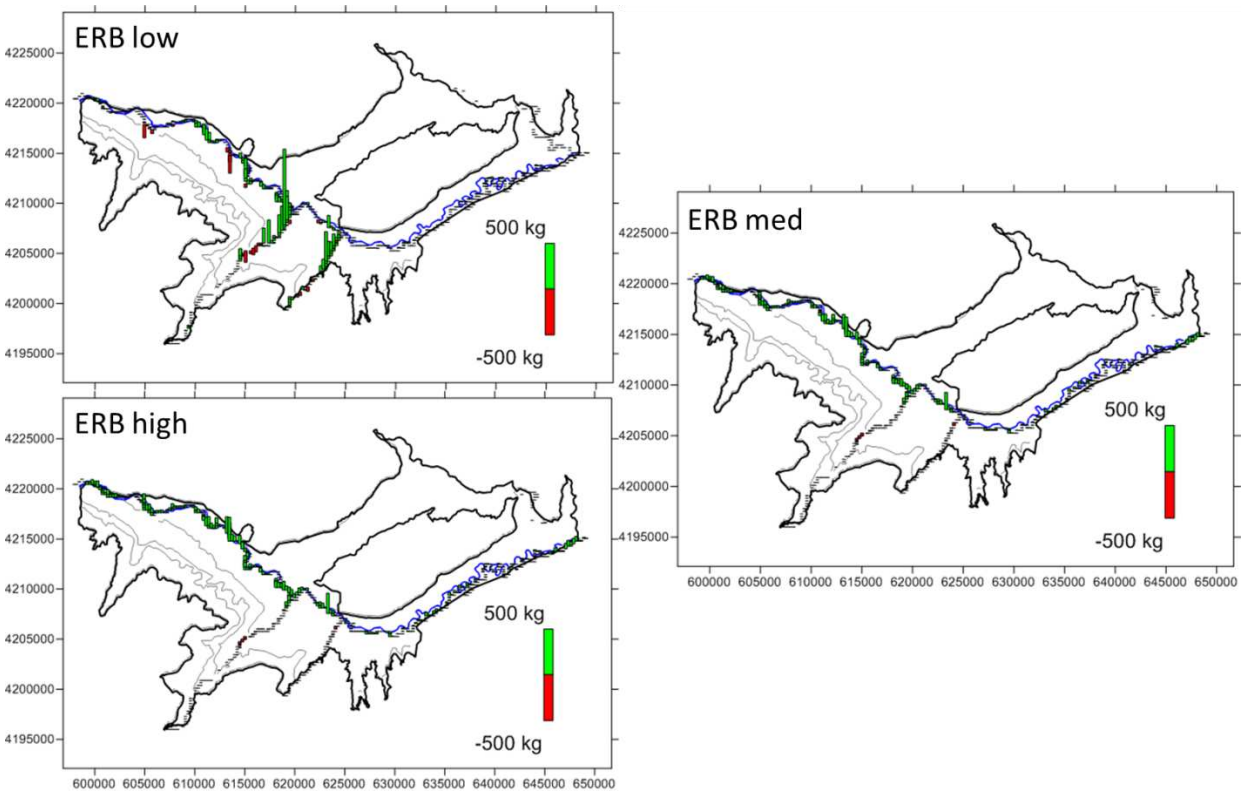

Figure C-4. The spatial distribution of temporally-averaged simulated Se mass loading differences from the Baseline for enhanced riparian buffer scenarios

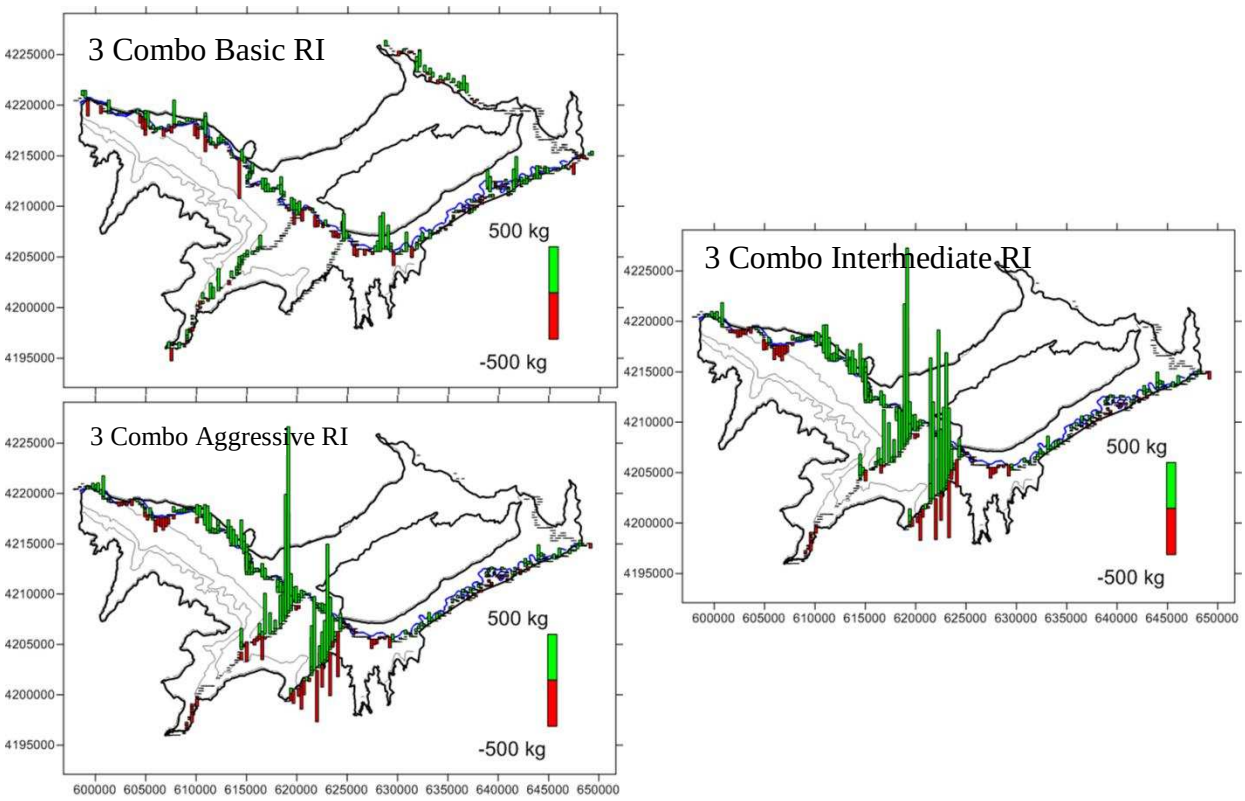

Figure C-5. The spatial distribution of temporally-averaged simulated Se mass loading differences from the Baseline for three combination reduced irrigation scenarios

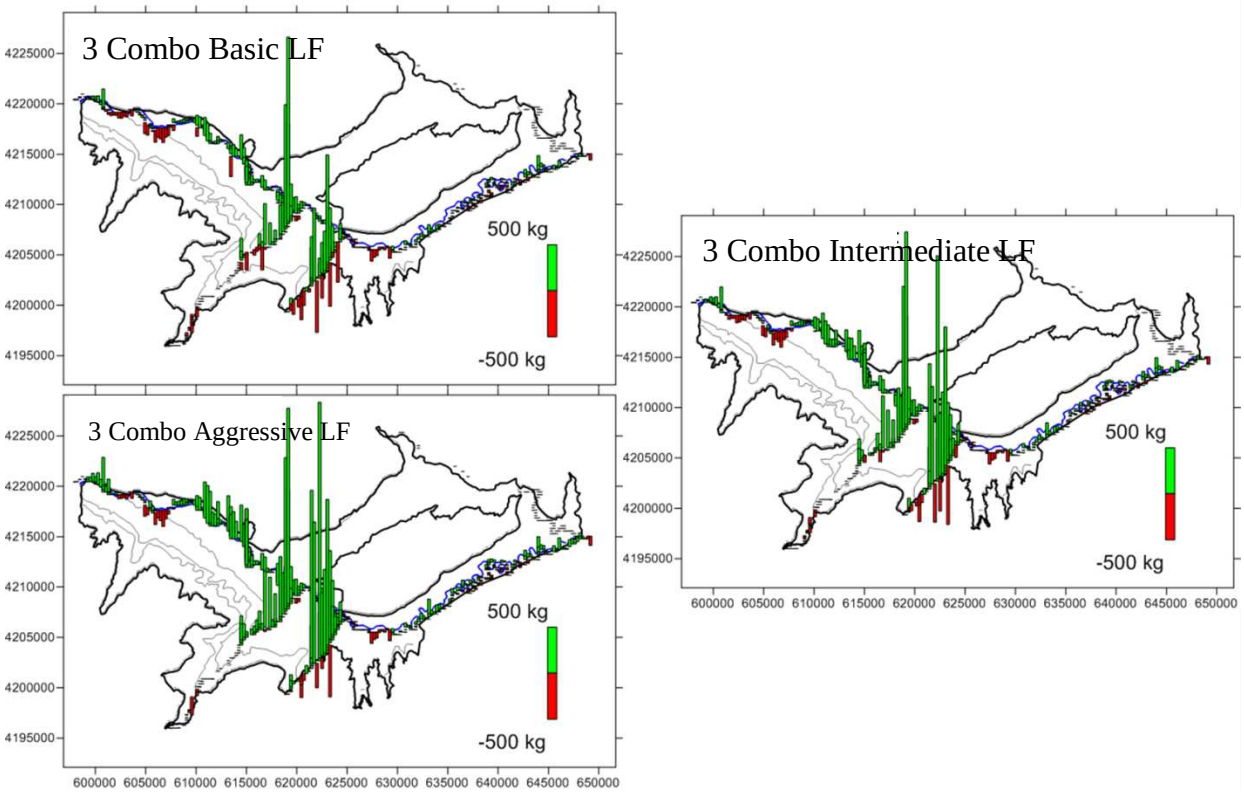

Figure C-6. The spatial distribution of temporally-averaged simulated Se mass loading differences from the Baseline for three combination lease fallowing scenarios

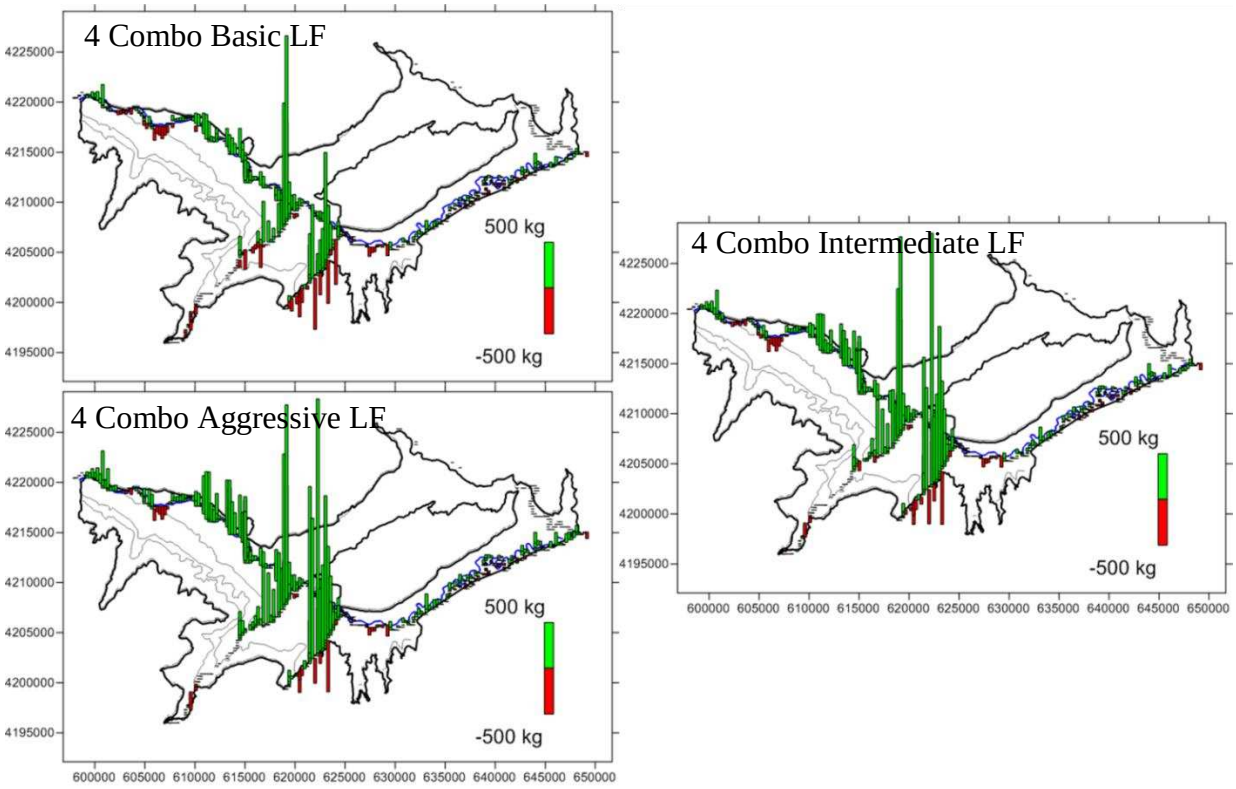

Figure C-7. The spatial distribution of temporally-averaged simulated Se mass loading differences from the Baseline for three combination lease fallowing scenarios